

1 Journal: Ecological Monographs  
2 Manuscript type: Article  
3 Running Head: Carbon cycling in a mid-latitude forest  
4  
5

6 **Carbon budget of the Harvard Forest Long-Term Ecological Research site: pattern,**  
7 **process, and response to global change**  
8

9 Adrien C. Finzi<sup>1</sup>, Marc-André Giasson<sup>1</sup>, Audrey A. Barker Plotkin<sup>2,\*</sup>, John D. Aber<sup>3</sup>, Emery R.  
10 Boose<sup>2</sup>, Eric A. Davidson<sup>4</sup>, Michael C., Dietze<sup>5</sup>, Aaron M. Ellison<sup>2</sup>, Serita D. Frey<sup>3</sup>, Evan  
11 Goldman<sup>6</sup>, Trevor F. Keenan<sup>7,8</sup>, Jerry M. Melillo<sup>9</sup>, J. William Munger<sup>6</sup>, Knute J. Nadelhoffer<sup>10</sup>,  
12 Scott V. Ollinger<sup>3,11</sup>, David A. Orwig<sup>2</sup>, Neil Pederson<sup>2</sup>, Andrew D. Richardson<sup>12,13</sup>, Kathleen  
13 Savage<sup>14</sup>, Jianwu Tang<sup>9</sup>, Jonathan R. Thompson<sup>2</sup>, Christopher A. Williams<sup>15</sup>, Steven C. Wofsy<sup>6</sup>,  
14 Zaixing Zhou<sup>11</sup>, and David R. Foster<sup>2</sup>  
15

16 <sup>1</sup> Department of Biology, Boston University, Boston, Massachusetts 02215 USA

17 <sup>2</sup> Harvard Forest, Harvard University, Petersham, Massachusetts 01366 USA

18 <sup>3</sup> Department of Natural Resources and the Environment, University of New Hampshire,  
19 Durham, New Hampshire 03824 USA

20 <sup>4</sup> University of Maryland Center for Environmental Science, Appalachian Laboratory, Frostburg,  
21 Maryland 21532 USA

22 <sup>5</sup> Department of Earth & Environment, Boston University, Boston, Massachusetts 02215 USA

23 <sup>6</sup> School of Engineering and Applied Sciences, Harvard University, Cambridge, Massachusetts  
24 02138 USA

25 <sup>7</sup> Lawrence Berkeley National Laboratory, Berkeley, California 94720 USA

26 <sup>8</sup> Department of Environmental Science, Policy and Management, UC Berkeley, Berkeley,  
27 California 94720 USA

28 <sup>9</sup> The Ecosystems Center, Marine Biological laboratory, Woods Hole, Massachusetts 02543 USA

29 <sup>10</sup> Department of Ecology and Evolutionary Biology, University of Michigan, Ann Arbor,  
30 Michigan 48109 USA

This is the author manuscript accepted for publication and has undergone full peer review but has not been through the copyediting, typesetting, pagination and proofreading process, which may lead to differences between this version and the [Version of Record](#). Please cite this article as [doi: 10.1002/ECM.1423](https://doi.org/10.1002/ECM.1423)

This article is protected by copyright. All rights reserved

31 <sup>11</sup> Earth Systems Research Center, University of New Hampshire, Durham, New Hampshire  
32 03824 USA

33 <sup>12</sup> School of Informatics, Computing and Cyber Systems, Northern Arizona University, Flagstaff,  
34 Arizona 86011 USA

35 <sup>13</sup> Center for Ecosystem Science and Society, Northern Arizona University, Flagstaff, Arizona  
36 86011 USA

37 <sup>14</sup> Woods Hole Research Center, 149 Woods Hole Road, Falmouth, MA, 02540 USA

38 <sup>15</sup> Graduate School of Geography and Department of Biology, Clark University, Worcester,  
39 Massachusetts 01610 USA

40

41

42 \* **Corresponding Author:** Audrey Barker Plotkin ([aabarker@fas.harvard.edu](mailto:aabarker@fas.harvard.edu))

43

44 Manuscript received 23 January 2020; accepted 22 May 2020; final version received 16 June  
45 2020.

46

#### ABSTRACT

47 How, where, and why carbon (C) moves into and out of an ecosystem through time are long-  
48 standing questions in biogeochemistry. Here, we bring together hundreds of thousands of C-  
49 cycle observations at the Harvard Forest in central Massachusetts, USA, a mid-latitude landscape  
50 dominated by 80–120-year-old closed-canopy forests. These data answered four questions:

51 (i) where and how much C is presently stored in dominant forest types; (ii) what are current  
52 rates of C accrual and loss; (iii) what biotic and abiotic factors contribute to variability in these  
53 rates; and (iv) how has climate change affected the forest's C cycle? Harvard Forest is an active  
54 C sink resulting from forest regrowth following land abandonment. Soil and tree biomass  
55 comprise nearly equal portions of existing C stocks. Net primary production (NPP) averaged  
56 680–750 g C m<sup>-2</sup> yr<sup>-1</sup>; belowground NPP contributed 38–47% of the total, but with large  
57 uncertainty. Mineral soil C measured in the same inventory plots in 1992 and 2013 were too  
58 heterogeneous to detect change in soil-C pools; however, radiocarbon data suggest a small but  
59 persistent sink of 10–30 g C m<sup>-2</sup> yr<sup>-1</sup>. Net ecosystem production (NEP) in hardwood stands  
60 averaged ~300 g C m<sup>-2</sup> yr<sup>-1</sup>. NEP in hemlock-dominated forests averaged ~450 g C m<sup>-2</sup> yr<sup>-1</sup> until  
61 infestation by the hemlock woolly adelgid turned these stands into a net C source. Since 2000,

62 NPP has increased by 26%. For the period 1992–2015, NEP increased 93%. The increase in  
63 mean annual temperature and growing season length alone accounted for ~30% of the increase in  
64 productivity. Interannual variations in GPP and NEP were also correlated with increases in red  
65 oak biomass, forest leaf area, and canopy-scale light-use efficiency. Compared to long-term  
66 global change experiments at the Harvard Forest, the C sink in regrowing biomass equaled or  
67 exceeded C cycle modifications imposed by soil warming, N saturation, and hemlock removal.  
68 Results of this synthesis and comparison to simulation models suggest that forests across the  
69 region are likely to accrue C for decades to come but may be disrupted if the frequency or  
70 severity of biotic and abiotic disturbances increase.

71

72

### KEYWORDS

73 forest ecosystems, ecosystem ecology, carbon cycling, net primary production, gross primary  
74 production, belowground production, disturbance, eddy covariance, permanent plots, climate  
75 change, long-term ecological research

76

### INTRODUCTION

77 Understanding how, where, and why C moves through an ecosystem is a long-standing goal in  
78 biogeochemistry (e.g., Brown and Escombe 1902, Isaac and Hopkins 1937, Kira and Shidei  
79 1967, Raich and Nadelhoffer 1989, Ryan et al. 1997, Litton et al. 2007). It is an especially  
80 important present-day issue because forest C balances both affect and are influenced by climatic  
81 and atmospheric changes such as warming and rising concentrations of atmospheric CO<sub>2</sub>  
82 (Melillo et al. 1990, Schimel 1995). Understanding feedbacks between forests and the  
83 atmosphere is key to understanding whether, how, and for how long the terrestrial biosphere will  
84 continue to mitigate anthropogenic CO<sub>2</sub> emissions.

85

86 Eastern North American forests have accumulated significant C in recent decades (Urbanski et  
87 al. 2007, Pan et al. 2011, Williams et al. 2012, Fahey et al. 2013, Eisen and Barker Plotkin  
88 2015). Recovery from agricultural abandonment and intensive forest harvesting is considered the  
89 primary driver of this sink along with episodic disturbance such as the 1938 hurricane (Albani et  
90 al. 2006, Thompson et al. 2011, Duveneck et al. 2017). As many forests in this region mature, it  
91 is relevant to ask how long they will remain C sinks. Will the sinks disappear as predicted by  
92 original theories of forest development because photosynthetic C gain is offset by growing

93 respiratory costs (Kira and Shidei 1967, Odum 1969)? Or, in the absence of large-scale  
94 disturbance, will these mature forests remain C sinks long into the future (Carey et al. 2001,  
95 Pregitzer and Euskirchen 2004, Zhou et al. 2006, Luysaert et al. 2008)?

96  
97 Most research attributes the C sink to the growth of woody biomass. Soil C is lost as a result of  
98 row crop agriculture and grazing (Sanderman et al. 2017). In the 18<sup>th</sup> and 19<sup>th</sup> centuries, row crop  
99 agriculture and livestock grazing were active land uses in New England. There is evidence that  
100 regrowth following land abandonment contributes to a persistent C sink (Barford et al. 2001,  
101 Urbanski et al. 2007), but to what extent and whether C also accumulates in soils remains  
102 uncertain (Compton and Boone 2000, Gaudinski et al. 2000, Sierra et al. 2012).

103  
104 While forests are regrowing from land abandonment, atmospheric chemistry and climate are  
105 changing. In Massachusetts since 1900, atmospheric CO<sub>2</sub> has increased 38% (Sargent et al.  
106 2018). Atmospheric N deposition more than doubled, but is now declining in response to air  
107 quality regulations (Bowen and Valiela 2001, Waller et al. 2012). Since 1964, the average annual  
108 temperature in central Massachusetts has increased 1.5 °C and total precipitation has increased  
109 by 188 mm (SRCC 2019). These factors, alone or together, are likely to affect the C cycle.  
110 Indeed, longer growing seasons (Richardson et al. 2010, Yang et al. 2012, Keenan et al. 2014),  
111 CO<sub>2</sub> fertilization (Keenan et al. 2016, Williams et al. 2016), enhanced water-use efficiency  
112 (Keenan et al. 2013), atmospheric N deposition (Frey et al. 2014), and increasing moisture  
113 availability (Schwalm et al. 2011, Pederson et al. 2013) are variously implicated in the increasing  
114 rate of C accumulation in New England forests.

115  
116 The Harvard Forest in central Massachusetts, USA, is one of the most intensively studied forests  
117 in the world. Its land-use history of harvesting and agricultural land clearance, reforestation, and  
118 subsequent partial harvesting is well-documented and similar to that experienced by much of  
119 eastern North America (Foster and Aber 2004). This Long-Term Ecological Research (LTER)  
120 site is home to more than a century of study and three decades of intensive measurements of  
121 forest compositional and structural change, and C fluxes between the forest, the soil, and the  
122 atmosphere (Fig. 1).

123

124 A cornerstone of C-cycle research at the Harvard Forest are continuous measurements of forest-  
125 atmosphere exchanges of CO<sub>2</sub> that began in 1990 in a mixed hardwood-conifer forest. In a  
126 seminal paper, Wofsy et al. (1993) showed that net C uptake in regrowing forests exceeded those  
127 assumed for temperate forests at that time. This paper led, in part, to the hypothesis that global  
128 changes such as rising atmospheric CO<sub>2</sub> and N deposition may be enhancing the terrestrial sink  
129 for atmospheric CO<sub>2</sub> above that due to land-use change. It also catalyzed interest in developing  
130 long-term, whole-ecosystem free-air CO<sub>2</sub> enrichment studies to assess the validity of the CO<sub>2</sub>  
131 fertilization and N deposition hypotheses (DeLucia et al. 1999, Finzi et al. 2007, Reich et al.  
132 2014). Their paper was followed by an analysis of eight years of C-flux data (Barford et al.  
133 2001) that documented large interannual variations in forest-atmosphere fluxes of C, which they  
134 related to growing season length and cloudiness. It also showed comparatively small year-to-year  
135 variations in woody biomass increment and the potential importance of C allocation, particularly  
136 to storage compounds, in explaining the difference between the variability in tree growth and  
137 that of C exchange. A third study by Urbanski et al. (2007) published 13 years of forest-  
138 atmosphere CO<sub>2</sub> exchange at the Harvard Forest (1992–2004). They found that net C uptake by  
139 the forest nearly doubled during this 13-year period, which they correlated with increases in leaf-  
140 area index, midsummer photosynthetic capacity and the growth of red oak as a canopy dominant.  
141 The doubling of C uptake was a surprising result because the changes in the driving variables—  
142 e.g., atmospheric CO<sub>2</sub> concentration and N deposition, leaf area index, and growing season  
143 length— did not appear to change by a similar magnitude nor could present-day biogeochemical  
144 models simulate the observed increase.

145  
146 A long-term, site-based analysis of these eddy-flux observations has not been published since  
147 2007 and hence a major goal of this synthesis paper is to explore how C fluxes have evolved in  
148 this mixed hardwood-conifer site over the period 1992–2015. Two additional eddy-flux towers in  
149 an old hemlock and young hardwood forest, and a recent synthesis of soil respiration  
150 measurements (Giasson et al. 2013), expand our understanding of ecosystem C flux. A large  
151 portfolio of permanent plots provides detailed information on C storage and fluxes in live  
152 biomass, dead biomass, and soils, and how storage and uptake have changed over the past  
153 quarter-century. A meteorological station on site, ecophysiological studies, and remote sensing

154 data allow investigation of biotic and abiotic factors that potentially control variation in C  
155 cycling.

156  
157 The Harvard Forest hosts several global change experiments designed to simulate soil warming  
158 (e.g., Melillo et al. 2017), atmospheric N deposition (e.g., Nadelhoffer et al. 1999a, b, Frey et al.  
159 2014), and invasive insects (Orwig et al. 2013). Each of the experiments pushes the forest in a  
160 new direction with consequences for C cycling. Twenty-six years of soil warming at the Harvard  
161 Forest resulted in an enhanced rate of soil respiration and a putative loss of soil C of 17% at an  
162 average, annualized rate of  $60 \text{ g C m}^{-2} \text{ yr}^{-1}$  (Melillo et al. 2017). Interestingly, the increase in soil  
163 respiration was marked by four phases. Two phases were characterized by substantial increases  
164 with warming, which alternated with two phases when there was no significant effect of  
165 warming on soil respiration. Similarly, a 20-year study simulating the effects of N deposition  
166 found substantial increases in biomass and soil C storage in hardwood stands. These stands  
167 sequestered C above that in control plots at an average annual rate of  $125 \text{ g C m}^{-2} \text{ yr}^{-1}$  with a  
168 fertilization rate of  $50 \text{ kg N ha}^{-1} \text{ yr}^{-1}$ , and  $460 \text{ g C m}^{-2} \text{ yr}^{-1}$  at a fertilization rate of  $150 \text{ kg N ha}^{-1}$   
169  $\text{yr}^{-1}$  (Frey et al. 2014). Most of the additional C was sequestered in biomass, and in the surface  
170 soil as a result of reduced rates of organic matter decomposition, but some was also sequestered  
171 in deep mineral soil in the N15 treatment (Nadelhoffer et al. 1999a, Frey et al. 2014). In red pine  
172 plantations, fertilization with N did not result in soil C accumulation. At the high level of  
173 fertilization, red pine trees died, indicating that extreme N deposition has the capacity to  
174 fundamentally change the C cycle of forests dominated by red pine. It is unknown, however, how  
175 the magnitude of changes in the C cycle elicited by the experimental studies compare to the rate  
176 of C sequestration owing to forest regrowth following land-use change. Thus, as a part of this  
177 synthesis, we make explicit comparisons of C gains and losses from the experiments to present-  
178 day estimates of C sequestration by the forest ecosystem.

179  
180 Integrating site-based, long-term data sets (e.g., Fahey et al. 2005) provides the opportunity to  
181 separate the contributions of C accumulation into internal drivers of ecosystem development  
182 (i.e., regrowth and structural and compositional changes following disturbance, nutrient cycling)  
183 and global change drivers (e.g., temperature,  $\text{CO}_2$ , invasive insects, atmospheric deposition, land  
184 use). For example, Keenan et al. (2013) suggested that increases in C uptake at the Harvard

185 Forest was in part attributable to increases in water-use efficiency associated with the rise in  
186 atmospheric CO<sub>2</sub>. Similarly, Keenan et al. (2014) suggested that warming-induced increases in  
187 growing season length also contributed to the increase in C uptake. How and whether these  
188 patterns persist are a key point for discussion in the present manuscript.

189  
190 Here, we bring together hundreds of thousands of observations on the C cycle for the Harvard  
191 Forest in central Massachusetts, USA, a mid-latitude landscape dominated by closed-canopy  
192 forests 80–120 years old. We synthesized these data to answer four key research questions in C-  
193 cycle science: (i) where and how much C is presently stored in dominant forest types; (ii) what  
194 are rates of C accrual or loss from 1992–2015, the period of intensive measurements; (iii) what  
195 biotic and abiotic factors contribute to variability in these rates; and (iv) is there evidence that  
196 climate change is affecting the magnitude and seasonality of the C fluxes? We then placed these  
197 results into context. We compared the magnitude of change in the C cycle from forest regrowth  
198 and recent climate change to published results from three long-term global change experiments  
199 at the Harvard Forest: soil warming, N saturation, and hemlock removal. Finally, we evaluated to  
200 what extent the C stocks and accrual rates in the 1500 ha Harvard Forest represent forests in the  
201 surrounding ecoregion.

202

203

## METHODS

### 204 **Site overview**

205 The ~1500 ha Harvard Forest is in the New England Upland physiographic region of north-  
206 central Massachusetts (42.5° N, 72.2° W). Elevation across the Harvard Forest ranges from 220  
207 m to 410 m above sea level. Soils are primarily stony, acidic glacial tills that overlay  
208 metamorphic bedrock. The climate is cool and moist; based on data from 1961–1990, July mean  
209 temperature is 20.1 °C, January mean temperature is –6.8 °C, and the 1066 mm average annual  
210 precipitation is distributed evenly throughout the year (Greenland and Kittel 1997).

211

212 Since its establishment in 1907, the Harvard Forest has been a long-term forestry and ecological  
213 research site. It is part of several major research networks including the LTER program, the  
214 National Ecological Observatory Network (NEON), AmeriFlux, and the Forest Global Earth  
215 Observatory (ForestGEO). Research infrastructure includes three eddy-flux towers, a network of

216 phenology observation sites, two gauged headwater streams, a meteorological station, long-term  
217 experiments, permanent plots, and extensive records of land-use history and ecological  
218 dynamics. The research program integrates historical and reconstructive studies, long-term  
219 measurements, large experimental manipulations, and local to regional modeling (Foster and  
220 Aber 2004).

221  
222 Major forest types include oak–maple (*Quercus rubra*–*Acer rubrum*), eastern hemlock (*Tsuga*  
223 *canadensis*), and red maple (*A. rubrum*), with some oak–pine (*Q. rubra*–*Pinus strobus*) stands  
224 and remnant conifer plantations (Motzkin et al. 1999). Many stands contain multiple age cohorts,  
225 but overall forest age as of 2015 was mainly 80–120 years. A few trees exceed 200 years in age.  
226 Nearly all the forests in the region are second-growth as a consequence of repeated harvesting  
227 and agricultural clearing that peaked in the mid-1800s, followed by regional reforestation (Foster  
228 and Aber 2004). In 1938, a major hurricane damaged 70% of the standing timber of the Harvard  
229 Forest. More limited natural disturbances have included a major gypsy moth (*Lymantria dispar*)  
230 outbreak in 1981, ice storms, wind damage, and the recent establishment and spread of the  
231 hemlock woolly adelgid (*Adelges tsugae*, HWA). Recent timber harvesting (1990–2014) rates at  
232 the Harvard Forest averaged 0.4% of the forest land per year, removing an average of  
233 approximately 590 m<sup>3</sup> per year (Harvard Forest Archives). This is a lower frequency of  
234 harvesting disturbance than the surrounding regions (Worcester Plateau and Lower Worcester  
235 Plateau ecoregions), where about 1.4% per year was harvested (mostly at low to moderate  
236 intensity) during 1984–2015 (McDonald et al. 2006, Thompson et al. 2017).

237

### 238 **Data sources**

239 The Harvard Forest has an extensive portfolio of permanent forest plots and experiments, many  
240 with consistent measurements initiated when the LTER program began in 1988 (Fig. 1). Data  
241 sets, including those used in this analysis (Appendix S1: Tables S1 and S2) and associated code,  
242 are freely available via the Environmental Data Initiative Data Portal (see Data Availability).  
243 Unless otherwise noted, we used measurements only from closed-canopy forests. The notable  
244 exception is the use of eddy-covariance data from a recently clear-cut site to understand rates of  
245 C cycling in a rapidly aggrading stand. For the purposes of C budgeting, we excluded data  
246 collected from experimental treatments but retained data from their corresponding control plots.



247 We also compared our C cycle synthesis to published syntheses of global change experiments  
248 based at the Harvard Forest (Fig. 1). See Table 1 for abbreviations and acronyms used in the  
249 paper.

250

### 251 **Climatic and atmospheric data sets**

252 Data for temperature and precipitation from 1964–2015 are available from an on-site  
253 meteorological station. When available, we used meteorological data collected at the three eddy-  
254 flux towers included in this analysis. For variables that were not measured at the towers  
255 themselves (e.g., precipitation), we used the Harvard Forest meteorological station data. We  
256 filled gaps in data series by determining the relationship between the variable of interest and the  
257 same variable measured at other sites, namely the Environmental Measurement Site (EMS),  
258 hemlock (HEM), and clear-cut (CC) flux towers, and the Harvard Forest meteorological station.  
259 We ranked the relationships by quality-of-fit of the regressions and used them to fill gaps in the  
260 master data sets. Meteorological variables used in this analysis include air temperature, soil  
261 temperature at 10 cm (HEM, CC tower site) or 20 cm depth (EMS), photosynthetic photon flux  
262 density, soil water content, vapor pressure deficit, and precipitation.

263

264 To examine temporal trends in other global change factors during the study period, we used  
265 publicly available atmospheric data, including annual mean CO<sub>2</sub> concentration measured at the  
266 Mauna Loa Observatory (Tans and Keeling 2019), ground-level O<sub>3</sub> concentration recorded in  
267 Ware Center, MA, 25 km south of the Harvard Forest (EPA 2019), and total N and SO<sub>4</sub><sup>2-</sup>  
268 deposition observed at the Quabbin Reservoir, 17 km southwest of the Harvard Forest (NADP  
269 2019).

270

### 271 **Plot-based measurements of carbon pools and fluxes**

272 We used measurements of trees, dead wood, litterfall, soil C, fine root biomass, and root  
273 exudates from permanent plot studies and control plots of long-term experiments to estimate  
274 current C stocks and temporal trends in C stocks and fluxes. Plot size and number varied by  
275 project; since the Harvard Forest is the study site, each plot was considered a replicate sample  
276 within the study site, with all units standardized to g C m<sup>-2</sup> (pools) or g C m<sup>-2</sup> yr<sup>-1</sup> (fluxes).  
277 Estimates of C flux used varying numbers of plots for each year, depending on the sample

278 frequency of the different studies. Plots were grouped as “hardwood” (mostly oak–maple, along  
279 with some maple–birch–ash) or “hemlock” based on a cluster analysis (Fig. 1b; R version 3.3.1,  
280 *k*-means function) of the most recent measurement of biomass by species for each plot. We  
281 excluded plots in plantation forests from this synthesis; plantations (mainly *Pinus resinosa*,  
282 *Picea glauca*, and *Picea abies*) are a small and declining component of the Harvard Forest (< 5%  
283 of the land base) and southern New England in general. Pine–oak is another minor forest type at  
284 the Harvard Forest, but none of the plots with tagged trees were of this forest type, so these were  
285 not included in our analyses.

286

### 287 **Trends in live tree biomass (aboveground and coarse roots)**

288 Individual tree measurements from nine studies using repeated measurements from 1988–2015  
289 (115 plots total) were used to characterize live tree C stocks (Appendix S1: Table S3). The  
290 studies varied in plot size (from ~120 m<sup>2</sup> to 3 ha), number of plots (1–60), and measurement  
291 frequency (mostly annual to decadal). The suite of 34 plots (each 314 m<sup>2</sup>) in the EMS tower  
292 footprint were first measured in 1993, and tree growth and mortality have been censused  
293 annually since 1998. Plots from other studies added data for other forest types and locations in  
294 the Harvard Forest. Most of these were censused every 5 or 10 years. One large (2.9 ha) plot has  
295 been censused about every decade since 1969. The minimum tree size included varied by study,  
296 from 2.5 to 10 cm diameter at breast height (DBH). This is a minor source of variation among  
297 studies, because small trees contribute very little to plot-level metrics of C storage and  
298 increment. However, estimates of percent mortality used a common minimum DBH of 10 cm,  
299 since mortality was more frequent in smaller diameter classes (Appendix S1: Fig. S1). Data from  
300 the most recent measure of each plot (varied by project, 2008–2015) were used to calculate  
301 current C storage in aboveground and coarse root biomass. We calculated aboveground  
302 increment, coarse root increment, and mortality using the subset of nine studies (60 plots) that  
303 tracked individual tagged trees and had  $\geq 10$  years of measurements.

304

305 We estimated whole-tree aboveground biomass using species-specific allometric equations (43  
306 species in total, Appendix S1: Table S4). Most of the equations excluded the stump and root  
307 crown and included foliage, but there were some exceptions. We developed new allometric  
308 equations for 14 of the most common species using a Bayesian data analytic approach that

309 ‘fuses’ above-stump biomass equations presented in Jenkins et al. (2004; Dietze 2015). These 14  
310 species represented 88% of the individual live tree measurements in the database (>120,000  
311 measurements total). The biomass of the remaining 29 species was estimated using allometric  
312 equations chosen from a variety of sources based on: a) availability of data for that species, b)  
313 equations developed for the range of diameters represented in our data set, and c) geographic  
314 proximity. We estimated C content as 50% of dry woody biomass for all species. Using  
315 parameters and equations of Jenkins et al. (2003), we estimated coarse root biomass for each tree  
316 based on a proportion of the aboveground biomass that varied based on diameter and species  
317 group. Total tree biomass (aboveground + coarse roots) reported here excludes the stump and  
318 root crown, so is a slight underestimate of this pool.

319

### 320 **Fine litterfall (foliar and non-foliar)**

321 Foliar litterfall was collected in ten different studies (Appendix S1: Table S5). Litterfall of fine,  
322 non-foliar material (e.g., twigs, bark, flowers, acorns, etc.) was reported in four of those studies.  
323 One study reported only total (foliar + non-foliar) litterfall and no study reported branchfall.  
324 Because litterfall was generally collected more than once per year, annual litterfall was  
325 calculated as the total mass of fine litter material collected between August and the subsequent  
326 July. For plots with multiple litter baskets, the mean litterfall per plot was used as the unit of  
327 replication. We measured C content of leaves and it averaged 50% of dry biomass for all species,  
328 so litterfall mass was converted to litterfall C content using a C content of 50%.

329

### 330 **Woody debris and standing dead wood**

331 Coarse (diameter > 7.5 cm) and fine (0.6–7.5 cm) woody debris and standing dead wood were  
332 measured in 4, 4, and 3 studies, respectively (Appendix S1: Table S6), using either the line  
333 transect or fixed-radius plot method (Harmon and Sexton 1996). The data sets used contained  
334 woody debris mass but no information on C content. Thus, to estimate the C content of the dead  
335 wood, we used the percent C content of hemlock coarse woody debris, stumps, and snags  
336 measured by Raymer et al. (2013) and of red oak woody debris published by Currie and  
337 Nadelhoffer (2002). We calculated the mean percent C content of each decay class for conifers  
338 and deciduous trees, and used it to convert dead wood mass into C content for the hardwood and

339 hemlock plots of all studies. For samples in which the decay class was not noted, we used the  
340 average percent C content of the five decay classes.

341

### 342 **Soil carbon**

343 Soil organic C content was the most widely measured belowground C pool. It was measured in  
344 17 studies over a variety of forest types, topography, and drainage conditions (Appendix S1:  
345 Table S7). Organic horizon soil monoliths (of surface area generally  $10 \times 10$ ,  $10 \times 20$ ,  $15 \times 15$ ,  
346 or  $20 \times 20$  cm) and mineral soil cores (5 or 10 cm diameter, collected using a hammer corer or  
347 power auger, respectively) were brought back to the lab. Samples were sieved to remove rocks  
348 and roots, homogenized, and then dried and ground into a fine powder before dry combustion in  
349 an elemental analyzer to determine soil organic C content.

350

351 Most of the measurements were of the organic horizon or the top 15 cm of the mineral soil, but  
352 in eight studies samples were also collected deeper in the mineral soil (Appendix S1: Table S7).  
353 In studies where mineral soil C content was not measured at 15 cm increments (e.g., 10 cm  
354 increments), we estimated the C content of a hypothetical 15 cm-thick soil layer by evaluating  
355 the distribution of C through the soil profile (regressing C content against depth) and  
356 extrapolating the C content of 15 cm-thick soil layers.

357

### 358 **Fine root biomass**

359 Fine root (diameter < 2 mm) biomass and C content were measured in eight studies (Appendix  
360 S1: Table S8). As with mineral-soil C content, most measurements were from the organic  
361 horizon or the top 15 cm of the mineral soil. Only two studies provided deeper measurements in  
362 a hemlock stand, and one in a deciduous stand. Samples were collected using the same  
363 methodology as for soil C content. Roots were picked manually. Most studies did not separate  
364 live and dead roots, so these were pooled together if reported separately. Roots were then  
365 washed, dried, and weighed to obtain the dry root biomass content of the samples. In some  
366 studies, roots were ground into a fine powder and combusted in an elemental analyzer to  
367 determine root percent-C content, which was used to convert root biomass into total root C. For  
368 studies where root biomass was known but not root C content, we used root percent C content  
369 measured in other studies located in the same or other closely located plots to convert biomass to

370 C stock. When C concentration data were unavailable, we used 43% C content as the conversion  
371 factor, the average of the fine root data available.

### 372 **Dissolved organic carbon export**

373 Dissolved organic carbon (DOC) in stream water was measured during one year in Arthur Brook  
374 on the Prospect Hill Tract of the Harvard Forest. Water was sampled ( $n = 125$ ) and DOC  
375 concentration was quantified using a TOC analyzer. The annual export of DOC by the headwater  
376 stream was estimated as the product of DOC concentration and streamflow (Wilson et al. 2013).

377

### 378 **Root exudates**

379 Two studies reported root C exudation (Brzostek et al. 2013, Abramoff and Finzi 2016). In both  
380 cases, exudates were collected using a modified version of the method developed by Phillips et  
381 al. (2008). In brief, live roots were carefully excavated, washed, and incubated overnight in a  
382 moist soil-sand mixture while remaining attached to the tree. Roots were then placed into glass  
383 cuvettes filled with glass beads and a C-free nutrient solution for 24 hours prior to exudate  
384 collection. At the time of collection, the now exudate-containing nutrient solution was extracted  
385 with two additional flushes of C-free nutrient solution to ensure complete recovery of the  
386 exudates. Samples were frozen at  $-20\text{ }^{\circ}\text{C}$  until analysis for organic carbon content on a TOC  
387 analyzer. The daily rate of root exudation was converted to annual fluxes by multiplying the  
388 mean daily flux by the mean number of days in the growing season.

389

### 390 **Correction for rock content**

391 Because the belowground measurements were based on soil samples containing no large rocks,  
392 we corrected the data to account for soil rock volume when not already done for a project. Soil  
393 rock fraction was measured in two  $0.5\text{ m}^3$  pits located in a hemlock stand (Raymer et al. 2013)  
394 and 70 plots from five different studies in deciduous stands (Borken et al. 2006, Lajtha et al.  
395 2014, Frey et al. 2014).

396

### 397 **Aboveground net primary production**

398 Aboveground net primary production (ANPP) was calculated as the sum of aboveground  
399 increments, recruitment, and foliar litterfall for each measurement interval. The biomass  
400 increment of new recruits was based on the biomass of the tree in the first year it grew above the

401 minimum diameter minus the biomass of the tree at the minimum diameter (Clark et al. 2001).  
402 Any growth of trees that died between two consecutive measurements was not included. We  
403 used total litterfall from the five studies with > 5 years of total (foliar + non-foliar) annual  
404 litterfall measurements. As is true for most studies in forested ecosystems, ANPP is likely  
405 underestimated by excluding the following components: branch turnover, woody increment and  
406 turnover of shrub and herbaceous vegetation, reductions in litterfall-measured foliar turnover due  
407 to herbivory and possibly some decomposition in the baskets, and changes in non-structural  
408 carbohydrates (Clark et al. 2001, Chapin et al. 2006, Ouimette et al. 2018). None of the plots  
409 included in the analysis was subject to timber harvest during 1992–2015 (although data from an  
410 eddy-flux tower sited in a recently harvested site is part of this overall study), so removal by  
411 timber harvest was not a flux considered in the plot-based ANPP calculations.

412  
413 We examined trends over time for the components of ANPP in the suite of hardwood plots for  
414 the period 1998–2014, and in the suite of hemlock plots for the period 2005–2014. In addition to  
415 the combined analysis of ANPP across studies, we examined annual woody biomass increment  
416 for a longer period, 1960–2011, using tree-ring analysis in two hardwood stands on the Prospect  
417 Hill tract. All trees  $\geq 10$  cm DBH were surveyed and cored in five 13 m radius (531 m<sup>2</sup>) plots  
418 (two in one stand, and three in the other). We calculated annual biomass increment for each stand  
419 and then averaged those results to get annual biomass increment. For detailed methods see Dye  
420 et al. (2016). The correlation between growth and climate for *Quercus rubra* and *Acer rubrum*,  
421 the two species producing the most biomass in these plots, was calculated using annual radial  
422 growth indices and monthly climatic variables from prior June through current August from  
423 1920–2012. The ARSTAN chronology was used for this analysis of tree sensitivity to climate  
424 (Cook and Krusic 2005).

425

### 426 **Belowground net primary production**

427 Belowground net primary production (BNPP) was calculated as the sum of fine and coarse root  
428 production, fine root turnover, and root exudation. There are three published estimates of fine  
429 root production plus turnover (i.e., root NPP) for oak-dominated hardwood stands at the Harvard  
430 Forest. Gaudinski et al. (2010) used radiocarbon data to estimate fine root NPP at 72 g C m<sup>-2</sup> yr<sup>-1</sup>.  
431 McClaugherty et al. (1982) used sequential coring to estimate fine root NPP at 270 g C m<sup>-2</sup> yr<sup>-1</sup>

432 (assuming 50% C content). Abramoff and Finzi (2016) used minirhizotrons to estimate fine root  
433 NPP and turnover time, which we applied to the far broader data set of fine root biomass  
434 available in this paper. In particular, fine root turnover time ( $FR_{\text{turnover time}}$ , yr) was estimated for  
435 the hemlock and hardwood stands by dividing the mean fine root biomass ( $FR_{\text{mass}}$ , g C m<sup>-2</sup>) by  
436 fine root production ( $FR_{\text{production}}$ , g C m<sup>-2</sup> yr<sup>-1</sup>) estimated from minirhizotrons. For the hemlock  
437 stand,  $FR_{\text{turnover time}}$  was calculated using  $FR_{\text{production}}$  values for 2012, before the hemlock started  
438 declining in vigor because of the hemlock woolly adelgid infestation. In the hardwood stand, the  
439 installation of 6 out of 10 minirhizotron tubes in the fall of 2012 might have increased root  
440 growth rates in subsequent years due to the severing of roots during tube placement. Thus, to  
441 minimize the potential for overestimation,  $FR_{\text{turnover time}}$  was calculated using  $FR_{\text{production}}$  values  
442 for 2014, the second year after tube installation and the most recent data available. Abramoff and  
443 Finzi (2016) estimated fine root turnover times for oak and hemlock of  $1.25 \pm 1.40$  yr and  $2.51 \pm$   
444  $1.88$  yr, respectively. Fine root NPP was then estimated as fine root biomass divided by turnover  
445 (pool / flux method, Schlesinger and Bernhardt 2013). This results in estimates of  $333 \pm 385$  g C  
446 m<sup>-2</sup> yr<sup>-1</sup> and  $218 \pm 174$  g C m<sup>-2</sup> yr<sup>-1</sup> for oak- and hemlock-dominated forests, respectively.

447  
448 Unfortunately, there is no simple or straightforward method for determining which of the  
449 estimates is closest to the true value (Strand et al. 2008, but see Tierney and Fahey 2002). The  
450 minirhizotron study reported here is particularly good at observing the production of fast-  
451 turnover fine roots but is sensitive to the amount of time since minirhizotron tubes were installed  
452 and technical considerations related to depth of view and root architecture to extrapolate to units  
453 of g C m<sup>-2</sup> yr<sup>-1</sup>. The sequential coring technique can provide time-resolved estimates of root  
454 biomass and root production but is likely to miss the population of roots that were produced and  
455 turned over between the time soil cores are collected (c.f., Fahey and Hughes 1994). It also  
456 includes substantial spatial variability in its estimate because one cannot sample the same  
457 location more than once. Radiocarbon provides very precise estimates of root age and turnover  
458 times but may be biased by the assumption of a constant probability of root mortality regardless  
459 of age or order (Tierney and Fahey 2002), and stored or recycled carbohydrates (i.e., “older” C)  
460 that may contribute to the production of roots years after the C was fixed. No one method works  
461 perfectly for estimating fine root production. Therefore, in this study we chose to present the  
462 average rate of fine root NPP from three studies.

463 **Soil respiration**

464 Soil respiration ( $R_s$ ) has been measured at the Harvard Forest using a combination of manual and  
465 automated soil respiration chambers for over 20 years. We previously published a synthesis of >  
466 100,000 observations of soil respiration measurements collected through 2010 at the Harvard  
467 Forest (Giasson et al. 2013). For this paper, we extended this data set through 2015 using an  
468 empirical function relating  $R_s$  to soil temperature (Fig. A4 in Giasson et al. 2013).

469  
470 **Eddy covariance measurements**

471 Ecosystem-scale  $\text{CO}_2$  fluxes have been measured continuously since 1992 at the Harvard  
472 Forest's EMS tower, since 2004 at the HEM tower, and since 2009 at the CC tower using the  
473 eddy covariance (EC) technique. The EMS tower samples from a mosaic of oak–maple stands  
474 established between 1900–1945 with small components of eastern hemlock, white pine (*Pinus*  
475 *strobus*), planted red pine (*Pinus resinosa*), and a shrub swamp (Urbanski et al. 2007). Most of  
476 the footprint was historically cleared for pasture, with smaller components of permanent woodlot  
477 and historically tilled soils (Motzkin et al. 1999). The HEM tower is located at the northeast  
478 corner of a stand dominated by eastern hemlock 100–230 years old and large white pine (Hadley  
479 and Schedlbauer 2002, Hadley et al. 2008). The sector from  $180^\circ$  to  $270^\circ$  overlaps the hemlock-  
480 dominated stand. Most of the forest in the hemlock sector has never been cleared for agriculture  
481 but was used as a woodlot during the 1700s and 1800s and was subject to partial harvests into the  
482 20<sup>th</sup> century (Foster et al. 1992). The sector from  $270^\circ$ – $180^\circ$  includes stands of oak and maple, a  
483 red pine plantation, and a large forested swamp. Flux data are separated into hemlock and non-  
484 hemlock based on wind direction being from the hemlock sector or not. Defoliation of hemlock  
485 by HWA was underway by 2012 (Kim et al. 2017). The CC tower is located in an early  
486 successional hardwood stand. Formerly a white and Norway spruce (*Picea glauca* and *Picea*  
487 *abies*) plantation where native hardwood trees had grown into gaps (Williams et al. 2013), an  
488 area roughly  $200 \times 400$  m, which encompasses most of the flux tower footprint, was harvested in  
489 the fall of 2008. All trees were cut except for a few hardwood seed trees.

490  
491 In this study, we analyzed 24 complete years of data (1992–2015) from the EMS tower, 11  
492 complete years (2005–2015) from the HEM tower, and 6 complete years of data (2010–2015)  
493 from the CC tower. EC towers measure net ecosystem exchange (NEE), which is the difference



494 between total ecosystem respiration ( $R_e$ ) and photosynthesis that we refer to as gross primary  
495 production (GPP):

$$496 \quad NEE = R_e - GPP \quad \text{Eq. 1}$$

497  
498 NEE is reported with respect to a vertical coordinate defined as positive upward so that negative  
499 values of NEE are fluxes of C from the atmosphere to the land surface and as such calculates  
500 gains or loss of C from the atmospheric pool. This analysis is interested in gains or losses of C  
501 from the forest itself, so we present the eddy-covariance fluxes using the opposite sign  
502 convention, which are hereafter referred to as net ecosystem production (NEP):

$$503 \quad NEP = -NEE = GPP - R_e \quad \text{Eq. 2}$$

504  
505 Data collections invariably include measurement gaps owing to unfavorable meteorological  
506 conditions, instrument calibrations, or malfunctions. Hence, it is standard to gap-fill data sets  
507 based on well-established numerical methods (Falge et al. 2001, Reichstein et al. 2005) in order  
508 to integrate fluxes to annual sums. All the approaches used here are based on response functions  
509 relating respiration to temperature and GPP to light, and excluding data during periods that are  
510 too calm ( $u^*$  filter) to generate reliable flux measurements. Analysis of component fluxes to  
511 environmental variables include only periods when data series were intact and not subject to gap  
512 filling.

513  
514 In this study, we used eddy-covariance data series with the gaps filled by the principal  
515 investigator (PI); these data sets are available on the Harvard Forest Data Archive website and  
516 are referred herein as “PI-preferred”. Gaps in the EMS-tower NEE data set represented 59% of  
517 the data and were filled using the algorithm developed by Urbanski et al. (2007). Data from the  
518 CC tower contained nearly 72% of gaps which were gap-filled following a marginal distribution  
519 sampling method. Briefly, biweekly mean half-hourly estimates were calculated and assigned to  
520 missing values or low quality-control values. If gaps were still persistent, biweekly mean half-  
521 hourly values averaged from one year prior to one year after a particular gap of concern were  
522 used to fill the gap. NEE was then partitioned into  $R_e$  and GPP following the approach of  
523 Reichstein et al. (2005). The NEE series for the HEM tower contained only data from 180° to  
524 270°, the region of hemlock dominance. The series therefore contained ~70% gaps. Most of the

525 2004–2007 HEM data, with the main exception of two approximately two-month-long gaps,  
526 were gap-filled and partitioned by the PI using non-linear regression (Hadley et al. 2008). We  
527 filled the remaining gaps and completed the partitioning for 2008–2015 using the Fluxnet-  
528 Canada Research Network (FCRN) gap-filling procedure (Barr et al. 2004, Amiro et al. 2006)  
529 with the same  $u^*$  threshold estimated by the PI and used to fill gaps in 2004–2007 data. That  
530 method gave good agreement with PI-gap-filled data (Giasson et al. 2013). For both the EC and  
531  $R_s$  data sets, we used the gap-filled half-hourly or hourly fluxes to calculate daily and monthly  
532 fluxes. We also calculated annual sums based on “ecological years” beginning on 1 November,  
533 the transition to winter. We estimated aboveground respiration ( $R_{\text{above}}$ ) as the difference between  
534 EC-based  $R_e$  and chamber-based  $R_s$ .

535  
536 Furthermore, we used two different gap-filling and partitioning algorithms to fill all gaps in the  
537 three sites’ NEE data series and partition them into NEP, GPP, and  $R_e$ . This allowed a common  
538 comparison among annual NEP, GPP, and  $R_e$  totals of the three sites and to the PI-preferred  
539 values. First, we used the REddyProc R package V1.0.0 (Reichstein et al. 2016), which uses a  
540 seasonally-varying  $u^*$  threshold estimated with the procedure developed by Papale et al. (2006).  
541 Second, we filled the same gaps using the FCRN gap-filling procedure (Barr et al. 2004, Amiro  
542 et al. 2006) with the same seasonally varying  $u^*$  threshold estimated following Papale et al.  
543 (2006). The choice of the  $u^*$  threshold is the largest source of uncertainty in eddy-covariance  
544 data series (Ellison et al. 2006, Papale et al. 2006). Thus, for both the REddyProc and FCRN  
545 algorithms, we estimated this uncertainty by repeating the  $u^*$  threshold estimation 200 times on a  
546 bootstrapped sample. We reported the uncertainty as the 2.5% and 97.5% quantiles of the  
547 bootstrapped sample.

548

#### 549 **Autotrophic and heterotrophic respiration**

550 Autotrophic respiration ( $R_a$ ), the C respired by vegetation, was calculated as the difference  
551 between GPP, NPP and soil C sequestration. Root respiration ( $R_r$ ) was calculated as the  
552 difference between  $R_a$  and  $R_{\text{above}}$ . Heterotrophic respiration, the C emitted by soil microbes and  
553 fauna, was calculated as the difference between soil respiration ( $R_s$ ) and  $R_r$ .

554

555 **GPP response to light**

556 To study interannual variations in whole-canopy photosynthetic rates, we characterized canopy-  
557 scale light-use efficiency (LUE) during the height of the growing season. Non-gap-filled GPP  
558 was plotted as a function of PPFD from July 1 to July 31 of a given calendar year. We fitted a  
559 rectangular hyperbola function to estimate light-response curve parameters:

560 
$$GPP = \frac{\alpha A_{\max} PPFD}{\alpha PPFD + A_{\max}} \quad \text{Eq. 3}$$

561 where  $\alpha$  is the apparent quantum yield ( $\text{mol mol}^{-1}$ ) and  $A_{\max}$  is the ecosystem photosynthetic  
562 capacity ( $\mu\text{mol C m}^{-2} \text{s}^{-1}$ ).

563

564 **Plant area index**

565 Plant area index (PAI) was measured within the EMS and HEM flux tower footprints using a  
566 LAI-2000 Plant Canopy Analyzer (LI-COR, Inc., Lincoln, NE, USA). The data are reported as  
567 PAI rather than leaf area index because they include woody material. Within the EMS tower  
568 footprint, PAI was measured in the biometric inventory plots in 1998–1999 and 2005–2015. It  
569 was measured at least monthly in mid-summer and more frequently in spring and fall during leaf  
570 out and senescence. Within the HEM tower footprint, PAI was measured each August in 2008–  
571 2009 and 2012–2016 in 12 plots. At the CC site, leaf area index (LAI, which excludes woody  
572 biomass) was measured as described in Khomik et al. (2014). From 2009–2012, LAI at the CC  
573 site was measured by destructively sampling all green leaves on representative individuals of  
574 dominant species, scanning the area of each leaf with a LI-3000 leaf area meter (LI-COR, Inc.,  
575 Lincoln, NE, USA), and scaling the total leaf area per square meter of each species by the areal  
576 coverage of each species measured with the line-intercept method. In 2013, CC-site LAI was  
577 measured with a ceptometer (LI-191, LI-COR, Inc., Lincoln, NE, USA). We converted the CC-  
578 site LAI to PAI using a site-specific conversion factor of 1.22 on the tree and shrub portions of  
579 total LAI.

580

581 **Spring and autumn phenology dates**

582 We estimated the duration of the growing season following the approach of Keenan et al. (2014).  
583 First, we used singular spectrum analysis to smooth the daily NEP data from the EMS and HEM  
584 towers. We then determined the maximum daily NEP for each year from the smoothed time

585 series and calculated the mean maximum daily NEP for each site. We defined the onset of the  
586 growing season as the first day of the year when daily NEP exceeded 30% of the mean  
587 maximum daily NEP (Richardson et al. 2010, Keenan et al. 2014). Similarly, the last day of the  
588 growing season was defined by the calendar day when NEP fell below this threshold.

589  
590 We also used a long-term (1990–present) data set of phenological observations recorded at the  
591 Harvard Forest (O’Keefe 2015) to estimate the date of bud break (first day when at least 50% of  
592 the buds on a tree had leaves), full leaf out (90% of the leaves on a tree reached at least 95% of  
593 their final size), and leaf abscission (leaf coloration; the day when at least 20% of the leaves on a  
594 tree had changed color). We calculated the average date of occurrence of each phenological  
595 event for four red oak trees and five red maples, deemed representative of the EMS-tower  
596 footprint, or for five hemlock trees, representing the HEM-tower footprint, and averaged the  
597 results across years (1992–2014).

598

### 599 **Change over time in aboveground and soil carbon stocks**

600 We examined the C stocks in live tree biomass and deadwood for trends over time. Changes in  
601 live tree biomass were estimated as plot-level aboveground growth and recruitment minus  
602 mortality. Changes in deadwood were examined in the few studies with repeated measurements  
603 of downed and standing dead wood. We also examined the mortality estimates for trends in  
604 mortality inputs over time. Finally, we tested for change over time in mineral soil C content in  
605 the one study (42 plots) that had repeated measures of soil C over time (1992 and 2013); data for  
606 only the 0–15 cm mineral soil layer were available. The soil C stock data included in this  
607 analysis was supplemented by published estimates of soil C turnover at the Harvard Forest based  
608 on <sup>14</sup>C measurements (Gaudinski et al. 2000, Sierra et al. 2012, McFarlane et al. 2013).

609

### 610 **Comparison to global change experiments**

611 We compared trends in C fluxes from observational studies to published results from three global  
612 change experiments at the Harvard Forest: the Prospect Hill Soil Warming Experiment  
613 (established 1990; Melillo et al. 2017), the Chronic Nitrogen Amendment Study (established  
614 1988; Aber et al. 1989, Frey et al. 2014), and the Hemlock Removal Experiment (established  
615 2004; Ellison et al. 2010, Orwig et al. 2013). We updated data from the Hemlock Removal

616 Experiment that were presented in Orwig et al. (2013) with newer data for litterfall (Barker  
617 Plotkin 2017), live biomass (Ellison and Barker Plotkin 2015), and coarse woody debris (Ellison  
618 and Barker Plotkin 2018).

619

## 620 **Regional comparisons**

621 We evaluated the degree to which forests at the Harvard Forest represent those of the  
622 surrounding landscape (Fig. 2) in terms of: 1) GPP, and 2) aboveground biomass stocks. Zhou et  
623 al. (2018) estimated GPP for the Harvard Forest and the surrounding 165 km<sup>2</sup> area using the  
624 PnET-II ecosystem model. After validation of modeled GPP with estimates from the Harvard  
625 Forest EMS tower, the model was run spatially using remotely-sensed estimates of foliar %N for  
626 the Harvard Forest and the surrounding 11 × 15 km area. This area was defined by a 2003  
627 aircraft data acquisition from NASA's Airborne Visible / Infrared Imaging Spectrometer  
628 (AVIRIS), which was used to generate estimates of foliar %N (Ollinger et al. 2008). Foliar %N  
629 is a critical input to PnET-II because it determines photosynthetic capacity (Aber et al. 1996).

630

631 We compared field-measured aboveground biomass stocks from the Harvard Forest with  
632 estimates obtained from the U.S. Forest Service's Forest Inventory and Analysis (FIA) plot  
633 network. There were only 9 FIA plots in the 11 × 15 km area used for the GPP comparison,  
634 which showed a mean aboveground C of 7,600 g C m<sup>-2</sup>. Given the small sample size, we also  
635 used FIA data from 184 plots within the two adjoining U.S. EPA Level IV Ecoregions that  
636 surround the Harvard Forest (Fig. 2; 58g and 59b; Griffith et al. 2009). Only plots that had not  
637 been subject to harvest within the past remeasurement period (ca. 5 years) were included,  
638 although the effects of timber harvesting over the past 5–20 years would be apparent in the  
639 biomass estimates from these plots.

640

## 641 **Statistical analyses**

642 Calculations and statistical analyses were made using R version 3.3.1 and MATLAB R2017b.  
643 The standard deviation (SD) of the mean we presented (e.g., Tables 2–4) are the standard  
644 variation of the mean across all plots from all studies and all measurement years. When adding  
645 different components, each with an error term, we propagated the errors such as  $SD = \sqrt{SD_1^2$   
646  $+ SD_2^2 + \dots + SD_n^2}$ . We used a two-sample t-test to determine if C pools and fluxes were

647 significantly different between the hemlock and hardwood stands (Tables 2, 3) or between the  
648 HEM and EMS tower sites (Table 4). We used linear models (lm function, R Core Team 2016)  
649 to examine components of NPP and NEP for trends over time. We used nonlinear least square  
650 regression in Matlab R2017b to fit light-response curves (Eq. 3).

651

652

## RESULTS

### 653 Climate and atmospheric trends

654 Climate data indicated trends of increasing temperature and precipitation (Fig. 3a, b) at the  
655 Harvard Forest during the study period (1992–2015). The trends included increases in mean  
656 annual air temperature (MAT;  $+0.05\text{ }^{\circ}\text{C yr}^{-1}$ ;  $p = 0.0134$ ) as well as in individual seasons. Air  
657 temperature increased significantly in April–June ( $0.07\text{ }^{\circ}\text{C yr}^{-1}$ ;  $p = 0.0038$ ), in September–  
658 November ( $0.08\text{ }^{\circ}\text{C yr}^{-1}$ ;  $p = 0.0014$ ), and in the April–September periods ( $0.08\text{ }^{\circ}\text{C yr}^{-1}$ ;  $p =$   
659  $0.0009$ ). Although the 1992–2015 increase in mean annual precipitation through time was not  
660 statistically significant (MAP;  $+7.4\text{ mm yr}^{-1}$ ;  $p = 0.2500$ ), there were significant changes in total  
661 precipitation during the non-winter months. Precipitation from May to October increased by an  
662 average of  $+7.9\text{ mm yr}^{-1}$  ( $p = 0.0435$ ).

663

664 When considering the 52-year record from the Harvard Forest meteorological station (1964–  
665 2015), we detected significant trends in mean annual air temperature ( $+0.02\text{ }^{\circ}\text{C yr}^{-1}$ ;  $p < 0.001$ ;  
666 Fig. 3a) and precipitation ( $+6.9\text{ mm yr}^{-1}$ ;  $p < 0.001$ ; Fig. 3b). The rates of increase in seasonal  
667 mean air temperature and precipitation were smaller over the 1964–2015 record than over the  
668 last two decades (1992–2015), with increases in air temperature of  $0.02\text{ }^{\circ}\text{C yr}^{-1}$  in April–June ( $p$   
669  $= 0.0021$ ),  $0.03\text{ }^{\circ}\text{C yr}^{-1}$  in September–November ( $p = 0.0011$ ), and  $0.03\text{ }^{\circ}\text{C yr}^{-1}$  throughout the  
670 growing season (April–September,  $p < 0.0001$ ) while May–October precipitation increased an  
671 average of  $+5.4\text{ mm yr}^{-1}$  ( $p < 0.0001$ ). Over the 1964–2015 period, the increase in precipitation  
672 at the Harvard Forest was larger than that reported for the entire central Massachusetts region  
673 ( $+3.7\text{ mm yr}^{-1}$ ) whereas the increase in temperature was  $0.01\text{ }^{\circ}\text{C yr}^{-1}$  smaller (SRCC 2019).

674

675 The atmospheric  $\text{CO}_2$  concentration measured at the Mauna Loa Observatory has been increasing  
676 by  $1.52 \pm 0.02\text{ ppm yr}^{-1}$  since 1959 ( $p < 0.0001$ ), a trend that rose to  $1.96 \pm 0.02\text{ ppm yr}^{-1}$  during  
677 the study period ( $p < 0.0001$ ; Fig. 3c). A decreasing trend ( $p < 0.0001$ ) in ground-level ozone

678 concentration has been observed at a U.S. Environmental Protection Agency monitoring site  
679 located in a rural setting 25 km south of the Harvard Forest. O<sub>3</sub> concentration decreased by 18%  
680 between 1981 and 2015 and by the same percentage between 1992 and 2015 (Fig. 3d). Similarly,  
681 measured total N and SO<sub>4</sub><sup>2-</sup> deposition at the Quabbin Reservoir measurement station of the  
682 National Atmospheric Deposition Program, located 17 km southwest of the Harvard Forest,  
683 followed decreasing trends over the past several decades ( $p < 0.0001$  and  $p = 0.0002$ ,  
684 respectively). Total N deposition decreased by 41% between 1982 and 2015 (Fig. 3e) while  
685 SO<sub>4</sub><sup>2-</sup> deposition declined by 75% over the same period (Fig. 3f). Total N and SO<sub>4</sub><sup>2-</sup> deposition  
686 decreased by 45 % and 71% between 1992 and 2015, respectively.

687

### 688 **Changes in forest species composition and biomass**

689 The Harvard Forest has accrued woody biomass as the forest recovered from past agricultural  
690 land use, timber harvest, and hurricane damage. Measurements in 1937, 1992, and 2013 of 60  
691 plots distributed across the Prospect Hill Tract (Fig. 1b) show that red oak represented only 12%  
692 of the forest biomass in 1937 but came to dominate forest-wide woody biomass (Fig. 4a). In  
693 1937, white pine comprised 38% of total biomass at the Harvard Forest (Fig. 4a), but much of  
694 this was blown down in a major hurricane in 1938 and salvage-logged. We observed modest  
695 shifts in species composition during the focal study period (1992–2013). Red oak increased its  
696 share of total biomass from 30% in 1992 to 34% in 2013, whereas red maple decreased from  
697 17% to 14% of total biomass. From 1992 to 2013, white pine and hemlock each maintained  
698 about 18% of total biomass. Tree-ring data indicate that red oak biomass increment has  
699 dominated total forest growth since at least 1960 (Fig. 4b), and red oak's contribution to total  
700 biomass increment increased about 5% from 1992–2012 ( $p = 0.003$ ).

701

### 702 **Carbon pools**

703 Ecosystem C stock averaged  $34,600 \pm 5,400$  (mean  $\pm$  SD) and  $29,600 \pm 4,700$  g C m<sup>-2</sup> in  
704 hemlock and hardwood stands, respectively (Table 2). Of this, 44% was in soil C pools to a  
705 depth of 45 cm, 40% was in live aboveground biomass, ~6% was in woody debris, and ~10%  
706 was in root biomass in both stand types. Aboveground live biomass, fine woody debris, coarse  
707 and fine roots, and C in the organic horizon and 45 cm deep in the mineral soil were all

708 significantly greater in hemlock than in hardwood stands (Table 2). The only C pool that was  
709 significantly larger in hardwood stands was coarse woody debris.

710

711 C stocks for individual research projects are summarized for live trees (aboveground plus coarse  
712 roots), deadwood, soil, and fine roots in Supplemental Tables S3, S6, S7, and S8, respectively.

713

#### 714 **Carbon fluxes**

##### 715 *NPP*

716 Annual NPP for hemlock- and hardwood-dominated forests averaged  $746 \pm 239 \text{ g C m}^{-2} \text{ yr}^{-1}$  and  
717  $733 \pm 197 \text{ g C m}^{-2} \text{ yr}^{-1}$ , respectively (Table 3). ANPP was ~54% of NPP, with foliage production  
718 representing 50–60% of ANPP. BNPP was  $349 \pm 196 \text{ g C m}^{-2} \text{ yr}^{-1}$  and  $332 \pm 149 \text{ g C m}^{-2} \text{ yr}^{-1}$  in  
719 the hemlock- and hardwood-dominated forests, respectively. Root NPP accounted for  $\geq 72\%$  of  
720 BNPP with the remaining 21–28% accounted for by root exudation (Table 3). For the subset of  
721 plots surrounding the HEM and EMS tower sites, NPP and its distribution above- and below-  
722 ground were similar to the forest as a whole (Table 4). For brevity, subtle distinctions between  
723 tower plots and the entire data set are not described in the text (but compare Table 3 with Table  
724 4).

725

726 For the period 1998–2014, mean annual aboveground biomass increment was  $200 \pm 118 \text{ g C m}^{-2}$   
727  $\text{yr}^{-1}$  for hardwood-dominated plots (Table 3). Aboveground biomass increment in the hemlock-  
728 dominated plots averaged  $166 \pm 99 \text{ g C m}^{-2} \text{ yr}^{-1}$ . Aboveground biomass increment, based on  
729 allometric equations, included both woody and foliar increments, whereas foliage production  
730 was measured separately. Nearly all aboveground biomass accrued on existing stems, as  
731 recruitment of new trees was  $< 1\%$  of aboveground biomass increment in all the undisturbed  
732 permanent-plot studies.

733

734 Total litterfall (a proxy for foliar production) averaged  $201 \pm 51 \text{ g C m}^{-2} \text{ yr}^{-1}$  for hardwood plots  
735 and  $231 \pm 94 \text{ g C m}^{-2} \text{ yr}^{-1}$  for hemlock plots. Litterfall was the only C flux that was significantly  
736 different between the forest types (Table 3). It was also significantly greater at the HEM than at  
737 the EMS site (Table 4).

738



739 For the hardwood plots, both biomass increment and annual litterfall increased over the period  
740 1998–2014 (Fig. 5a, b). Biomass increment was  $168 \text{ g C m}^{-2} \text{ yr}^{-1}$  in 1998 and increased  $7.8 \text{ g C}$   
741  $\text{m}^{-2} \text{ yr}^{-1}$  (SE of slope = 1.22; lm, aboveground and coarse root increment~year,  $F_{1,506} = 40.7$ ,  $p <$   
742  $0.05$ ). Foliar litterfall was  $136 \text{ g C m}^{-2} \text{ yr}^{-1}$  in 1998 and increased  $2.26 \text{ g C m}^{-2} \text{ yr}^{-1}$  (SE of slope =  
743  $0.37$ ; lm, litterfall~year,  $F_{1,699} = 37.7$ ,  $p < 0.05$ ). For the period 2000–2014 (total litterfall data,  
744 including foliar and woody components, was not available prior to 2000), NPP (excluding fine  
745 roots and root exudates) increased at a rate of  $\sim 9.2 \text{ g C m}^{-2} \text{ yr}^{-1}$  from a modeled starting value of  
746  $372 \text{ g C m}^{-2} \text{ yr}^{-1}$  in 2000 (Fig. 5c; SE of slope = 3.3; lm NPP~year,  $F_{1,13} = 7.7$ ,  $p < 0.05$ ). Over 14  
747 years, NPP of the hardwood stands increased by nearly  $130 \text{ g C m}^{-2}$  or  $\sim 26\%$ . There were fewer  
748 data and years of measurement for hemlock-dominated plots. No trends over time were detected  
749 in this forest type (Fig. 6a–c), although decreased foliar production is notable after 2012, as  
750 HWA established at the Harvard Forest and hemlock health began to decline.

751  
752 Annual increment of coarse roots averaged  $34 \pm 20$  and  $38 \pm 23 \text{ g C m}^{-2} \text{ yr}^{-1}$  for hemlock and  
753 hardwood plots, respectively. Fine root production was the largest component of BNPP,  
754 averaging  $218 \pm 174$  and  $225 \pm 136 \text{ g C m}^{-2} \text{ yr}^{-1}$  in hemlock and hardwood plots, respectively  
755 (Table 3). Root exudates contributed  $97 \pm 88$  (hemlock) and  $69 \pm 56 \text{ g C m}^{-2} \text{ yr}^{-1}$  (hardwood).  
756 Neither of these fluxes were sampled consistently enough to estimate change over time.

757

#### 758 *NEP*

759 Eddy-covariance flux estimates of NEP indicated that the EMS and HEM tower sites were net C  
760 sinks of  $298 \pm 153 \text{ g C m}^{-2} \text{ yr}^{-1}$  and  $465 \pm 83 \text{ g C m}^{-2} \text{ yr}^{-1}$ , respectively, before hemlock trees  
761 started declining because of the hemlock woolly adelgid infestation (Table 4, Fig. 7a). At the  
762 EMS site, there was an increase in net C uptake for the period 1992–2008 followed by an abrupt  
763 decline in 2009–2011 and return to near average conditions thereafter (Fig. 7b). For the full EMS  
764 record (1992–2015), there was a non-significant trend of increasing C uptake with time of  $6.9 \text{ g}$   
765  $\text{C m}^{-2} \text{ yr}^{-1}$  ( $p = 0.13$ ). Over 24 years, NEP increased by nearly  $168 \text{ g C m}^{-2}$  or  $\sim 93\%$ .

766

767 NEP during the first 8 years of the 11-year record at the HEM site did not suggest a significant  
768 trend in net C uptake (Fig. 7b). Beginning in 2013, however, there was a steep decline in NEP  
769 following the outbreak of the hemlock woolly adelgid at the site. Cumulative NEP indicated that

770 both tower sites were growing C sinks until 2014 (Fig. 7a), when the HEM tower site turned into  
771 a net C source to the atmosphere on an annual basis (Fig. 7b). The CC site was a strong net C  
772 source in the years immediately after harvest, but it turned into a net C sink on an annual basis in  
773 2013, the fifth year after the disturbance (Fig. 7b). By the end of 2015, seven years after harvest,  
774 the CC site had regained about two thirds of the C it had lost to the atmosphere from on-site  
775 decomposition since the harvest (Fig. 7a) and it is expected to become a C sink in the next 3–5  
776 years barring major disturbance.

777  
778 At the EMS site, GPP ranged from 1,176 to 2,133 g C m<sup>-2</sup> yr<sup>-1</sup> (mean = 1,526 g C m<sup>-2</sup> yr<sup>-1</sup>) and  
779 R<sub>e</sub> ranged from 879 to 2,013 g C m<sup>-2</sup> yr<sup>-1</sup> (mean = 1,228 g C m<sup>-2</sup> yr<sup>-1</sup>; Appendix S1: Table S9).  
780 Soil and total ecosystem respiration were significantly larger at the EMS site than at the HEM  
781 site (Table 4). Partitioning of the eddy-covariance fluxes suggested that GPP increased more  
782 rapidly than R<sub>e</sub> for the period 1992–2008 at the EMS site (Fig. 7c, d), leading to the site's growth  
783 as a C sink. From 2009 to 2016 the EMS site remained a C sink but the size of the sink declined  
784 to the long-term average of ~200–300 g C m<sup>-2</sup> yr<sup>-1</sup> (Fig. 7b). At the HEM site, GPP ranged from  
785 1,083 to 1,614 g C m<sup>-2</sup> yr<sup>-1</sup> (mean = 1,370 g C m<sup>-2</sup> yr<sup>-1</sup>) and R<sub>e</sub> from 843 to 1,228 g C m<sup>-2</sup> yr<sup>-1</sup>  
786 (mean = 1,022 g C m<sup>-2</sup> yr<sup>-1</sup>; Appendix S1: Table S9). Initially, there was no clear temporal trend  
787 in the partitioned fluxes at the HEM tower site (Fig. 7c, d). Beginning in 2011, however, GPP  
788 declined precipitously. At the CC site, GPP ranged from 1,171 to 2,339 g C m<sup>-2</sup> yr<sup>-1</sup> and R<sub>e</sub>  
789 ranged from 1,421 to 2,078 g C m<sup>-2</sup> yr<sup>-1</sup> (Appendix S1: Table S9). GPP generally increased from  
790 year to year while R<sub>e</sub> tended to decrease with time, resulting in a steady increase in NEP (Fig. 7).

791  
792 There was generally good agreement between annual NEP, GPP, and R<sub>e</sub> estimated with the  
793 REddyProc, FCRN, or PI-preferred gap-filling and partitioning algorithms (Appendix S1: Fig.  
794 S2). At times, one of the methods gave results very different from the others (e.g., EMS-NEP in  
795 2005 and 2011 [Appendix S1: Fig. S2a], CC-NEP in 2015 [Appendix S1: Fig. S2g]). This was  
796 usually in years when one or multiple very large gaps (> 40 days) occurred in the data series  
797 during the growing season, or when a larger proportion of data than usual was missing during the  
798 growing season. For example, this was the case in 2005 when a storm caused instrument damage.  
799

800 Interannual variation in mid-summer ecosystem photosynthetic capacity ( $A_{\max}$ ) was > 2-fold at  
801 the three tower sites (Fig. 8a–c, Appendix S1: Fig. S3). At saturating light (> 1000  $\mu\text{mol PPFD}$   
802  $\text{m}^{-2} \text{s}^{-1}$ ) GPP varied between 14 and 49  $\mu\text{mol C m}^{-2} \text{s}^{-1}$  at the EMS site, 5 and 32  $\mu\text{mol C m}^{-2} \text{s}^{-1}$  at  
803 the HEM site, and 9 and 45  $\mu\text{mol C m}^{-2} \text{s}^{-1}$  at the CC site (Fig. 8a–c). There were significant  
804 increases in NEP with LUE (Fig. 9a) and in GPP with  $A_{\max}$  (Fig. 9b). Plant area index varied by  
805  $1 \text{ m}^2 \text{ m}^{-2}$  among years at the EMS site, reflecting variation in summer leaf area, not branch or  
806 stem area as indicated by consistent winter PAI minimum (Fig. 8d). GPP increased linearly with  
807 PAI at the CC tower site (Fig. 8e) while NEP increased with PAI at the EMS site (Fig. 9c). GPP  
808 per unit leaf area was lowest at the HEM tower site (Fig. 8e). Red oak tree-ring increment varied  
809 25% around the 1992–2012 mean, and increment was positively correlated with NEP at the EMS  
810 tower (Fig. 9d).

811  
812 Interannual variation in PAI was not significantly related to interannual variation in  $A_{\max}$ .  
813 Urbanski et al. (2007) found a positive correlation between  $A_{\max}$  and PAI, but for a limited  
814 number of years at the EMS tower site. Data collected since then find high  $A_{\max}$  for both high and  
815 low PAI (Fig. 8, Appendix S1: Fig. S3).

816  
817 There was pronounced seasonality in the respiratory fluxes of C at the Harvard Forest (Fig. 10).  
818 At the EMS tower site,  $R_e$  increased with air temperature in the spring following snowmelt and  
819 was initially driven by aboveground respiration (Fig. 10a). As the soil warmed, peaking an  
820 average of 18 days later than air temperature, belowground respiration came to dominate  $R_e$  and  
821 aboveground respiration declined. The initial increase in  $R_e$  at EMS coincided with increases in  
822 tree diameter (measured every one to two weeks by dendrometer bands) and the deployment of  
823 leaves (Fig. 11). By mid-August, aboveground growth was largely complete and the  
824 preponderance of  $R_e$  was from belowground. A similar phenology was observed at the HEM  
825 tower site (Fig. 10b) with the exception that the spring increase in  $R_e$  was more equitably  
826 distributed between above- and belowground respiration. Interestingly, the autumnal increase of  
827 aboveground respiration at the EMS site was not observed at the HEM tower site.

828  
829 Tree growth was sensitive to interannual and seasonal variation in both temperature and  
830 precipitation. Correlations between monthly temperature and precipitation for red oak and red

831 maple (the two dominant hardwood tree species at the Harvard Forest) are presented in Appendix  
832 S1: Table S10.

833  
834 Annual soil respiration ( $R_s$ ) varied from 628 to 876 g C m<sup>-2</sup> yr<sup>-1</sup> (Appendix S1: Table S9). Mean  
835 annual  $R_s$  was  $738 \pm 42$  g C m<sup>-2</sup> yr<sup>-1</sup> and  $659 \pm 18$  g C m<sup>-2</sup> yr<sup>-1</sup> in hardwood- and hemlock-  
836 dominated forests, respectively. As a percentage of total ecosystem respiration,  $R_s$  accounted for  
837  $63 \pm 9\%$  of the total flux (range: 38–83%, Appendix S1: Table S9).

838  
839 One year of stream DOC measurements showed an export of  $1.72 \pm 0.01$  g C m<sup>-2</sup> yr<sup>-1</sup> over the 24  
840 ha catchment area (Wilson et al. 2013), two orders of magnitude less than NEP.

#### 841 842 **Spring and autumn phenology**

843 The duration of the growing season, the period between the first and last day of the year when  
844 NEP exceeded 30% of the mean maximum daily NEP, increased with time (Fig. 12). At the EMS  
845 site, the length of the growing season increased significantly at a rate of 0.85 d yr<sup>-1</sup> because of  
846 both an earlier onset (0.38 d yr<sup>-1</sup>) and a later end (0.47 d yr<sup>-1</sup>). At the HEM site the length of the  
847 growing season increased, but not statistically significantly so, at a rate of 2.68 d yr<sup>-1</sup> due to an  
848 earlier onset (1.51 d yr<sup>-1</sup>) and a later end (1.17 d yr<sup>-1</sup>).

849  
850 Predictably, there were significant relationships between the timing of the onset and the end of  
851 the growing season, and the magnitude of seasonal NEP at the EMS site (Fig. 13a, c). On  
852 average, an earlier onset of the growing season by one day resulted in a 3.6 g C m<sup>-2</sup> increase in  
853 March–May NEP. Likewise, a one-day delay in the end of the growing season corresponded to a  
854 5.3 g C m<sup>-2</sup> increase in September–November NEP. The relationships between phenology dates  
855 and seasonal NEP were statistically significant in the spring but not in the autumn at the HEM  
856 site (Fig. 13b, d).

857  
858 Based on these data, we calculated the contribution of a longer growing season to ANPP and  
859 NEP at the EMS site as follows. Assuming a growing season length of 120 days per year (Fig.  
860 12) and an annual rate of ANPP of 390 g C m<sup>-2</sup> yr<sup>-1</sup> (Table 4), gives an average daily rate of  
861 ANPP of 3.2 g C m<sup>-2</sup> d<sup>-1</sup>. Given that the growing season length has increased 0.85 days yr<sup>-1</sup> (Fig.

862 12), lengthening of the growing season alone accounts for an additional  $2.7 \text{ g C m}^{-2} \text{ yr}^{-1}$  (i.e.,  
863  $0.85 \times 3.2 \text{ g C m}^{-2} \text{ d}^{-1}$ ) in ANPP. Similarly, NEP at the EMS site was  $298 \pm 153 \text{ g C m}^{-2} \text{ yr}^{-1}$   
864 (Table 4). Given a 120-day growing season, the average daily rate of NEP is  $2.5 \text{ g C m}^{-2} \text{ d}^{-1}$ .  
865 Lengthening of the growing season therefore accounts for an additional  $2.1 \text{ g C m}^{-2} \text{ yr}^{-1}$  in NEP.

### 867 **Decadal changes in C stocks**

868 We documented a net increase in ecosystem C in the live-tree pool for hardwood and hemlock  
869 forests. Based on the nine plot-based studies with multiple tree censuses spanning at least 10  
870 years, net accrual of aboveground C (growth + recruitment – mortality; mean  $\pm$  SD) averaged  
871  $150 \pm 125 \text{ g C m}^{-2} \text{ yr}^{-1}$  for hardwood-dominated plots and  $19 \pm 259 \text{ g C m}^{-2} \text{ yr}^{-1}$  for hemlock-  
872 dominated plots (Appendix S1: Table S3). The background annual mortality rate in the  
873 permanent plots and experimental controls averaged  $1.3 \pm 0.7\%$ . Smaller diameter trees had a  
874 disproportionately high mortality rate (Appendix S1: Fig. S1). Annual C loss to mortality  
875 averaged  $57 \pm 162 \text{ g C m}^{-2} \text{ yr}^{-1}$  for hardwood plots and  $124 \pm 224 \text{ g C m}^{-2} \text{ yr}^{-1}$  for hemlock plots  
876 and showed no trend over time in either forest type (Appendix S1: Fig. S4). No plot in this  
877 analysis experienced timber harvest during the period of study, but averaged across the entire  
878 Harvard Forest's  $\sim 1500$  ha, timber harvest records indicated that removals of C in harvested  
879 trees averaged  $\sim 11 \text{ g C m}^{-2} \text{ yr}^{-1}$  during the period of 1990–2015.

880  
881 We detected minor and equivocal changes over time in deadwood C pools (Appendix S1: Fig.  
882 S5). For all hardwood plots with deadwood measurements combined, there was no trend over  
883 time in standing dead wood stocks. Coarse woody debris (CWD; downed wood  $> 7.5$  cm  
884 diameter) pools began at  $1,411 \pm 241 \text{ g C m}^{-2}$  ( $p < 0.001$ ) and decreased slightly by  $-31.2 \pm 15.7$   
885  $\text{g C m}^{-2} \text{ yr}^{-1}$  ( $p = 0.049$ ). Fine woody debris (FWD; downed wood 0.6–7.5 cm diameter) pools  
886 began at  $112 \pm 38 \text{ g C m}^{-2}$  and increased slightly by  $7.2 \pm 2.5 \text{ g C m}^{-2} \text{ yr}^{-1}$ . For the EMS tower  
887 plots, CWD had a significantly positive slope ( $69 \pm 30 \text{ g C m}^{-2} \text{ yr}^{-1}$ ) in contrast to the overall  
888 hardwood trend, and there were no changes over time in standing deadwood or FWD. Although  
889 we had many one-time measurements of deadwood C pools in hemlock-dominated sites and a  
890 robust estimate of average pools of CWD, FWD, and standing dead wood (Table 2), there were  
891 too few repeated measures of deadwood measurements to examine trends over time for the  
892 hemlock forests overall or at the HEM tower site.

893

894 Nearly all the studies reporting soil C data were from one or two years of study. As a  
895 consequence, only data from the PHOREST plots (mineral soil C content sampled in 1992 and  
896 2013 in 42 plots) could provide information on changes in soil C pools through time. In this data  
897 set, there was no apparent net accrual of soil C through time (Appendix S1: Table S11). For the  
898 period 1992–2013, soil bulk density declined on average  $0.05 \pm 0.15 \text{ g cm}^{-3}$  whereas soil %C  
899 increased on average  $0.50 \pm 2.01\%$  such that the total quantity of C in the soil did not change for  
900 the period 1992–2013 (Appendix S1: Table S11).

901

### 902 **Regional comparisons**

903 Based on FIA plot data, aboveground C in the two ecoregions surrounding the Harvard Forest  
904 ranged from 1,500 to 15,200  $\text{g C m}^{-2}$  with a median of 6,500  $\text{g C m}^{-2}$  (Fig. 2). This is  
905 considerably lower than the median for the Harvard Forest, 11,600  $\text{g C m}^{-2}$ .

906

907 The PnET-II estimate of GPP for the region ranged from 797 to 1,622  $\text{g C m}^{-2} \text{ yr}^{-1}$  with a mean  
908 of 1,324  $\text{g C m}^{-2} \text{ yr}^{-1}$  (Zhou et al. 2018, Fig. 2). Predicted GPP for the Harvard Forest (mean of  
909 1,329  $\text{g C m}^{-2} \text{ yr}^{-1}$ ) did not differ from the region-wide mean. The PnET-II estimate of GPP  
910 closely matched that estimated from the HEM tower fluxes, for the period 2004–2011. For the  
911 EMS tower, mean GPP predicted by the model was 5.6% lower than the tower-based estimate  
912 and the model did not capture the observed trend of increasing GPP for the period 1992–2010  
913 (Zhou et al. 2018).

914

915

## DISCUSSION

916 This work synthesized hundreds of thousands of observations to quantify the C cycle for the  
917 Harvard Forest in central Massachusetts, USA and to place the Harvard Forest within a regional  
918 context. These data, collected at a wide range of temporal and spatial scales, consistently  
919 described undisturbed forests as active C sinks. The climate of the Harvard Forest has  
920 measurably changed with increasing temperature leading to longer growing seasons and higher  
921 precipitation during the growing season. There has also been a continuous increase in  
922 atmospheric  $\text{CO}_2$  concurrent with a decline in ground-level  $\text{O}_3$ , and sulfate and total N  
923 deposition. The results of this study alongside simulation modeling suggest that land-use

924 abandonment at the turn of the last century, a reduction in forest harvesting, and climate and  
925 atmospheric changes drive the slow but steady increase in ecosystem C content (Ollinger et al.  
926 2002, Albani et al. 2006, Thompson et al. 2011, Duveneck et al. 2017).

927  
928 Prior to the outbreak of the hemlock woolly adelgid (HWA), C stocks within hardwood- and  
929 hemlock-dominated stands were not significantly different and nearly equally divided between  
930 soil and biomass pools. Carbon continued to accumulate, with NEP averaging  $298 \pm 153 \text{ g C m}^{-2}$   
931  $\text{yr}^{-1}$  in hardwood stands and  $465 \pm 83 \text{ g C m}^{-2} \text{ yr}^{-1}$  in hemlock stands prior to the widespread  
932 outbreak of HWA in 2013. Since 2013, however, hemlock-dominated stands have become a  
933 source of C to the atmosphere. Whereas direct measurements of soil C stocks showed no change  
934 between 1992 and 2013 (Appendix S1: Table S11), soil radiocarbon studies suggest a small sink  
935 on the order of  $10\text{--}30 \text{ g C m}^{-2} \text{ yr}^{-1}$  (Gaudinski et al. 2000, Sierra et al. 2012).

936  
937 Although climate change for the period of intensive measurements reported here (1992–2015) is  
938 modest compared to predictions for the future, our findings suggest that it has had a discernible  
939 impact on the C cycle. The progressive lengthening and warming of the growing season through  
940 time has increased net C uptake in hardwood stands. This is likely reinforced by increasing  
941 precipitation,  $\text{CO}_2$  fertilization, increases in water-use efficiency (WUE), and changes in  
942 atmospheric deposition (Thomas et al. 2010, Keenan et al. 2013). In hemlock stands, a similar  
943 phenomenon occurred until 2013 when a growing regional HWA population led to increased  
944 hemlock mortality. Invasive insects alongside other major disturbances (e.g., logging, hurricanes,  
945 extreme climate events) are the largest threats to continued atmospheric  $\text{CO}_2$  sequestration at this  
946 site.

947

#### 948 **The present-day carbon cycle**

949 There was a near-equal distribution of total ecosystem C between that in live biomass (~50%)  
950 and the soil to 45 cm depth (~45%) with the remaining ~5% as woody debris (Table 2). The  
951 quantities of C in live aboveground biomass and in soil were similar in hardwood- and hemlock-  
952 dominated plots, but the soil organic horizon in hemlock stands contained  $\sim 1500 \text{ g C m}^{-2}$  more  
953 than that found in the hardwood stands. Root biomass was a small C pool at the Harvard Forest,  
954 comprising ~20% of total biomass and ~10% of total ecosystem C, consistent with an analysis of

955 global temperate forests in which belowground biomass comprised 20–30% of aboveground  
956 biomass (Cairns et al. 1997). It was also consistent with the Hubbard Brook Experimental Forest  
957 in central New Hampshire; there, estimated root biomass was ~21% of total biomass (Fahey et  
958 al. 2005).

959  
960 ANPP at the Harvard Forest averaged 390–430 g C m<sup>-2</sup> yr<sup>-1</sup> and total NPP averaged 680–750 g C  
961 m<sup>-2</sup> yr<sup>-1</sup> (Tables 3, 4). Root NPP (BNPP; coarse roots, fine roots, root exudates) averaged 47%  
962 and 45% of total NPP in hemlock- and hardwood-dominated stands, respectively (Table 3).

963 Thus, roots represent a major portion of NPP at the site. Unlike aboveground C pools, however,  
964 automated measurements and inventories of both root and soil C pools are comparatively scarce  
965 for the Harvard Forest, and indeed most forests. There is therefore great uncertainty in this aspect  
966 of the C budget. The estimates of root NPP in this study are similar, but by no means identical, to  
967 values reported in the literature. For healthy hemlock stands, the only estimate of root NPP is  
968 that reported here and it is based on the work of Abramoff and Finzi (2016). For hardwood  
969 stands, we report root NPP of 332 ± 149 g C m<sup>-2</sup> yr<sup>-1</sup> (Table 3). This is higher than that reported  
970 by McClaugherty et al. (1982; 270 g C m<sup>-2</sup> yr<sup>-1</sup>) and Gaudinski et al. (2010; 72 g C m<sup>-2</sup> yr<sup>-1</sup>).  
971 The substantial variability, particularly the standard deviation of the mean BNPP we report in  
972 Tables 3 and 4, argues that more plots, more samples per plot, and more longitudinal studies are  
973 needed to constrain these values for the Harvard Forest.

974  
975 At present, we estimate that soil C pools are neutral to small sinks for atmospheric CO<sub>2</sub>. There  
976 are, however, only two longitudinal studies of soil C at the Harvard Forest. In the first study  
977 (PHOREST), bulk soil C content was surveyed in 1992 (Mozkin et al. 1999) and again in 2013  
978 (Appendix S1: Table S11). This study showed that small and statistically non-significant  
979 increases in soil C concentration through time were offset by similarly small and non-significant  
980 decreases in soil bulk density such that there was no net change in total soil C in the top 15 cm of  
981 mineral soil in hardwood- (*n* = 31) and hemlock- (*n* = 11) dominated plots. In the second study,  
982 <sup>14</sup>C was used to estimate the turnover time of different soil C pools (litter, humified, mineral-  
983 associated) in well-drained glacial till, the most prevalent soil type at the Harvard Forest  
984 (Gaudinski et al. 2000). Their radiocarbon mass balance estimated a soil-C accrual rate of 10–30  
985 g C m<sup>-2</sup> yr<sup>-1</sup>. This rate may have been more rapid immediately following agricultural



986 abandonment in the late 1800s, but nevertheless this approach suggests that a small C sink  
987 persists in the soil to this day. Adding confidence to the assessment of Gaudinski et al. (2000),  
988 Sierra et al. (2012) resampled the same soil pits and found close agreement with earlier estimates  
989 of C pool sizes, fluxes, and turnover times. Although we cannot be sure that these data apply to  
990 all forest and soil types at the Harvard Forest, the rate of soil C accrual based on radiocarbon is  
991 consistent with data showing generally negligible to small increases in soil organic carbon (SOC)  
992 following agricultural abandonment at the Harvard Forest (Compton and Boone 2000), in central  
993 New England (Hooker and Compton 2003), the Great Lakes region (Morris et al. 2007), and  
994 North American forests more generally (Nave et al. 2013).

995  
996 Resolving the uncertainty in SOC change a century into forest regrowth is a major challenge.  
997 The annual change in SOC, whether positive or negative, is small but the pool of C is large,  
998 making it difficult to detect a significant change. As a case in point, we collected 77 soil samples  
999 (5 cm diam., from the soil surface to 30 cm depth in the mineral soil) from hemlock forests  
1000 surrounding the HEM tower to conduct a power analysis for SOC change in the years to come as  
1001 hemlock declines (Appendix S1: Fig. S6). Using Monte Carlo resampling, we estimated that  
1002 2,919 samples would be required to detect a significant change ( $p < 0.05$ ) for a relatively large  
1003 change in SOC of 150 g C m<sup>-2</sup>. For a more realistic change on the order of 20 g C m<sup>-2</sup> the number  
1004 of samples skyrockets to 164,194. However, the likelihood of detecting small annual changes in  
1005 SOC increases if samples are collected many years from one another. For example, to detect a  
1006 change in SOC of 20 g C m<sup>-2</sup> yr<sup>-1</sup> over the 21 years the PHOREST study has been ongoing would  
1007 require 372 samples for detection at  $p < 0.05$ . Admittedly, this is a formidable soil processing  
1008 challenge, but it is possible with sufficient resources and time.

1009  
1010 In contrast to an inventory-based approach, the benefit of the radiocarbon approach is that it  
1011 integrates information on the ages of C in different pools (i.e., SOC, roots). These ages can then  
1012 be transformed into residence times and fluxes of C in the belowground system (Gaudinski et al.  
1013 2000). The radiocarbon approach does, however, require a number of assumptions to calculate C  
1014 ages, C turnover times, production and consumption of litter inputs, and so on, each of which has  
1015 its own uncertainty. So, it too must be used in combination with other approaches to build a  
1016 comprehensive understanding of belowground C cycling. To this end, the recent establishment of

1017 a belowground C observatory at the Harvard Forest that uses long-term resampling plots coupled  
1018 with an array of measurements (i.e., soil respiration, trenching,  $\Delta^{14}\text{C}$ ,  $\delta^{13}\text{C}$ ) should deepen our  
1019 understanding of the belowground C cycle at this site.

1020

### 1021 **Seasonal and interannual variations in carbon fluxes**

1022 Differences between conifer and hardwood leaf longevity and physiology led to distinct seasonal  
1023 variations in GPP,  $R_e$ , and the DOY the stands became net C sinks (Fig. 10, Appendix S1: Table  
1024 S12). Atmospheric warming during the transition from winter to spring stimulates ecosystem  
1025 respiration in advance of the uptick in photosynthesis in both forest types. However, it was not  
1026 until ~1 July at the EMS tower that carbon uptake balanced the carbon loss from respiration over  
1027 the non-growing season. By contrast, C uptake at the HEM site balanced C loss from the winter  
1028 far earlier, on average April 3 (Appendix S1: Table S12). At the CC site, this balance occurred  
1029 around May 11. The earlier date of net annual C uptake at the HEM site reflects the persistence  
1030 of a live, overwinter canopy that can actively photosynthesize once temperatures are consistently  
1031 above 0 °C (Hadley and Schedlbauer 2002). Although photosynthesis can occur at low  
1032 temperatures, -5 to -11 °C (Burkle and Logan 2003), the data suggest this makes a very minor  
1033 contribution to overall ecosystem C uptake. At the deciduous-dominated EMS and CC sites, GPP  
1034 remained very low throughout the winter, but not necessarily zero because there are some  
1035 conifers within their footprints. The later DOY for net C uptake at the EMS site is also explained  
1036 by the comparatively large winter respiration flux, whose source remains as yet unresolved.

1037

1038 At the EMS site, the springtime lag between the increase in air temperature and the later increase  
1039 in soil temperature resulted in a larger proportion of  $R_e$  derived from aboveground biomass and  
1040 an earlier peak in  $R_e$  compared to  $R_s$  (Fig. 10). There was strong synchrony between  
1041 aboveground respiration, leaf area expansion, and diameter growth from spring until peak LAI  
1042 (Fig. 11). By mid-August, however, aboveground growth was largely complete and the  
1043 preponderance of  $R_e$  was from  $R_s$  until the fall when there was an uptick in aboveground  
1044 respiration that may be related to foliar nutrient retranslocation, foliar senescence, and winter  
1045 hardening (Fig. 11). The phenology of  $R_e$  at the EMS site is consistent with a recent meta-  
1046 analysis demonstrating that root growth lags behind shoot growth in temperate and boreal forests  
1047 (Abramoff and Finzi 2015). The phenology of C fluxes at the HEM tower site were similar to

1048 those at the EMS site with one notable exception:  $R_e$  peaked approximately two weeks later, on  
1049 average, and declined more rapidly thereafter compared to the EMS site (Fig. 10).

1050

1051 The updated eddy-covariance analysis reported here presents a dynamic picture of forest–  
1052 atmosphere C exchanges. In particular, among the flux sites analyzed by Keenan et al. (2013),  
1053 the EMS tower data showed the strongest increase in annual net C uptake. For the 1992 to 2009  
1054 period of their analysis, NEP increased an average of  $23 \text{ g C m}^{-2} \text{ yr}^{-1}$ , resulting in a gain of  $400 \text{ g}$   
1055  $\text{C m}^{-2} \text{ yr}^{-1}$  in NEP in those 18 years. For the 24-year period (1992–2015) analyzed here, average  
1056 annual NEP increased  $6.9 \text{ g C m}^{-2} \text{ yr}^{-1}$ , or about  $168 \text{ g C m}^{-2} \text{ yr}^{-1}$  more uptake in 2015 compared  
1057 to 1992 (Fig. 7b). This brings the annual increase in NEP at the EMS site in line with the other  
1058 sites analyzed by Keenan et al. (2013). Importantly, the long-term trend reported here suggests  
1059 that the rapid increase in NEP between 1998 and 2008 was transient.

1060

1061 Interpretation of the very high NEP from 2004–2008, and very low NEP in 2010–2011 is  
1062 complex. Advances in flux partitioning, including Wehr et al.’s (2016) work using isotopologues  
1063 of  $\text{CO}_2$  at the EMS site can help discern the net balance of photosynthesis and  $R_e$ . However,  
1064 Wehr’s results apply directly only to the period of that study, which encompasses the 2011–2013  
1065 growing seasons. A detailed analysis of the environmental drivers and biotic responses (*sensu*  
1066 Richardson et al. 2007), and how to apply partitioning studies to the full NEE record, is  
1067 underway.

1068

1069 There was large inter-annual variation (50–100%) in maximum canopy photosynthetic rate ( $A_{\text{max}}$ ,  
1070 Fig. 8a–c, Appendix S1: Fig. S3b, Appendix S1: Table S13) and light use efficiency (LUE;  $\alpha$ ,  
1071 Appendix S1: Fig. S3a, Appendix S1: Table S13). At the early-successional CC tower site,  
1072 annual increases in LUE and  $A_{\text{max}}$  were driven by the accrual of leaf area in this rapidly  
1073 aggrading stand (Fig. 8c, e). At the closed-canopy EMS tower site, interannual variations in NEP  
1074 were positively correlated with PAI (Fig. 9c). The slope of this regression line implies that NEP  
1075 increases by  $\sim 280 \text{ g C m}^{-2} \text{ yr}^{-1}$  for every  $1 \text{ m}^2 \text{ m}^{-2}$  increase in PAI, which is the maximum  
1076 variation observed in the data set. We also find that NEP is positively correlated with canopy-  
1077 scale LUE (Fig. 9a), and that GPP is positively correlated with canopy-scale  $A_{\text{max}}$  (Fig. 9b).

1078 These results suggest that plasticity in canopy-scale attributes like photosynthetic rate and leaf

1079 area have a measurable impact on C uptake at this site. However, the causality between  
1080 interannual variations in C fluxes and those of canopy-scale attributes remains unclear. For  
1081 example, do increases in  $A_{\max}$  and PAI drive increases in C uptake or are they the consequence of  
1082 favorable growing conditions and high C uptake, or both?

1083  
1084 Different methods of measuring ecosystem carbon accrual were well correlated, although some  
1085 differences remained. We compared the difference in net ecosystem production assessed by  
1086 tower- and ground-based measurements for the two mature forest types (Table 4). Tower-based  
1087 NEP was higher than plot-based NEP, which corroborates earlier analyses reported by Barford et  
1088 al. (2001). Twenty-four years of data from the hardwood forest site narrowed the difference  
1089 between these two measurement approaches to 36%, whereas the difference was 61% after eight  
1090 years of study of the hemlock forest site. Ecologically, it stands to reason that the difference in  
1091 NEP estimates narrows through time since biomass is produced from a combination of current-  
1092 year and stored photosynthate. With many years of data (i.e., a larger sample size), the  
1093 interannual variations in climate and forest productivity converge towards a mean value whose  
1094 uncertainty declines.

1095

#### 1096 **Stand dynamics and recent global change**

1097 At annual to decadal time scales, neither stand biomass nor rates of NPP are at steady state in the  
1098 mature hardwood-dominated stands at the Harvard Forest. Rather, the stands remain active C  
1099 sinks as they accrue biomass following land-use abandonment and low rates of forest harvest.  
1100 This general pattern of land-use history and ecosystem recovery characterizes temperate forests  
1101 across much of eastern North America (Gough et al. 2016, Nave et al. 2017). At the Harvard  
1102 Forest, NPP also increased by ~26% from 2000 to 2014 (Fig. 5). Both stand dynamics and global  
1103 change likely contribute to the observed NPP increase.

1104

1105 Species composition change, particularly increasing red oak dominance, likely contributed to the  
1106 trend of increasing NPP. Red oak tree-ring increment positively correlated with tower-based  
1107 NEP (Fig. 9d). Maples and birches initially dominated the mixed-species hardwood forests that  
1108 developed after agricultural clearing, after old-field white pine harvest, or the 1938 hurricane.  
1109 Red oak height growth then accelerated and within about 30 years red oak rose to its current

1110 dominance in the canopy (Oliver 1975, 1978, Oliver and Stephens 1977). Red oak relative  
1111 abundance increased from 30% of total biomass in 1992 to 34% in 2013 (Fig. 4a), contributing  
1112 45% of the overall increase in live tree biomass during the study period. Its increasing  
1113 dominance is corroborated by previous, site-specific studies at the Harvard Forest (Fig. 4b;  
1114 Urbanski et al. 2007, Eisen and Barker Plotkin 2015).

1115  
1116 It appears that red oak has an inherently higher growth capacity than the other abundant species  
1117 at the Harvard Forest. Of the major tree species, it has the highest concentration of N in foliage  
1118 and the most rapid rate of net photosynthesis (Bassow and Bazzaz 1997). Red oak also has a high  
1119 water-use efficiency (Turnbull et al. 2002). These ecophysiological traits alongside the fact that  
1120 red oak trees at Harvard Forest have an average diameter larger than that of the other species  
1121 present, likely gives rise to red oak's outsized contribution to NPP and NEP (Lutz et al. 2012,  
1122 Stephenson et al. 2014).

1123  
1124 The majority of the NPP at the Harvard Forest is allocated to the production of fast-cycling C  
1125 pools: leaves (22%), fine roots (29%), and root exudates (8%, Table 4). Leaves and roots have  
1126 high N concentration, so the increase in total tree biomass and NPP implies an increase in N  
1127 uptake through time, or possibly an increase in N-use efficiency (c.f., Finzi et al. 2007). As an  
1128 ectomycorrhizal (ECM) tree species, red oak can access soil N via fungal symbionts. ECM fungi  
1129 produce both oxidative and hydrolytic enzymes that are released into soil (Chalot and Brun  
1130 1998). These enzymes are often within mucopolysaccharides produced by the fungus that are  
1131 reabsorbed after the decomposition of organic matter (Lindahl et al. 2005, Hobbie and Hobbie  
1132 2008). This strategy confers a competitive advantage for N to the ECM trees relative to free-  
1133 living microbes and non-ECM trees (Averill et al. 2014). This suggests that ECM fungal  
1134 association should be added to the list of autecological factors contributing to red oak's  
1135 dominance and high productivity at the Harvard Forest.

1136  
1137 Recent warming trends have altered the rate of C cycling in hardwood- and hemlock-dominated  
1138 stands. At the EMS site, spring is occurring earlier, the onset of fall is occurring later, and the  
1139 length of the growing season is increasing with time (Fig. 12). Such changes have decreased

1140 springtime net C losses because of earlier onset of C uptake (Fig. 13a), increased fall C uptake  
1141 (Fig. 13c), and enhanced NEP through time (Fig. 7b).

1142  
1143 At the EMS site we found that the length of the growing season increased by just under one day  
1144 per year. This means ANPP has increased by  $2.7 \text{ g C m}^{-2} \text{ yr}^{-1}$  (see *Methods* for details of the  
1145 calculation). Since the average annual increase in ANPP was  $9.2 \pm 3.3 \text{ g C m}^{-2} \text{ yr}^{-1}$  (Fig. 5c),  
1146 lengthening of the growing season alone accounts for up to 30% of the observed annual average  
1147 increase in ANPP. A similar calculation is possible for NEP. Here we estimate that lengthening  
1148 of the growing season increases NEP by  $2.1 \text{ g C m}^{-2} \text{ yr}^{-1}$ . Because the average annual increase in  
1149 NEP at the EMS site is  $6.9 \pm 9.0 \text{ g C m}^{-2} \text{ yr}^{-1}$  (Fig. 7b), lengthening of the growing season alone  
1150 also accounts for 30% of the annual increase in NEP.

1151  
1152 The signature of a changing climate on hemlock forest productivity was also in evidence. The  
1153 most important of these is the spread of HWA into the footprint of the Harvard Forest and the  
1154 decline in hemlock (Ellison et al. 2018). The spread of this invasive insect is closely tied to  
1155 climate, with a northward expansion facilitated by warming temperature. Prior to infestation of  
1156 the HEM tower site, however, we observed an earlier onset of springtime, later onset of leaf off  
1157 of the deciduous component of the forest and lengthening of the growing season (Fig. 12b).  
1158 None of these trends was statistically significant because there are fewer years of data available  
1159 at this site (Fig. 12b). Similar to the EMS site, there was a significant relationship of earlier  
1160 spring resulting in greater C uptake at the HEM site (Fig. 13). By contrast, lengthening of the  
1161 growing season in the autumn was negatively, albeit not significantly, correlated with NEP.  
1162 Lengthening of the growing season at the HEM site did not increase net C uptake.

1163  
1164 At the same time that the growing season is lengthening, other global change factors are  
1165 concurrently changing. These include a rise in atmospheric  $\text{CO}_2$ , a decrease in atmospheric  
1166 deposition of N and  $\text{SO}_4^{2-}$ , a decrease in ground-level  $\text{O}_3$  concentrations, and the previously  
1167 discussed increases in temperature and precipitation (Fig. 3). These changes in atmospheric  
1168 chemistry may be collectively important. For example, the declines in total N and  $\text{SO}_4^{2-}$   
1169 deposition, and the increase in the pH of precipitation (*data not shown*) are leading to a gradual  
1170 deacidification of soils and soil water in New England and in Europe (Driscoll et al. 1998,

1171 Stoddard et al. 1999). It seems reasonable to hypothesize that collectively, the accumulated effect  
1172 of all these small but significant global changes may also be contributing to the increase in  
1173 productivity through time (c.f., Fernández-Martínez et al. 2017).

1174  
1175 With specific respect to rising atmospheric CO<sub>2</sub>, the average annual concentration of CO<sub>2</sub> has  
1176 increased 13%, from 356 ppm in 1992 to 401 ppm 2015 (+45 ppm, NOAA 2019). Previous  
1177 research at eddy-covariance sites throughout the northeast correlated increases in NEP over time  
1178 with increases in WUE owing to rising CO<sub>2</sub> (Keenan et al. 2013). Mechanistically, this occurs  
1179 because stomatal aperture can decline with rising CO<sub>2</sub> because of the increasing CO<sub>2</sub>  
1180 concentration gradient between the atmosphere and leaf mesophyll cells. As such, rising CO<sub>2</sub> can  
1181 allow plants to conserve water, maintain photosynthetic rates, and increase the ratio of C fixed to  
1182 water transpired (i.e., WUE; Battipaglia et al. 2013).

1183  
1184 While there are no whole-system CO<sub>2</sub> exposure studies at the Harvard Forest, greenhouse work  
1185 with the dominant species at the forest showed that they are responsive to CO<sub>2</sub> under limiting  
1186 and non-limiting nutrient conditions (Bazzaz and Miao 1992, Miao 1995, Driscoll et al. 1998).  
1187 While a formal study of attribution (*sensu* Bindoff et al. 2013) has not been conducted with  
1188 respect to the CO<sub>2</sub> effect on productivity at the Harvard Forest, Fernández-Martínez et al. (2017)  
1189 suggest a direct CO<sub>2</sub> enhancement of 1% on NEP across eastern North American and European  
1190 forests for the period 1995–2011. Regionally, Ollinger et al. (2002) used the simulation model  
1191 PnET-II to show that rising atmospheric CO<sub>2</sub> and N deposition, alone and in combination, had  
1192 significant, positive effects on northeastern forest productivity. It therefore seems reasonable to  
1193 suggest that rising atmospheric CO<sub>2</sub> is having an effect on C exchange at the Harvard Forest. At  
1194 present, however, we do not have direct, site-specific evidence for a CO<sub>2</sub>-fertilization effect on  
1195 productivity.

1196  
1197 Increasing precipitation over the study period (Fig. 3b) also likely contributed to the observed  
1198 increases in NPP and NEP at the EMS site. Most of the increased precipitation fell during the  
1199 growing season (May–October). Co-analysis of tree rings and climate variables in red oak  
1200 indicates that late-summer precipitation can increase growth, suggesting that even mesic forests  
1201 like the Harvard Forest (Belmecheri et al. 2014), and eastern temperate forests in general, are

1202 sensitive to water availability (Martin-Benito and Pederson 2015, D'Orangeville et al. 2018).  
1203 Regionally, the number of rainless days declined during the past 30 years, suggesting a decline in  
1204 drought conditions (Bishop and Pederson 2015). Our study period was during one of the wettest  
1205 eras of not only the last 500 years (Pederson et al. 2013, 2015), but perhaps of the last 5000+  
1206 years (Shuman and Marsicek 2016, Marlon et al. 2017). Other drivers of carbon dynamics may  
1207 be more apparent during this period of measurement because, relative to the past, the occurrence  
1208 of drought stress has been less frequent.

1209

### 1210 **Comparisons to global change experiments**

1211 Forest regrowth following land-use abandonment is likely the largest contributor to the observed  
1212 C sink at the Harvard Forest during the last century. After that, our findings suggest that climate  
1213 change and other global change drivers have enhanced the C sink in biomass over the last three  
1214 decades. Climate and other global change factors may have had an effect further back in time,  
1215 but prior to 1990 there are fewer systematic measurements of C stocks and fluxes to help us  
1216 assess earlier changes.

1217

1218 The Harvard Forest hosts long-term global change experiments that simulate aspects of climate  
1219 change, atmospheric chemistry change, and the spread of invasive insects. Each of these factors  
1220 affects the C cycle and other ecosystem processes. We compared C-cycle responses from three  
1221 experimental studies—soil warming, N deposition, and hemlock removal—to the observational  
1222 data presented here to provide a broad context within which we can interpret the experimental  
1223 work.

1224

1225 One of the largest uncertainties in the global C cycle is the response of soil C to warming.  
1226 Globally, soils store more C than is present in the Earth's atmosphere and vegetation combined  
1227 (Scharlemann et al. 2014, Jackson et al. 2017), so small changes in soil-C cycling may have a  
1228 large effect on the future climate. Beginning in 1991, soil warming experiments at the Harvard  
1229 Forest heated the soil +5 °C above ambient (Melillo et al. 2002, 2011, 2017). The IPCC's 5<sup>th</sup>  
1230 assessment reported that this level of soil warming would only be achieved under the most  
1231 extreme scenario for climate change, RCP 8.5, in about the year 2140 (Collins et al. 2013). The  
1232 initial results from the longest-running soil warming study at this site found that putative soil C



1233 losses ranged from 90 to 180 g C m<sup>-2</sup> yr<sup>-1</sup> for up to 7 years (Melillo et al. 2002, 2011). This  
1234 declined to an annual average rate of 60 g C m<sup>-2</sup> yr<sup>-1</sup> over 26 years of warming interspersed by  
1235 periods when there was no effect of +5 °C on soil respiration or C mineralization (Melillo et al.  
1236 2017). The average annual rate of C loss with warming is 2–6 fold larger than the estimated soil  
1237 C sink based on radiocarbon data (10–30 g C m<sup>-2</sup> yr<sup>-1</sup>).

1238  
1239 Melillo et al. (2017) used a mass-balance approach to estimate that 17% of total soil C was lost  
1240 from the organic horizon to 60 cm depth in the mineral soil over 26 years of warming. This was  
1241 not observed directly in the soil samples that were collected from the experimental plots. We can  
1242 use the soil power analysis to estimate the number of samples required to detect a significant  
1243 change in soil C content. Melillo et al. (2017) reported an average C loss of 800 g C m<sup>-2</sup> in the  
1244 organic horizon of warmed compared to control plots over 26 years. We estimate it would take  
1245 73 and 103 samples to detect this change at  $p < 0.10$  and  $p < 0.05$ , respectively. Across the entire  
1246 profile, they estimate a loss just in excess of 1,500 g C m<sup>-2</sup> in 26 years. Theoretically, detection  
1247 would require only 21 and 29 samples at  $p < 0.10$  and  $p < 0.05$ , respectively. In practice,  
1248 however, the soil C loss was across 60 cm of mineral soil with presumably variable amounts of  
1249 loss at different increments of depth. Therefore, it seems that the mass-balance approach they  
1250 employed is the only means of estimating soil C loss in the absence of terminating the  
1251 experiment and extracting several hundred soil cores to increase statistical power.

1252  
1253 More broadly, ecosystem C gains from forest regrowth overwhelm changes in C uptake and loss  
1254 rates from observed and simulated climate change. For the 24-year period 1992–2015, coincident  
1255 with the years of long-term soil warming, hardwood forest NEP averaged  $298 \pm 153$  g C m<sup>-2</sup> yr<sup>-1</sup>  
1256 (Table 4). Since NEP includes C in aboveground biomass and soil, C emissions from the soil in  
1257 response to extreme warming would need to be 2–7 fold higher to entirely offset C gains from  
1258 forest regrowth and other potential contributions from climate change, rising CO<sub>2</sub>, and  
1259 atmospheric N deposition. Soil warming may reduce the magnitude of the C sink, but the  
1260 Harvard Forest will likely remain a net carbon sink because of the large effect of recovery from  
1261 previous land-use change coupled to longer growing seasons and rising atmospheric CO<sub>2</sub>.

1262

1263 Concerns over enhanced N loading from atmospheric deposition motivated a second flagship  
1264 global change experiment at the Harvard Forest: long-term simulated N deposition in hardwood  
1265 and red pine plantation forests to assess the N saturation hypotheses of Ågren and Bosatta (1988)  
1266 and Aber et al. (1989). The Chronic Nitrogen Amendment Study was established in 1988 at two  
1267 levels of N addition, 5 g N m<sup>-2</sup> yr<sup>-1</sup> (N5) and 15 g N m<sup>-2</sup> yr<sup>-1</sup> (N15) (Frey et al. 2014). Over 20  
1268 years, the hardwood stand sequestered C in biomass and soil above that in control plots at an  
1269 average annual rate of 125 g C m<sup>-2</sup> yr<sup>-1</sup> (N5) and 460 g C m<sup>-2</sup> yr<sup>-1</sup> (N15). Most additional C was  
1270 sequestered in biomass, and in the surface organic horizon via suppressed decomposition, but  
1271 some was sequestered in deep mineral soil in the N15 treatment (Nadelhoffer et al. 1999a, Frey  
1272 et al. 2014). In the N5 treatment, 55% of the additional C sink was in the organic horizon and  
1273 mineral soil, and in the N15 treatment, 63% of the additional C sink was in these same horizons.  
1274 In the red pine stand, the N5 treatments neither gained nor lost C at a rate different from control  
1275 plots. In the N15 treatments, however, red pine trees died, indicating that extreme N deposition  
1276 has the capacity to fundamentally change the C cycle. Widespread tree decline and mortality  
1277 were observed in parts of Europe and, to a lesser extent, eastern North America, in the 1980s and  
1278 1990s (Schulze 1989, Högberg et al. 1996, Emmett et al. 1998). Red pine, an abandoned  
1279 plantation species at the Harvard Forest, does not occur in non-plantation areas of the forest and  
1280 is naturally in decline throughout the research area. Therefore, we do not consider red pine  
1281 responses further in this study.

1282  
1283 Relative to the effects of soil warming and forest regrowth, high (N5) to extreme (N15)  
1284 fertilization levels stimulate an ecosystem C sink that is 2–7 fold greater than the rate of C loss  
1285 from soils exposed to extreme warming, and 0.7 to 2 times higher than that of forest regrowth.  
1286 Nitrogen is thus a potent modifier of ecosystem C capital. Given that the 1990 amendments to  
1287 the Clean Air Act (U.S., 104 Stat. 2399, Pub.L. 101–549) have decreased atmospheric N  
1288 deposition across northeastern North America, primarily through reductions in NO<sub>x</sub> emissions,  
1289 the stimulatory effect of N deposition on the C sink may decline in the future (Du et al. 2014,  
1290 Beachley et al. 2016). We note, however, that NH<sub>3</sub> deposition is presently increasing at a modest  
1291 rate throughout much of the U.S. including the northeast (Butler et al. 2016). Simultaneous  
1292 reductions in atmospheric acidity (e.g., SO<sub>4</sub><sup>2-</sup>, NO<sub>3</sub><sup>-</sup>), the primary sink for NH<sub>3</sub>, may increase the

1293 concentration of  $\text{NH}_4^+$  in the soil and contribute to a C sink. At present this remains highly  
1294 uncertain.

1295  
1296 The northeastern U.S. has the greatest number of invasive forest insects in the country (Liebhold  
1297 et al. 2013), and they have major ecological and economic impacts (Lovett et al. 2016). In central  
1298 New England, prominent forest invasive insects include the hemlock woolly adelgid (*Adelges*  
1299 *tsugae*), gypsy moth (*Lymantria dispar*), emerald ash borer (*Agrilus planipennis*), and localized  
1300 outbreaks of Asian longhorned beetle (*Anoplophora glabripennis*) (Dodds and Orwig 2011).  
1301 These insects are poised to selectively impact or in some cases extirpate eastern hemlock, oaks,  
1302 ash, or various hardwood species, respectively. At the Harvard Forest, gypsy moth outbreaks  
1303 temporarily reduced oak biomass increment in the early 1980s (Fig. 4b), and now the hemlock  
1304 woolly adelgid (HWA) is progressively eliminating eastern hemlock. The ecosystem  
1305 consequences of hemlock loss via HWA has been a research focus at the Harvard Forest since  
1306 the 1990s (Orwig and Foster 1998, Orwig et al. 2008, 2012) and HWA is now causing decline  
1307 and mortality at the Harvard Forest (Kim et al. 2017, Orwig et al. 2018).

1308  
1309 Prior to HWA's arrival at the Harvard Forest, a third flagship experiment used girdling to kill all  
1310 hemlock trees in a second-growth forest to simulate the effects of the adelgid on ecosystem  
1311 processes (Ellison et al. 2010). The transfer of live aboveground biomass to the coarse woody  
1312 debris (CWD) pool dominated the C cycle consequences of this manipulation. Nine years after  
1313 girdling, live woody biomass in the girdled plots was about 40% of that in the intact hemlock  
1314 plots (Orwig et al. 2013). Despite greater productivity in the girdled plots than in control stands  
1315 (Orwig et al. 2013), C loss from decaying CWD exceeded net uptake for over a decade (Ellison  
1316 and Barker Plotkin 2018). Using a chronosequence approach, Raymer et al. (2013) estimated that  
1317 it would take ~20 years for ecosystem C content to recoup losses following hemlock loss in  
1318 second-growth forests, but nearly 140 years to accumulate as much C as that measured in the  
1319 primary-growth hemlock stand in which the HEM eddy-covariance tower is located and which is  
1320 now rapidly declining. Eventually, the predicted loss of C from the thick organic soil horizon in  
1321 the primary forest would be compensated by greater rates of NPP and C accumulation in biomass  
1322 by the rapidly aggrading hardwood forest (Finzi et al. 2014).

1323

1324 In and around the HEM tower site, visible signs of hemlock canopy loss began in 2013. The  
1325 eddy-covariance data show that the HEM site is now a net source of C to the atmosphere on an  
1326 annual basis (Fig. 7b). For the three-year period 2013–2015, NEP averaged  $36 \text{ g C m}^{-2} \text{ yr}^{-1}$  and  
1327 was lowest in 2015 ( $-129 \text{ g C m}^{-2} \text{ yr}^{-1}$ ). Relative to 2002, peak growing season  
1328 evapotranspiration decreased  $> 25\%$  while annual water yield increased 15% in 2013 and 2014  
1329 (Kim et al. 2017). Thus, hydrologic and C cycle changes are underway at this site. An intensified  
1330 effort is now ongoing to quantify changes in C pools and fluxes throughout areas experiencing  
1331 hemlock decline to test hypotheses generated by both experimental and chronosequence  
1332 approaches.

1333

### 1334 **Comparison of C cycling at the Harvard Forest to the surrounding region**

1335 The continuity and breadth of data, and detailed site history at an intensive ecological research  
1336 site such as the Harvard Forest LTER offer an unparalleled opportunity to integrate multiple data  
1337 streams over decades to discern long-term patterns of C cycling and the historical, biotic, and  
1338 climate factors driving these patterns. Yet by concentrating work at a particular location,  
1339 questions arise about how representative a site is compared to the broader region (Fahey et al.  
1340 2015). We know that the land use and wind disturbance history at the Harvard Forest are broadly  
1341 representative of the central New England region. The timing of major land-use changes and  
1342 percentage of land in agriculture were consistent across Massachusetts (Hall et al. 2002).

1343 Hurricane wind damage follows a strong gradient in frequency and intensity from southeastern to  
1344 northwestern New England, and the most recent major hurricane at the Harvard Forest (1938)  
1345 affected the surrounding central New England area similarly (Boose et al. 2001). However,  
1346 nuances in site characteristics and disturbance patterns may lead to differences in C stocks and  
1347 fluxes between the Harvard Forest, its surrounding ecoregion, and other intensively studied sites.

1348

1349 Based on the remote sensing estimates of GPP, productivity at the Harvard Forest is similar to  
1350 that of the surrounding ecoregion (Zhou et al. 2018). ANPP at the Harvard Forest averaged 390–  
1351  $430 \text{ g C m}^{-2} \text{ yr}^{-1}$  and total NPP averaged  $680\text{--}750 \text{ g C m}^{-2} \text{ yr}^{-1}$  (Tables 3, 4), reasonable values  
1352 compared to estimates of forest NPP in northern New England and New York. Net primary  
1353 production at the Hubbard Brook Experimental Forest in New Hampshire averaged  $585 \text{ g C m}^{-2}$   
1354  $\text{yr}^{-1}$  with  $\sim 350\text{--}400 \text{ g C m}^{-2} \text{ yr}^{-1}$  in ANPP alone (Fahey et al. 2005). ANPP at the Bartlett

1355 Experimental Forest, New Hampshire, ranged from 140 to 376 g C m<sup>-2</sup> yr<sup>-1</sup> with a mean of 257 g  
1356 C m<sup>-2</sup> yr<sup>-1</sup> (Ollinger and Smith 2005) and total NPP for the site was estimated to be 615 ± 118 g  
1357 C m<sup>-2</sup> yr<sup>-1</sup> (Ouimette et al. 2018). In the Allegheny Plateau of central New York, Fahey et al.  
1358 (2013) reported ANPP rates of 386 g C m<sup>-2</sup> yr<sup>-1</sup>. In the Catskill Mountains of New York, Lovett  
1359 et al. (2013) reported ANPP of 160–350 g C m<sup>-2</sup> yr<sup>-1</sup>, and in the Adirondack Mountains, Joshi et  
1360 al. (2003) reported ANPP rates of ~200 g C m<sup>-2</sup> yr<sup>-1</sup> for low elevation hardwood stands. The  
1361 higher overall ranges of NPP and ANPP at the Harvard Forest probably reflect its more southerly  
1362 location and warmer climate, which likely drive higher rates of net C uptake.

1363  
1364 C stocks in biomass are notably higher at the Harvard Forest compared to FIA plots in the  
1365 surrounding ecoregion. We hypothesize that this reflects a higher intensity of forest management  
1366 outside of the Harvard Forest during the last half century, as productivity recovers quickly after  
1367 partial disturbance (Fig. 7d, Amiro et al. 2010, Barker Plotkin et al. 2013), but C stocks can take  
1368 decades to recover. Recent (1990–2014) timber harvesting rates at the Harvard Forest averaged  
1369 0.4% of the land base per year and did not affect the plots included in this study. This is a lower  
1370 frequency of harvesting disturbance than the surrounding regions (Worcester Plateau and Lower  
1371 Worcester Plateau ecoregions), where about 1.4% of the land base per year was harvested during  
1372 the period of 1984–2015 (McDonald et al. 2006, Thompson et al. 2017). Indeed, timber  
1373 harvesting is the leading cause of adult tree mortality in northeastern forests (Canham et al.  
1374 2013). Partial harvest (20–40% live basal area removed) is most prevalent (Thompson et al.  
1375 2017), leading to intermittent removals of live aboveground C that take decades to regrow.

1376  
1377 Local site conditions and forest management practices at the Harvard Forest over the past  
1378 century also lead to differences in forest composition compared to the surrounding region. Oak  
1379 dominated live biomass C storage and uptake at the Harvard Forest over the study period and  
1380 increased in relative importance over the past 25 years (Urbanski et al. 2007, Eisen and Barker  
1381 Plotkin 2015). In contrast, red maple abundance has increased in New England over the past 400  
1382 years (Thompson et al. 2013) and surpasses oak biomass in much of the region (McEwan et al.  
1383 2011, Butler 2016, 2017, 2018). As discussed above, oaks may have relatively high biomass and  
1384 production capacity relative to other major tree species at the Harvard Forest, and therefore may  
1385 partially explain the higher biomass reported in this study compared to the region.

1386

1387

## SUMMARY

1388 C accrual persists at the Harvard Forest, consistent with previous studies of long-term forest  
1389 development (Luyssaert et al. 2008, Urbano and Keeton 2017). Comparative analysis of the  
1390 observational and experimental data reported here suggests that the largest driver of the C sink at  
1391 the Harvard Forest is forest regrowth following widespread land-use abandonment.

1392 Superimposed on this driver, climate warming and wetting, longer growing seasons, altered  
1393 phenology, rising CO<sub>2</sub>, declines in sulfate and total N deposition, alongside declines in ground-  
1394 level ozone concentrations are also likely contributing to the forest C sink. In many instances,  
1395 temporal variations in C cycling were readily interpretable such as the strong seasonal  
1396 correspondence between R<sub>a</sub>, leaf area deployment, and tree diameter growth in hardwood stands.  
1397 In other instances, the underlying causes were more complicated. These include interannual  
1398 variations in NEP, PAI and > 2-fold interannual variation in A<sub>max</sub>. Developing appropriate  
1399 statistical methods to parse the contributions of regrowth and climatic and atmospheric changes  
1400 on the C cycle remains an area of high priority for research.

1401

1402 Estimates of live aboveground C at the Harvard Forest are beginning to approach levels observed  
1403 in remnant old-growth stands on sites characteristic of the broader region, which range from  
1404 17,500 to 25,000 g C m<sup>-2</sup> (Siccama et al. 2007, Keeton et al. 2011, McGarvey et al. 2015).

1405 Estimates of deadwood in old-growth forest are less well studied but a few studies show dead  
1406 wood stocks that are many times higher than what we observe at the Harvard Forest and other  
1407 secondary forests in the region (McGee et al. 1999, McGarvey et al. 2015, D'Amato et al. 2017).

1408 Simulations using diverse modeling approaches consistently forecast biomass accrual associated  
1409 with long-term stand development persisting throughout the next century (Albani et al. 2006,  
1410 Tang et al. 2014, Duveneck et al. 2017, Wang et al. 2017). Simulations also suggest that rising  
1411 atmospheric CO<sub>2</sub> concentration, higher average temperatures and precipitation, and enhancement  
1412 of N mineralization rates and possibly N deposition will increase C sequestration despite  
1413 concomitant increases in respiration (McGuire et al. 1992, Richardson et al. 2010, Savage et al.  
1414 2013, Duveneck and Thompson 2017). On this basis, we hypothesize that continued forest  
1415 regrowth and climate change in the coming century will maintain C sink activity at the Harvard  
1416 Forest. This hypothesis is predicated on the assumption that major disturbances including

1417 invasive insects, logging or other land-use change, hurricanes, and extreme climate events do not  
1418 increase in frequency or intensity across the forest in the 21<sup>st</sup> century.

1419

1420

#### ACKNOWLEDGMENTS

1421 Adrien Finzi, Marc-André Giasson, and Audrey Barker Plotkin are co-first authors of this paper;  
1422 each contributed equally to the conceptualization of ideas, preparation of data, data analysis and  
1423 writing. This research was supported in part by the National Science Foundation Harvard Forest  
1424 Long-Term Ecological Research Program (since 1988; NSF-DEB grant numbers 8811764,  
1425 9411975, 0080592, 0620443, and 1237491). Flux tower and associated plot measurements were  
1426 additionally supported by the AmeriFlux Management Project with funding by the U.S.  
1427 Department of Energy's Office of Science under Contract No. DE-AC02-05CH11231, and  
1428 previously through the DOE NIGEC program. Collection of soil carbon data from the soil  
1429 warming plots was supported by the NSF-Ecosystem Studies (DEB0447967) and the NSF Long-  
1430 Term Research in Environmental Biology (DEB1456610) Programs. Additional support for  
1431 A.C.F. and M.A.G. was provided by the U.S. Department of Energy-Terrestrial Ecosystems  
1432 Science (DE-SC0006741). T.F.K. acknowledges support by the Director, Office of Science,  
1433 Office of Biological and Environmental Research of the U.S. Department of Energy under  
1434 Contract DE-AC02-05CH11231 as part of the RGCM RuBiSCo SFA. S.V.O. and Z.Z.  
1435 acknowledge support from NSF grant number 1638688, NASA grant numbers NNX08AG14G,  
1436 NNX14AJ18G, and NNX11AB88G, and USDA-NIFA grant number 1006997. N.P.  
1437 acknowledges support for the tree-ring work from NSF EF-1241930. C.A.W. acknowledges  
1438 financial support from NASA's Carbon Monitoring System program (NNH14ZDA001N-CMS)  
1439 under award NNX14AR39G. We thank Brett Butler for helping to coordinate access to FIA plot  
1440 locations pursuant to a Memorandum of Understanding 09MU11242305123 between the U.S.  
1441 Forest Service and Harvard University. Thanks to Elizabeth Nicoll for contributing to data  
1442 compilation, and to Loïc D'Orangeville for providing the processed Hemlock Tower  
1443 dendrometer band data. Finally, the authors appreciate the helpful suggestions from anonymous  
1444 reviewers on a previous version of the manuscript.

1445

1446

#### LITERATURE CITED

- 1447 Aber, J. D., K. J. Nadelhoffer, P. Steudler, and J. M. Melillo. 1989. Nitrogen saturation in  
1448 northern forest ecosystems. *Bioscience* 39:378–386.
- 1449 Aber, J. D., P. B. Reich, and M. L. Goulden. 1996. Extrapolating leaf CO<sub>2</sub> exchange to the  
1450 canopy: a generalized model of forest photosynthesis compared with measurements by eddy  
1451 correlation. *Oecologia* 106:257–265.
- 1452 Abramoff, R. Z., and A. C. Finzi. 2015. Are above- and below-ground phenology in sync? *New*  
1453 *Phytologist* 205:1054–1061.
- 1454 Abramoff, R. Z., and A. C. Finzi. 2016. Seasonality and partitioning of root allocation to  
1455 rhizosphere soils in a midlatitude forest. *Ecosphere* 7:e01547.
- 1456 Ågren, G. I., and E. Bosatta. 1988. Nitrogen saturation of terrestrial ecosystems. *Environmental*  
1457 *Pollution* 54:185–197.
- 1458 Albani, M., D. Medvigy, G. C. Hurtt, and P. R. Moorcroft. 2006. The contributions of land-use  
1459 change, CO<sub>2</sub> fertilization, and climate variability to the Eastern US carbon sink. *Global*  
1460 *Change Biology* 12:2370–2390.
- 1461 Amiro, B., A. Barr, T. Black, H. Iwashita, N. Kljun, J. Mccaughey, K. Morgenstern, S.  
1462 Murayama, Z. Nesic, and A. Orchansky. 2006. Carbon, energy and water fluxes at mature  
1463 and disturbed forest sites, Saskatchewan, Canada. *Agricultural and Forest Meteorology*  
1464 136:237–251.
- 1465 Amiro, B. D., A. G. Barr, J. G. Barr, T. A. Black, R. Bracho, M. Brown, J. Chen, K. L. Clark, K.  
1466 J. Davis, A. R. Desai, S. Dore, V. Engel, J. D. Fuentes, A. H. Goldstein, M. L. Goulden, T.  
1467 E. Kolb, M. B. Lavigne, B. E. Law, H. A. Margolis, T. Martin, J. H. McCaughey, L.  
1468 Misson, M. Montes-Helu, A. Noormets, J. T. Randerson, G. Starr, and J. Xiao. 2010.  
1469 Ecosystem carbon dioxide fluxes after disturbance in forests of North America. *Journal of*  
1470 *Geophysical Research* 115:G00K02, doi:10.1029/2010JG001390.
- 1471 Averill, C., B. L. Turner, and A. C. Finzi. 2014. Mycorrhiza-mediated competition between  
1472 plants and decomposers drives soil carbon storage. *Nature* 505:543–545.
- 1473 Barford, C. C., S. C. Wofsy, M. L. Goulden, J. W. Munger, E. H. Pyle, S. P. Urbanski, L.  
1474 Hutyyra, S. R. Saleska, D. Fitzjarrald, and K. Moore. 2001. Factors controlling long- and  
1475 short-term sequestration of atmospheric CO<sub>2</sub> in a mid-latitude forest. *Science* 294:1688–  
1476 1691.



1477 Barker Plotkin, A. 2017. Litterfall in Hemlock Removal Experiment at Harvard Forest since  
1478 2005. Harvard Forest Data Archive. HF161.

1479 Barker Plotkin, A., D. R. Foster, J. Carlson, and A. H. Magill. 2013. Survivors, not invaders,  
1480 control forest development following simulated hurricane. *Ecology* 94:414–423.

1481 Barr, A. G., T. A. Black, E. H. Hogg, N. Kljun, K. Morgenstern, and Z. Nestic. 2004. Inter-annual  
1482 variability in the leaf area index of a boreal aspen-hazelnut forest in relation to net  
1483 ecosystem production. *Agricultural and Forest Meteorology* 126:237–255.

1484 Bassow, S. L., and F. A. Bazzaz. 1997. Intra- and inter-specific variation in canopy  
1485 photosynthesis in a mixed deciduous forest. *Oecologia* 109:507–515.

1486 Battipaglia, G., M. Saurer, P. Cherubini, C. Calfapietra, H. R. McCarthy, R. J. Norby, and M.  
1487 Francesca Cotrufo. 2013. Elevated CO<sub>2</sub> increases tree-level intrinsic water use efficiency:  
1488 insights from carbon and oxygen isotope analyses in tree rings across three forest FACE  
1489 sites. *New Phytologist* 197:544–554.

1490 Bazzaz, F. A., and S. L. Miao. 1993. Successional status, seed size, and responses of tree  
1491 seedlings to CO<sub>2</sub>, light, and nutrients. *Ecology* 74:104–112.

1492 Beachley, G., M. Puchalski, C. Rogers, and G. Lear. 2016. A summary of long-term trends in  
1493 sulfur and nitrogen deposition in the United States 1990–2013. *JSM Environmental Science  
1494 and Ecology* 4:1030.

1495 Belmecheri, S., R. S. Maxwell, A. H. Taylor, K. J. Davis, K. H. Freeman, and W. J. Munger.  
1496 2014. Tree-ring  $\delta^{13}\text{C}$  tracks flux tower ecosystem productivity estimates in a NE temperate  
1497 forest. *Environmental Research Letters* 9:074011.

1498 Bindoff, N. L., P. A. Stott, K. M. AchutaRao, M. R. Allen, N. Gillett, D. Gutzler, K. Hansingo,  
1499 G. Hegerl, Y. Hu, S. Jain, I. I. Mokhov, J. Overland, J. Perlwitz, R. Sebbari and X. Zhang,  
1500 2013: Detection and Attribution of Climate Change: from Global to Regional. In: *Climate  
1501 Change 2013: The Physical Science Basis. Contribution of Working Group I to the Fifth  
1502 Assessment Report of the Intergovernmental Panel on Climate Change* [Stocker, T. F., D.  
1503 Qin, G.-K. Plattner, M. Tignor, S. K. Allen, J. Boschung, A. Nauels, Y. Xia, V. Bex and P.  
1504 M. Midgley (eds.)]. Cambridge University Press, Cambridge, United Kingdom and New  
1505 York, NY, USA.

- 1506 Bishop, D. A., and N. Pederson. 2015. Regional variation of transient precipitation and rainless-  
1507 day frequency across a subcontinental hydroclimate gradient. *Journal of Extreme Events*  
1508 02:1550007.
- 1509 Boose, E. R., K. E. Chamberlin, and D. R. Foster. 2001. Landscape and regional impacts of  
1510 hurricanes in New England. *Ecological Monographs* 71:27–48.
- 1511 Borken, W., E. A. Davidson, K. Savage, E. T. Sundquist, and P. Steudler. 2006. Effect of  
1512 summer throughfall exclusion, summer drought, and winter snow cover on methane fluxes  
1513 in a temperate forest soil. *Soil Biology & Biochemistry* 38:1388–1395.
- 1514 Bowen, J. L., and I. Valiela. 2001. Historical changes in atmospheric nitrogen deposition to Cape  
1515 Cod, Massachusetts, USA. *Atmospheric Environment* 35:1039–1051.
- 1516 Brown, H. T., and F. Escombe. 1902. The influence of varying amounts of carbon dioxide in the  
1517 air on the photosynthetic process of leaves and on the mode of growth of plants. *Proceedings*  
1518 *of the Royal Society of London* 70:397–413.
- 1519 Brzostek, E. R., A. Greco, J. E. Drake, and A. C. Finzi. 2013. Root carbon inputs to the  
1520 rhizosphere stimulate extracellular enzyme activity and increase nitrogen availability in  
1521 temperate forest soils. *Biogeochemistry* 115:65–76.
- 1522 Burkle, L. A., and B. A. Logan. 2003. Seasonal acclimation of photosynthesis in eastern hemlock  
1523 and partridgeberry in different light environments. *Northeastern Naturalist* 10:1–16.
- 1524 Butler, B. J. 2016. *Forests of Massachusetts, 2015. Resource Update FS-89.* Newtown Square,  
1525 PA: U.S. Department of Agriculture, Forest Service, Northern Research Station. 4 p.
- 1526 Butler, B. J. 2017. *Forests of Massachusetts, 2016. Resource Update FS-138.* Newtown Square,  
1527 PA: U.S. Department of Agriculture, Forest Service, Northern Research Station. 4 p.
- 1528 Butler, B. J. 2018. *Forests of Massachusetts, 2017. Resource Update FS-161.* Newtown Square,  
1529 PA: U.S. Department of Agriculture, Forest Service, Northern Research Station. 3 p.
- 1530 Butler, T., F. Vermeulen, C. M. Lehmann, G. E. Likens, and M. Puchalski. 2016. Increasing  
1531 ammonia concentration trends in large regions of the USA derived from the NADP/AMoN  
1532 network. *Atmospheric Environment* 146:132–140.
- 1533 Cairns, M. A., S. Brown, E. H. Helmer, and G. A. Baumgardner. 1997. Root biomass allocation  
1534 in the world's upland forests. *Oecologia* 111:1–11.
- 1535 Canham, C. D., N. Rogers, and T. Buchholz. 2013. Regional variation in forest harvest regimes  
1536 in the northeastern United States. *Ecological Applications* 23:515–522.

- 1537 Carey, E. V., A. Sala, R. Keane, and R. M. Callaway. 2001. Are old forests underestimated as  
1538 global carbon sinks? *Global Change Biology* 7:339–344.
- 1539 Chalot, M., and A. Brun. 1998. Physiology of organic nitrogen acquisition by ectomycorrhizal  
1540 fungi and ectomycorrhizas. *FEMS Microbiology Reviews* 22:21–44.
- 1541 Chapin, F. S., G. M. Woodwell, J. T. Randerson, E. B. Rastetter, G. M. Lovett, D. D. Baldocchi,  
1542 D. A. Clark, M. E. Harmon, D. S. Schimel, R. Valentini, C. Wirth, J. D. Aber, J. J. Cole, M.  
1543 L. Goulden, J. W. Harden, M. Heimann, R. W. Howarth, P. A. Matson, A. D. McGuire, J.  
1544 M. Melillo, H. A. Mooney, J. C. Neff, R. A. Houghton, M. L. Pace, M. G. Ryan, S. W.  
1545 Running, O. E. Sala, W. H. Schlesinger, and E.-D. Schulze. 2006. Reconciling carbon-cycle  
1546 concepts, terminology, and methods. *Ecosystems* 9:1041–1050.
- 1547 Clark, D. A., S. Brown, D. W. Kicklighter, J. Q. Chambers, J. R. Thomlinson, and J. Ni. 2001.  
1548 Measuring net primary production in forests: concepts and field methods. *Ecological*  
1549 *Applications* 11:356–370.
- 1550 Collins, M., R. Knutti, J. Arblaster, J.-L. Dufresne, T. Fichet, P. Friedlingstein, X. Gao, W. J.  
1551 Gutowski, T. Johns, G. Krinner, M. Shongwe, C. Tebaldi, A. J. Weaver, and M. Wehner.  
1552 2013. Long-term climate change: projections, commitments and irreversibility. *in* T. F.  
1553 Stocker, D. Qin, G.-K. Plattner, M. Tignor, S. K. Allen, J. Boschung, A. Nauels, Y. Xia, V.  
1554 Bex, and P. M. Midgley, editors. *Climate Change 2013: The Physical Science Basis*.  
1555 Contribution of Working Group I to the Fifth Assessment Report of the Intergovernmental  
1556 Panel on Climate Change. Cambridge University Press, Cambridge, United Kingdom and  
1557 New York, NY, USA.
- 1558 Compton, J. E., and R. D. Boone. 2000. Long-term impacts of agriculture on soil carbon and  
1559 nitrogen in New England forests. *Ecology* 81:2314–2330.
- 1560 Cook, E. R., and P. J. Krusic. 2005. Program ARSTAN: a tree-ring standardization program  
1561 based on detrending and autoregressive time series modeling, with interactive graphics.  
1562 Lamont-Doherty Earth Observatory, Columbia University, Palisades, NY.
- 1563 Currie, W. S., and K. J. Nadelhoffer. 2002. The imprint of land-use history: patterns of carbon  
1564 and nitrogen in downed woody debris at the Harvard Forest. *Ecosystems* 5:446–460.
- 1565 D’Amato, A. W., D. A. Orwig, D. R. Foster, A. Barker Plotkin, P. K. Schoonmaker, and M. R.  
1566 Wagner. 2017. Long-term structural and biomass dynamics of virgin *Tsuga canadensis*–  
1567 *Pinus strobus* forests after hurricane disturbance. *Ecology* 98:721–733.

1568 DeLucia, E. H., J. G. Hamilton, S. L. Naidu, R. B. Thomas, J. A. Andrews, A. Finzi, M.  
1569 Lavine, R. Matamala, J. E. Mohan, G. R. Hendrey, and W. H. Schlesinger. 1999. Net  
1570 primary production of a forest ecosystem with experimental CO<sub>2</sub> enrichment. *Science*  
1571 284:1177–1179.

1572 Dietze, M. C. 2015. The PEcAn Project.  
1573 <https://github.com/PecanProject/pecan/blob/develop/modules/allometry/vignettes/AllomVig>  
1574 [nette.Rmd](#)

1575 Dodds, K. J., and D. A. Orwig. 2011. An invasive urban forest pest invades natural environments  
1576 — Asian longhorned beetle in northeastern US hardwood forests. *Canadian Journal of*  
1577 *Forest Research* 41:1729–1742.

1578 D’Orangeville, L., J. Maxwell, D. Kneeshaw, N. Pederson, L. Duchesne, T. Logan, D. Houle, D.  
1579 Arseneault, C. M. Beier, D. A. Bishop, D. Druckenbrod, S. Fraver, F. Girard, J. Halman, C.  
1580 Hansen, J. L. Hart, H. Hartmann, M. Kaye, D. Leblanc, S. Manzoni, R. Ouimet, S. Rayback,  
1581 C. R. Rollinson, and R. P. Phillips. 2018. Drought timing and local climate determine the  
1582 sensitivity of eastern temperate forests to drought. *Global Change Biology* 24:2339–2351.

1583 Driscoll, C. T., G. E. Likens, and M. R. Church. 1998. Recovery of surface waters in the  
1584 northeastern U.S. from decreases in atmospheric deposition of sulfur. *Water, Air, and Soil*  
1585 *Pollution* 105:319–329.

1586 Du, E., W. de Vries, J. N. Galloway, X. Hu, and J. Fang. 2014. Changes in wet nitrogen  
1587 deposition in the United States between 1985 and 2012. *Environmental Research Letters*  
1588 9:095004.

1589 Duveneck, M. J., and J. R. Thompson. 2017. Climate change imposes phenological tradeoffs on  
1590 forest net primary productivity. *Journal of Geophysical Research: Biogeosciences* 122,  
1591 doi:10.1002/2017JG004025.

1592 Duveneck, M. J., J. R. Thompson, E. J. Gustafson, Y. Liang, and A. de Bruijn. 2017. Recovery  
1593 dynamics and climate change effects to future New England forests. *Landscape Ecology*  
1594 32:1385–1397.

1595 Dye, A., A. Barker Plotkin, D. Bishop, N. Pederson, B. Poulter, and A. Hessler. 2016. Comparing  
1596 tree-ring and permanent plot estimates of aboveground net primary production in three  
1597 eastern U.S. forests. *Ecosphere* 7:e01454.

- 1598 Eisen, K., and A. Barker Plotkin. 2015. Forty years of forest measurements support steadily  
1599 increasing aboveground biomass in a maturing, *Quercus*-dominant northeastern forest.  
1600 *Journal of the Torrey Botanical Society* 142:97–112.
- 1601 Ellison, A., and A. Barker Plotkin. 2015. Overstory vegetation in Hemlock Removal Experiment  
1602 at Harvard Forest since 2003. Harvard Forest Data Archive. HF126.
- 1603 Ellison, A., and A. Barker Plotkin. 2018. Coarse woody debris in hemlock removal experiment at  
1604 Harvard Forest since 2005. Harvard Forest Data Archive. HF125.
- 1605 Ellison, A. M., L. J. Osterweil, J. L. Hadley, A. Wise, E. Boose, L. Clarke, D. R. Foster, A.  
1606 Hanson, D. Jensen, P. Kuzeja, E. Riseman, and H. Schultz. 2006. Analytic webs support the  
1607 synthesis of ecological data sets. *Ecology* 87:1345–1358.
- 1608 Ellison, A. M., A. A. Barker Plotkin, D. R. Foster, and D. A. Orwig. 2010. Experimentally  
1609 testing the role of foundation species in forests: the Harvard Forest Hemlock Removal  
1610 Experiment. *Methods in Ecology and Evolution* 1:168–179.
- 1611 Ellison, A. M., Orwig, D. A., Fitzpatrick, M. C., Preisser, E. L. 2018. The Past, Present, and  
1612 Future of the Hemlock Woolly Adelgid (*Adelges tsugae*) and Its Ecological Interactions  
1613 with Eastern Hemlock (*Tsuga canadensis*) Forests. *Insects* 9: 172-189.
- 1614 Emmett, B. A., D. Boxman, M. Bredemeier, P. Gundersen, O. J. Kjønaas, F. Moldan, P.  
1615 Schleppei, A. Tietema, and R. F. Wright. 1998. Predicting the effects of atmospheric nitrogen  
1616 deposition in conifer stands: evidence from the NITREX ecosystem-scale experiments.  
1617 *Ecosystems* 1:352–360.
- 1618 EPA. 2019. Air data: air quality data collected at outdoor monitors across the US.  
1619 <https://www.epa.gov/outdoor-air-quality-data> (accessed 27 November 2019).
- 1620 Fahey, T. J., and J. W. Hughes. 1994. Fine root dynamics in a northern hardwood forest  
1621 ecosystem, Hubbard Brook Experimental Forest, NH. *Journal of Ecology* 82:533–548.
- 1622 Fahey, T. J., T. G. Siccama, C. T. Driscoll, G. E. Likens, J. Campbell, C. E. Johnson, J. J.  
1623 Battles, J. D. Aber, J. J. Cole, M. C. Fisk, P. M. Groffman, S. P. Hamburg, R. T. Holmes, P.  
1624 A. Schwarz, and R. D. Yanai. 2005. The biogeochemistry of carbon at Hubbard Brook.  
1625 *Biogeochemistry* 75:109–176.
- 1626 Fahey, T. J., R. E. Sherman, and D. A. Weinstein. 2013. Demography, biomass and productivity  
1627 of a northern hardwood forest on the Allegheny Plateau. *Journal of the Torrey Botanical*  
1628 *Society* 140:52–64.

- 1629 Fahey, T. J., P. H. Templer, B. T. Anderson, J. J. Battles, J. L. Campbell, C. T. Driscoll, A. R.  
1630 Fusco, M. B. Green, K.-A. S. Kassam, N. L. Rodenhouse, L. Rustad, P. G. Schaberg, and M.  
1631 A. Vadeboncoeur. 2015. The promise and peril of intensive-site-based ecological research:  
1632 insights from the Hubbard Brook ecosystem study. *Ecology* 96:885–901.
- 1633 Falge, E., D. Baldocchi, R. Olson, P. Anthoni, M. Aubinet, C. Bernhofer, G. Burba, R.  
1634 Ceulemans, R. Clement, H. Dolman, A. Granier, P. Gross, T. Grünwald, D. Hollinger, N.-O.  
1635 Jensen, G. Katul, P. Keronen, A. Kowalski, C. T. Lai, B. E. Law, T. Meyers, J. Moncrieff,  
1636 E. Moors, J. W. Munger, K. Pilegaard, Ü. Rannik, C. Rebmann, A. Suyker, J. Tenhunen, K.  
1637 Tu, S. Verma, T. Vesala, K. Wilson, and S. Wofsy. 2001. Gap filling strategies for  
1638 defensible annual sums of net ecosystem exchange. *Agricultural and Forest Meteorology*  
1639 107:43–69.
- 1640 Fernández-Martínez, M., S. Vicca, I. A. Janssens, P. Ciais, M. Obersteiner, M. Bartrons, J.  
1641 Sardans, A. Verger, J. G. Canadell, F. Chevallier, X. Wang, C. Bernhofer, P. S. Curtis, D.  
1642 Gianelle, T. Grünwald, B. Heinesch, A. Ibrom, A. Knohl, T. Laurila, B. E. Law, J. M.  
1643 Limousin, B. Longdoz, D. Loustau, I. Mammarella, G. Matteucci, R. K. Monson, L.  
1644 Montagnani, E. J. Moors, J. W. Munger, D. Papale, S. L. Piao, and J. Peñuelas. 2017.  
1645 Atmospheric deposition, CO<sub>2</sub>, and change in the land carbon sink. *Scientific Reports* 7:9632.
- 1646 Finzi, A. C., R. J. Norby, C. Calfapietra, A. Gallet-Budynek, B. Gielen, W. E. Holmes, M. R.  
1647 Hoosbeek, C. M. Iversen, R. B. Jackson, M. E. Kubiske, J. Ledford, M. Liberloo, R. Oren,  
1648 A. Polle, S. Pritchard, D. R. Zak, W. H. Schlesinger, and R. Ceulemans. 2007. Increases in  
1649 nitrogen uptake rather than nitrogen-use efficiency support higher rates of temperate forest  
1650 productivity under elevated CO<sub>2</sub>. *Proceedings of the National Academy of*  
1651 *Sciences* 104:14014–14019.
- 1652 Finzi, A. C., P. C. L. Raymer, M.-A. Giasson, and D. A. Orwig. 2014. Net primary production  
1653 and soil respiration in New England hemlock forests affected by the hemlock woolly  
1654 adelgid. *Ecosphere* 5:art98.
- 1655 Foster, D. R., and J. D. Aber. 2004. *Forests in time: The environmental consequences of 1,000*  
1656 *years of change in New England*. Yale University Press, New Haven, CT, USA.
- 1657 Foster, D. R., T. Zebryk, P. Schoonmaker, and A. Lezberg. 1992. Post-settlement history of  
1658 human land-use and vegetation dynamics of a *Tsuga canadensis* (hemlock) woodlot in  
1659 central New England. *Journal of Ecology* 80:773–786.

1660 Frey, S. D., S. Ollinger, K. Nadelhoffer, R. Bowden, E. Brzostek, A. Burton, B. A. Caldwell, S.  
1661 Crow, C. L. Goodale, A. S. Grandy, A. Finzi, M. G. Kramer, K. Lajtha, J. LeMoine, M.  
1662 Martin, W. H. McDowell, R. Minocha, J. J. Sadowsky, P. H. Templer, and K. Wickings.  
1663 2014. Chronic nitrogen additions suppress decomposition and sequester soil carbon in  
1664 temperate forests. *Biogeochemistry* 121:305–316.

1665 Gaudinski, J. B., S. E. Trumbore, E. A. Davidson, and S. Zheng. 2000. Soil carbon cycling in a  
1666 temperate forest: radiocarbon-based estimates of residence times, sequestration rates and  
1667 partitioning of fluxes. *Biogeochemistry* 51:33–69.

1668 Gaudinski, J. B., M. S. Torn, W. J. Riley, T. E. Dawson, J. D. Joslin, and H. Majdi. 2010.  
1669 Measuring and modeling the spectrum of fine-root turnover times in three forests using  
1670 isotopes, minirhizotrons, and the Radix model. *Global Biogeochemical Cycles* 24, GB3029,  
1671 doi:10.1029/2009GB003649.

1672 Giasson, M.-A., A. M. Ellison, R. D. Bowden, P. M. Crill, E. A. Davidson, J. E. Drake, S. D.  
1673 Frey, J. L. Hadley, M. Lavine, J. M. Melillo, J. W. Munger, K. J. Nadelhoffer, L. Nicoll, S.  
1674 V. Ollinger, K. E. Savage, P. A. Steudler, J. Tang, R. K. Varner, S. C. Wofsy, D. R. Foster,  
1675 and A. C. Finzi. 2013. Soil respiration in a northeastern US temperate forest: a 22-year  
1676 synthesis. *Ecosphere* 4:art140.

1677 Gough, C. M., P. S. Curtis, B. S. Hardiman, C. M. Scheuermann, and B. Bond-Lamberty. 2016.  
1678 Disturbance, complexity, and succession of net ecosystem production in North America's  
1679 temperate deciduous forests. *Ecosphere* 7:art01375.

1680 Greenland, D., and T. Kittel. 1997. A climatic analysis of long-term ecological research sites.  
1681 <https://lternet.edu/wp-content/uploads/2013/12/CLIMDES.pdf> (accessed 1 August 2019).

1682 Griffith, G. E., J. M. Omernik, S. A. Bryce, J. Royte, W. D. Hoar, J. W. Homer, D. Keirstead, K.  
1683 J. Metzler, and G. and Hellyer. 2009. Ecoregions of New England (color poster with map,  
1684 descriptive text, summary tables, and photographs). U.S. Geological Survey, Reston,  
1685 Virginia.

1686 Hadley, J. L., and J. L. Schedlbauer. 2002. Carbon exchange of an old-growth eastern hemlock  
1687 (*Tsuga canadensis*) forest in central New England. *Tree Physiology* 22:1079–1092.

1688 Hadley, J. L., P. S. Kuzeja, M. J. Daley, N. G. Phillips, T. Mulcahy, and S. Singh. 2008. Water  
1689 use and carbon exchange of red oak- and eastern hemlock-dominated forests in the

- 1690 northeastern USA: implications for ecosystem-level effects of hemlock woolly adelgid. *Tree*  
1691 *Physiology* 28:615–627.
- 1692 Hall, B., G. Motzkin, D. R. Foster, M. Syfert, and J. Burk. 2002. Three hundred years of forest  
1693 and land-use change in Massachusetts, USA. *Journal of Biogeography* 29:1319–1335.
- 1694 Harmon, M. E., and J. Sexton. 1996. Guidelines for measurements of woody detritus in forest  
1695 ecosystems. U.S. LTER Publication No. 20.
- 1696 Hobbie, E. A., and J. E. Hobbie. 2008. Natural abundance of  $^{15}\text{N}$  in nitrogen-limited forests and  
1697 tundra can estimate nitrogen cycling through mycorrhizal fungi: a review. *Ecosystems*  
1698 11:815–830.
- 1699 Högberg, P., H. Fan, M. Quist, D. A. N. Binkley, and C. O. Tamm. 2006. Tree growth and soil  
1700 acidification in response to 30 years of experimental nitrogen loading on boreal forest.  
1701 *Global Change Biology* 12:489–499.
- 1702 Hooker, T. D., and J. E. Compton. 2003. Forest ecosystem carbon and nitrogen accumulation  
1703 during the first century after agricultural abandonment. *Ecological Applications* 13:299–  
1704 313.
- 1705 Isaac, L. A., and H. G. Hopkins. 1937. The forest soil of the Douglas fir region, and changes  
1706 wrought upon it by logging and slash burning. *Ecology* 18:264–279.
- 1707 Jackson, R. B., K. Lajtha, S. E. Crow, G. Hugelius, M. G. Kramer, and G. Piñeiro. 2017. The  
1708 ecology of soil carbon: pools, vulnerabilities, and biotic and abiotic controls. *Annual*  
1709 *Review of Ecology, Evolution, and Systematics* 48:419–445.
- 1710 Jenkins, J. C., D. C. Chojnacky, L. S. Heath, and R. A. Birdsey. 2003. National-scale biomass  
1711 estimators for United States tree species. *Forest Science* 49, 12–35.
- 1712 Jenkins, J. C., D. C. Chojnacky, L. S. Heath, and R. A. Birdsey. 2004. Comprehensive database  
1713 of diameter-based biomass regressions for North American tree species. Newtown Square,  
1714 PA: U.S. Department of Agriculture, Forest Service, Northeastern Research Station.
- 1715 Joshi, A. B., D. R. Vann, A. H. Johnson, and E. K. Miller. 2003. Nitrogen availability and forest  
1716 productivity along a climosequence on Whiteface Mountain, New York. *Canadian Journal*  
1717 *of Forest Research* 33:1880–1891.
- 1718 Keenan, T. F., D. Y. Hollinger, G. Bohrer, D. Dragoni, J. W. Munger, H. P. Schmid, and A. D.  
1719 Richardson. 2013. Increase in forest water-use efficiency as atmospheric carbon dioxide  
1720 concentrations rise. *Nature* 499:324–327.



1721 Keenan, T. F., J. Gray, M. A. Friedl, M. Toomey, G. Bohrer, D. Y. Hollinger, J. William  
1722 Munger, J. O’Keefe, H. P. Schmid, I. S. Wing, B. Yang, and A. D. Richardson. 2014. Net  
1723 carbon uptake has increased through warming-induced changes in temperate forest  
1724 phenology. *Nature Climate Change* 4:598–604.

1725 Keenan, T. F., I. C. Prentice, J. G. Canadell, C. A. Williams, H. Wang, M. Raupach, and G. J.  
1726 Collatz. 2016. Recent pause in the growth rate of atmospheric CO<sub>2</sub> due to enhanced  
1727 terrestrial carbon uptake. *Nature Communications* 7:13428.

1728 Keeton, W. S., A. A. Whitman, G. C. McGee, C. L. Goodale, G. C. Whitman, G. G. McGree,  
1729 and K. Goodale. 2011. Late-successional biomass development in northern hardwood-  
1730 conifer forests of the northeastern United States. *Forest Science* 57:489–505.

1731 Khomik, M., C. A. Williams, M. K. Vanderhoof, R. G. MacLean, and S. Y. Dillen. 2014. On the  
1732 causes of rising gross ecosystem productivity in a regenerating clearcut environment: leaf  
1733 area vs. species composition. *Tree Physiology* 34:686–700.

1734 Kim, J., T. Hwang, C. L. Schaaf, D. A. Orwig, E. Boose, and J. William Munger. 2017.  
1735 Increased water yield due to the hemlock woolly adelgid infestation in New England.  
1736 *Geophysical Research Letters* 44:2327–2335.

1737 Kira, T., and T. Shidei. 1967. Primary production and turnover of organic matter in different  
1738 forest ecosystems of the western Pacific. *Japanese Journal of Ecology* 17:70–87.

1739 Lajtha, K., R. D. Bowden, and K. Nadelhoffer. 2014. Litter and root manipulations provide  
1740 insights into soil organic matter dynamics and stability. *Soil Science Society of America*  
1741 *Journal* 78:S261–S269.

1742 Liebhold, A. M., D. G. McCullough, L. M. Blackburn, S. J. Frankel, B. Von Holle, and J. E.  
1743 Aukema. 2013. A highly aggregated geographical distribution of forest pest invasions in the  
1744 USA. *Diversity and Distributions* 19:1208–1216.

1745 Lindahl, B. D., R. D. Finlay, and J. W. G. Cairney. 2005. Enzymatic activities of mycelia in  
1746 mycorrhizal fungal communities. Pages 331–348 in J. Dighton, J. F. White, and P.  
1747 Oudemans, editors. *The fungal community: its organization and role in the ecosystem*, 3rd  
1748 edition. CRC Press, Boca Raton, FL, USA.

1749 Litton, C. M., J. W. Raich, and M. G. Ryan. 2007. Carbon allocation in forest ecosystems.  
1750 *Global Change Biology* 13:2089–2109.

- 1751 Lovett, G. M., M. A. Arthur, K. C. Weathers, R. D. Fitzhugh, and P. H. Templer. 2013. Nitrogen  
1752 addition increases carbon storage in soils, but not in trees, in an eastern US deciduous forest.  
1753 *Ecosystems* 16:980–1001.
- 1754 Lovett, G. M., M. Weiss, A. M. Liebhold, T. P. Holmes, B. Leung, K. F. Lambert, D. A. Orwig,  
1755 F. T. Campbell, J. Rosenthal, D. G. McCullough, R. Wildova, M. P. Ayres, C. D. Canham,  
1756 D. R. Foster, S. L. LaDeau, and T. Weldy. 2016. Nonnative forest insects and pathogens in  
1757 the United States: Impacts and policy options. *Ecological Applications* 26:1437–1455.
- 1758 Lutz, J. A., A. J. Larson, M. E. Swanson, and J. A. Freund. 2012. Ecological importance of  
1759 large-diameter trees in a temperate mixed-conifer forest. *PLoS ONE* 7:e36131.
- 1760 Luysaert, S., E. -Detlef Schulze, A. Börner, A. Knohl, D. Hessenmöller, B. E. Law, P. Ciais,  
1761 and J. Grace. 2008. Old-growth forests as global carbon sinks. *Nature* 455:213–215.
- 1762 Marlon, J. R., N. Pederson, C. Nolan, S. Goring, B. Shuman, A. Robertson, R. Booth, P. J.  
1763 Bartlein, M. A. Berke, M. Clifford, E. Cook, A. Dieffenbacher-Krall, M. C. Dietze, A.  
1764 Hessl, J. B. Hubeny, S. T. Jackson, J. Marsicek, J., McLachlan, C. J., Mock, D. J. P. Moore,  
1765 J. Nichols, D. Peteet, K. Schaefer, V. Trouet, C. Umbanhowar, J. W. Williams, and Z. Yu.  
1766 2017. Climatic history of the northeastern United States during the past 3000 years. *Climate*  
1767 *of the Past* 13:1355–1379.
- 1768 Martin-Benito, D., and N. Pederson. 2015. Convergence in drought stress, but a divergence of  
1769 climatic drivers across a latitudinal gradient in a temperate broadleaf forest. *Journal of*  
1770 *Biogeography* 42:925–937.
- 1771 McClaugherty, C. A., J. D. Aber, and J. M. Melillo. 1982. The role of fine roots in the organic  
1772 matter and nitrogen budgets of two forested ecosystems. *Ecology* 63:1481–1490.
- 1773 McDonald, R. I., G. Motzkin, M. S. Bank, D. B. Kittredge, J. Burk, and D. R. Foster. 2006.  
1774 Forest harvesting and land-use conversion over two decades in Massachusetts. *Forest*  
1775 *Ecology and Management* 227:31–41.
- 1776 McEwan, R. W., J. M. Dyer, and N. Pederson. 2011. Multiple interacting ecosystem drivers:  
1777 toward an encompassing hypothesis of oak forest dynamics across eastern North America.  
1778 *Ecography* 34:244–256.
- 1779 McFarlane, K. J., M. S. Torn, P. J. Hanson, R. C. Porras, C. W. Swanston, M. A. Callahan Jr.,  
1780 and T. P. Guilderson. 2013. Comparison of soil organic matter dynamics at five temperate

1781 deciduous forests with physical fractionation and radiocarbon measurements.  
1782 Biogeochemistry 112:457–476.

1783 McGarvey, J. C., J. R. Thompson, H. E. Epstein, and H. H. Shugart Jr. 2015. Carbon storage in  
1784 old-growth forests of the Mid-Atlantic: toward better understanding the eastern forest  
1785 carbon sink. Ecology 96:311–317.

1786 McGee, G. G., D. J. Leopold, and R. D. Nyland. 1999. Structural characteristics of old-growth,  
1787 maturing, and partially cut northern hardwood forests. Ecological Applications 9:1316–  
1788 1329.

1789 McGuire, A.D., J. M. Melillo, L. A. Joyce, D. W. Kicklighter, A. L. Grace, B. Moore III, and C.  
1790 J. Vorosmarty. 1992. Interactions between carbon and nitrogen dynamics in estimating net  
1791 primary productivity for potential vegetation in North America. Global Biogeochemical  
1792 Cycles 6:101–124.

1793 Melillo, J. M., T. V. Callaghan, F. I. Woodward, E. Salati, and S. K. Sinha. 1990. Climate  
1794 change-effects on ecosystems. in J. T. Houghton, G. J. Jenkins, and J. J. Ephraums, editors.  
1795 Climate Change - The IPCC Scientific Assessment. Cambridge University Press,  
1796 Cambridge, Great Britain, New York, NY, USA, and Melbourne, Australia.

1797 Melillo, J. M., P. A. Steudler, J. D. Aber, K. Newkirk, H. Lux, F. P. Bowles, C. Catricala, A.  
1798 Magill, T. Ahrens, and S. Morrisseau. 2002. Soil warming and carbon-cycle feedbacks to  
1799 the climate system. Science 298:2173–2176.

1800 Melillo, J. M., S. Butler, J. Johnson, J. Mohan, P. Steudler, H. Lux, E. Burrows, F. Bowles, R.  
1801 Smith, L. Scott, C. Vario, T. Hill, A. Burton, Y.-M. Zhou, and J. Tang. 2011. Soil warming,  
1802 carbon-nitrogen interactions, and forest carbon budgets. Proceedings of the National  
1803 Academy of Sciences of the United States of America 108:9508–9512.

1804 Melillo, J. M., S. D. Frey, K. M. DeAngelis, W. J. Werner, M. J. Bernard, F. P. Bowles, G. Pold,  
1805 M. A. Knorr, and A. S. Grandy. 2017. Long-term pattern and magnitude of soil carbon  
1806 feedback to the climate system in a warming world. Science 358:101–105.

1807 Miao, S. 1995. Acorn mass and seedling growth in *Quercus rubra* in response to elevated  
1808 CO<sub>2</sub>. Journal of Vegetation Science 6:697–700.

1809 Morris, S. J., S. Bohm, S. Haile-Mariam, and E. A. Paul. 2007. Evaluation of carbon accrual in  
1810 afforested agricultural soils. Global Change Biology 13:1145–1156.

1811 Motzkin, G., P. Wilson, D. R. Foster, and A. Allen. 1999. Vegetation patterns in heterogeneous  
1812 landscapes: The importance of history and environment. *Journal of Vegetation Science*  
1813 10:903–920.

1814 Nadelhoffer, K. J., M. R. Downs, and B. Fry. 1999a. Sinks for <sup>15</sup>N additions to an oak forest and  
1815 a red pine plantation. *Ecological Applications* 9:72–86.

1816 Nadelhoffer, K. J., B. A. Emmett, P. Gundersen, O. J. Kjønaas, C. J. Koopmans, P. Schleppei, A.  
1817 Tietema, and R. F. Wright. 1999b. Nitrogen deposition makes a minor contribution to  
1818 carbon sequestration in temperate forests. *Nature* 398:145–148.

1819 NADP. 2019. National Atmospheric Deposition Program data and maps.  
1820 <http://nadp.slh.wisc.edu/data> (accessed 27 November 2019).

1821 Nave, L. E., C. W. Swanston, U. Mishra, and K. J. Nadelhoffer. 2013. Afforestation effects on  
1822 soil carbon storage in the United States: a synthesis. *Soil Science Society of America*  
1823 *Journal* 77:1035–1047.

1824 Nave, L. E., C. M. Gough, C. H. Perry, K. L. Hofmeister, J. M. Le Moine, G. M. Domke, C. W.  
1825 Swanston, and K. J. Nadelhoffer. 2017. Physiographic factors underlie rates of biomass  
1826 production during succession in Great Lakes forest landscapes. *Forest Ecology and*  
1827 *Management* 397:157–173.

1828 NOAA. 2019. Average annual atmospheric CO<sub>2</sub> concentration at the Mauna Loa Observatory.  
1829 [ftp://afpp.cmdl.noaa.gov/products/trends/co2/co2\\_annmean\\_mlo.txt](ftp://afpp.cmdl.noaa.gov/products/trends/co2/co2_annmean_mlo.txt). (accessed 27 November  
1830 2019)

1831 Odum, E. P. 1969. The strategy of ecosystem development. *Science* 164:262–270.

1832 O’Keefe, J. 2015. Phenology of woody species. Harvard Forest Data Archive. HF003.

1833 Oliver, C. D. 1975. The development of northern red oak (*Quercus rubra* L.) in mixed species,  
1834 even-age stands in central New England. Yale University.

1835 Oliver, C. D. 1978. The development of northern red oak in mixed stands in central New  
1836 England. *Yale School of Forestry and Environmental Studies Bulletin* No. 91.

1837 Oliver, C. D., and E. P. Stephens. 1977. Reconstruction of a mixed-species forest in central New  
1838 England. *Ecology* 58:562–572.

1839 Ollinger, S. V., and M.-L. Smith. 2005. Net primary production and canopy nitrogen in a  
1840 temperate forest landscape: an analysis using imaging spectroscopy, modeling and field  
1841 data. *Ecosystems* 8:760–778.

- 1842 Ollinger, S. V., J. D. Aber, P. B. Reich, and R. J. Freuder. 2002. Interactive effects of nitrogen  
1843 deposition, tropospheric ozone, elevated CO<sub>2</sub> and land use history on the carbon dynamics  
1844 of northern hardwood forests. *Global Change Biology* 8:545–562.
- 1845 Ollinger, S. V., A. D. Richardson, M. E. Martin, D. Y. Hollinger, S. E. Frohking, P. B. Reich, L.  
1846 C. Plourde, G. G. Katul, J. W. Munger, R. Oren, M.-L. Smith, K. T. Paw U, P. V. Bolstad,  
1847 B. D. Cook, M. C. Day, T. A. Martin, R. K. Monson, and H. P. Schmid. 2008. Canopy  
1848 nitrogen, carbon assimilation, and albedo in temperate and boreal forests: Functional  
1849 relations and potential climate feedbacks. *Proceedings of the National Academy of Sciences*  
1850 of the United States of America 105:19336–19341.
- 1851 Orwig, D. A., and D. R. Foster. 1998. Forest response to the introduced hemlock woolly adelgid  
1852 in southern New England, USA. *The journal of the Torrey Botanical Society* 125:60–73.
- 1853 Orwig, D. A., R. C. Cobb, A. W. D’Amato, M. L. Kizlinski, and D. R. Foster. 2008. Multi-year  
1854 ecosystem response to hemlock woolly adelgid infestation in southern New England forests.  
1855 *Canadian Journal of Forest Research* 38:834–843.
- 1856 Orwig, D. A., J. R. Thompson, N. A. Povak, M. Manner, D. Niebyl, and D. R. Foster. 2012. A  
1857 foundation tree at the precipice: *Tsuga canadensis* health after the arrival of *Adelges tsugae*  
1858 in central New England. *Ecosphere* 3:art10.
- 1859 Orwig, D. A., A. A. Barker Plotkin, E. A. Davidson, H. Lux, K. E. Savage, and A. M. Ellison.  
1860 2013. Foundation species loss affects vegetation structure more than ecosystem function in a  
1861 northeastern USA forest. *PeerJ* 1:e41.
- 1862 Orwig, D.A., P. Boucher, I. Paynter, E. Saenz, Z. Li, and C. Schaaf. 2018. The potential to  
1863 characterize ecological data with terrestrial laser scanning in Harvard Forest, MA. *Interface*  
1864 *Focus* 8:20170044.
- 1865 Ouimette, A. P., S. V. Ollinger, A. D. Richardson, D. Y. Hollinger, T. Keenan, L. C. Lepine, and  
1866 M. Vadeboncoeur. 2018. Carbon fluxes and interannual drivers in a temperate forest  
1867 ecosystem assessed through comparison of top-down and bottom up approaches.  
1868 *Agricultural and Forest Meteorology* 256–257:420–430.
- 1869 Pan, Y., R. A. Birdsey, J. Fang, R. Houghton, P. E. Kauppi, W. A. Kurz, O. L. Phillips, A.  
1870 Shvidenko, S. L. Lewis, J. G. Canadell, P. Ciais, R. B. Jackson, S. W. Pacala, A. D.  
1871 McGuire, S. Piao, A. Rautiainen, S. Sitch, and D. Hayes. 2011. A large and persistent  
1872 carbon sink in the world’s forests. *Science* 333:988–993.

1873 Papale, D., M. Reichstein, M. Aubinet, E. Canfora, C. Bernhofer, W. Kutsch, B. Longdoz, S.  
1874 Rambal, R. Valentini, T. Vesala, and D. Yakir. 2006. Towards a standardized processing of  
1875 Net Ecosystem Exchange measured with eddy covariance technique: algorithms and  
1876 uncertainty estimation. *Biogeosciences* 3:571–583.

1877 Pederson, N., A. R. Bell, E. R. Cook, U. Lall, N. Devineni, R. Seager, K. Eggleston, and K. P.  
1878 Vranes. 2013. Is an epic pluvial masking the water insecurity of the greater New York City  
1879 region? *Journal of Climate* 26:1339–1354.

1880 Pederson, N., A. W. D'Amato, J. M. Dyer, D. R. Foster, D. Goldblum, J. L. Hart, A. E. Hessel, L.  
1881 R. Iverson, S. T. Jackson, D. Martin-Benito, B. C. McCarthy, R. W. McEwan, D. J.  
1882 Mladenoff, A. J. Parker, B. Shuman, and J. W. Williams. 2015. Climate remains an  
1883 important driver of post-European vegetation change in the eastern United States. *Global*  
1884 *Change Biology* 21:2105–2110.

1885 Phillips, R. P., Y. Ehlertz, R. Bier, and E. S. Bernhardt. 2008. New approach for capturing soluble  
1886 root exudates in forest soils. *Functional Ecology* 22:990–999.

1887 Pregitzer, K. S., and E. S. Euskirchen. 2004. Carbon cycling and storage in world forests: biome  
1888 patterns related to forest age. *Global Change Biology* 10:2052–2077.

1889 Raich, J. W., and K. J. Nadelhoffer. 1989. Belowground carbon allocation in forest ecosystems:  
1890 global trends. *Ecology* 70:1346–1354.

1891 Raymer, P. C. L., D. A. Orwig, and A. C. Finzi. 2013. Hemlock loss due to the hemlock woolly  
1892 adelgid does not affect ecosystem C storage but alters its distribution. *Ecosphere* 4:art63.

1893 R Core Team. 2016. R: A language and environment for statistical computing. R Foundation for  
1894 Statistical Computing, Vienna, Austria. <https://www.R-project.org>.

1895 Reich, P.B., Hobbie, S.E. and Lee, T.D., 2014. Plant growth enhancement by elevated CO<sub>2</sub>  
1896 eliminated by joint water and nitrogen limitation. *Nature Geoscience*, 7(12), p.920.

1897 Reichstein, M., E. Falge, D. Baldocchi, D. Papale, M. Aubinet, P. Berbigier, C. Bernhofer, N.  
1898 Buchmann, T. Gilmanov, A. Granier, T. Grunwald, K. Havrankova, H. Ilvesniemi, D.  
1899 Janous, A. Knohl, T. Laurila, A. Lohila, D. Loustau, G. Matteucci, T. Meyers, F. Miglietta,  
1900 J.-M. Ourcival, J. Pumpanen, S. Rambal, E. Rotenberg, M. Sanz, J. Tenhunen, G. Seufert, F.  
1901 Vaccari, T. Vesala, D. Yakir, and R. Valentini. 2005. On the separation of net ecosystem  
1902 exchange into assimilation and ecosystem respiration: review and improved algorithm.  
1903 *Global Change Biology* 11:1424–1439.

- 1904 Reichstein, M., A. M. Moffat, T. Wutzler, K. Sickel, O. Menzer, and M. Migliavacca. 2016.  
1905 REddyProc: Data processing and plotting utilities of (half-) hourly eddy-covariance  
1906 measurements. R package version 1.0.0. <http://cran.r-project.org/package=REddyProc>.
- 1907 Richardson, A. D., D. Y. Hollinger, J. D. Aber, S. V. Ollinger, and B. H. Braswell. 2007.  
1908 Environmental variation is directly responsible for short-but not long-term variation in  
1909 forest-atmosphere carbon exchange. *Global Change Biology* 13:788–803.
- 1910 Richardson, A. D., T. A. Black, P. Ciais, N. Delbart, M. A. Friedl, N. Gobron, D. Y. Hollinger,  
1911 W. L. Kutsch, B. Longdoz, S. Luysaert, M. Migliavacca, L. Montagnani, J. W. Munger, E.  
1912 Moors, S. Piao, C. Rebmann, M. Reichstein, N. Saigusa, E. Tomelleri, R. Vargas, and A.  
1913 Varlagin. 2010. Influence of spring and autumn phenological transitions on forest ecosystem  
1914 productivity. *Philosophical Transactions of the Royal Society of London. Series B,*  
1915 *Biological Sciences* 365:3227–3246.
- 1916 Ryan, M. G., D. Binkley, and J. H. Fownes. 1997. Age-related decline in forest productivity:  
1917 pattern and process. *Advances in Ecological Research* 27:213–262.
- 1918 Sanderman, J., T. Hengl, and G. J. Fiske. 2017. Soil carbon debt of 12,000 years of human land  
1919 use. *Proceedings of the National Academy of Sciences of the United States of America*  
1920 114:9575–9580.
- 1921 Sargent, M., S. C. Wofsy, and T. Nehrkorn. 2018. CO<sub>2</sub> observations, modeled emissions, and  
1922 NAM-HYSPLIT footprints, Boston MA, 2013–2014. ORNL DAAC, Oak Ridge, Tennessee,  
1923 USA. <https://doi.org/10.3334/ORNLDAAC/1586>
- 1924 Savage, K. E., W. J. Parton, E. A. Davidson, S. E. Trumbore, and S. D. Frey. 2013. Long-term  
1925 changes in forest carbon under temperature and nitrogen amendments in a temperate  
1926 northern hardwood forest. *Global Change Biology* 19:2389–2400.
- 1927 Scharlemann, J. P. W., E. V. J. Tanner, R. Hiederer, and V. Kapos. 2014. Global soil carbon:  
1928 understanding and managing the largest terrestrial carbon pool. *Carbon Management* 5:81–  
1929 91.
- 1930 Schimel, D. S. 1995. Terrestrial ecosystems and the carbon cycle. *Global Change Biology* 1:77–  
1931 91.
- 1932 Schlesinger, W. H., and E. S. Bernhardt. 2013. *Biogeochemistry: an analysis of global change,*  
1933 3<sup>rd</sup> ed. Academic press.

- 1934 Schulze, E. D. 1989. Air pollution and forest decline in a spruce (*Picea abies*) forest. *Science*  
1935 244:776–783.
- 1936 Schwalm, C. R., C. A. Williams, and K. Schaefer. 2011. Carbon consequences of global  
1937 hydrologic change, 1948–2009. *Journal of Geophysical Research* 116, G03042,  
1938 doi:10.1029/2011JG001674.
- 1939 Shuman, B. N., and J. Marsicek. 2016. The structure of Holocene climate change in mid-latitude  
1940 North America. *Quaternary Science Reviews* 141:38–51.
- 1941 Siccama, T. G., T. J. Fahey, C. E. Johnson, T. W. Sherry, E. G. Denny, E. Binney Girdler, G. E.  
1942 Likens, and P. A. Schwarz. 2007. Population and biomass dynamics of trees in a northern  
1943 hardwood forest at Hubbard Brook. *Canadian Journal of Forest Research* 37:737–749.
- 1944 Sierra, C. A., S. E. Trumbore, E. A. Davidson, S. D. Frey, K. E. Savage, and F. M. Hopkins.  
1945 2012. Predicting decadal trends and transient responses of radiocarbon storage and fluxes in  
1946 a temperate forest soil. *Biogeosciences* 9:3013–3028.
- 1947 SRCC. 2019. Southern Regional Climate Center – Climate Trends. Available from:  
1948 <http://charts.srcc.lsu.edu/trends/> (accessed 11 January 2019).
- 1949 Stephenson, N. L., A. J. Das, R. Condit, S. E. Russo, P. J. Baker, N. G. Beckman, D. A. Coomes,  
1950 E. R. Lines, W. K. Morris, N. Rüger, E. Álvarez, C. Blundo, S. Bunyavejchewin, G.  
1951 Chuyong, S. J. Davies, Á. Duque, C. N. Ewango, O. Flores, J. F. Franklin, H. R. Grau, Z.  
1952 Hao, M. E. Harmon, S. P. Hubbell, D. Kenfack, Y. Lin, J.-R. Makana, A. Malizia, L. R.  
1953 Malizia, R. J. Pabst, N. Pongpattananurak, S.-H. Su, I-F. Sun, S. Tan, D. Thomas, P. J. van  
1954 Mantgem, X. Wang, S. K. Wiser, and M. A. Zavala. 2014. Rate of tree carbon accumulation  
1955 increases continuously with tree size. *Nature* 507:90–93.
- 1956 Stoddard, J. L., D. S. Jeffries, A. Lükewille, T. A. Clair, P. J. Dillon, C. T. Driscoll, M. Forsius,  
1957 M. Johannessen, J. S. Kahl, J. H. Kellogg, A. Kemp, J. Mannio, D. T. Monteith, P. S.  
1958 Murdoch, S. Patrick, A. Rebsdorf, B. L. Skjelkvåle, M. P. Stainton, T. Traaen, H. van Dam,  
1959 K. E. Webster, J. Wieting, and A. Wilander. 1999. Regional trends in aquatic recovery from  
1960 acidification in North America and Europe. *Nature* 401:575–578.
- 1961 Strand, A. E., S. G. Pritchard, M. L. McCormack, M. A. Davis, and R. Oren. 2008. Irreconcilable  
1962 differences: fine-root life spans and soil carbon persistence. *Science* 319:456–458.



- 1963 Tang, G., B. Beckage, and B. Smith. 2014. Potential future dynamics of carbon fluxes and pools  
1964 in New England forests and their climatic sensitivities: A model-based study. *Global*  
1965 *Biogeochemical Cycles* 28:286–299.
- 1966 Tans, P., and R. Keeling. 2019. Trends in atmospheric carbon dioxide.  
1967 <https://www.esrl.noaa.gov/gmd/ccgg/trends/data.html> (accessed 27 November 2019).
- 1968 Teets, A., S. Fraver, D. Y. Hollinger, A. R. Weiskittel, R. S. Seymour, and A. D. Richardson.  
1969 2018. Linking annual tree growth with eddy-flux measurements of net ecosystem  
1970 productivity across twenty years of observation in a mixed conifer forest. *Agricultural and*  
1971 *Forest Meteorology* 249:479–487.
- 1972 Thomas, R. Q., C. D. Canham, K. C. Weathers, and C. L. Goodale. 2010. Increased tree carbon  
1973 storage in response to nitrogen deposition in the US. *Nature Geoscience* 3:13–17.
- 1974 Thompson, J. R., D. R. Foster, R. Scheller, and D. Kittredge. 2011. The influence of land use and  
1975 climate change on forest biomass and composition in Massachusetts, USA. *Ecological*  
1976 *Applications* 21:2425–2444.
- 1977 Thompson, J. R., D. N. Carpenter, C. V. Cogbill, and D. R. Foster. 2013. Four centuries of  
1978 change in northeastern United States forests. *PLoS ONE* 8:e72540.
- 1979 Thompson, J. R., C. D. Canham, L. Morreale, D. B. Kittredge, and B. Butler. 2017. Social and  
1980 biophysical variation in regional timber harvest regimes. *Ecological Applications* 27:942–  
1981 955.
- 1982 Tierney, G. L., and T. J. Fahey. 2002. Fine root turnover in a northern hardwood forest: a direct  
1983 comparison of the radiocarbon and minirhizotron methods. *Canadian Journal of Forest*  
1984 *Research* 32:1692–1697.
- 1985 Turnbull, M. H., D. Whitehead, D. T. Tissue, W. S. Schuster, K. J. Brown, V. C. Engel, and K.  
1986 L. Griffin. 2002. Photosynthetic characteristics in canopies of *Quercus rubra*, *Quercus*  
1987 *prinus* and *Acer rubrum* differ in response to soil water availability. *Oecologia* 130:515–  
1988 524.
- 1989 Urbano, A. R., and W. S. Keeton. 2017. Carbon dynamics and structural development in  
1990 recovering secondary forests of the northeastern U.S. *Forest Ecology and Management*  
1991 392:21–35.
- 1992 Urbanski, S., C. Barford, S. Wofsy, C. Kucharik, E. Pyle, J. Budney, K. McKain, D. Fitzjarrald,  
1993 M. Czikowsky, and J. W. Munger. 2007. Factors controlling CO<sub>2</sub> exchange on timescales

- 1994 from hourly to decadal at Harvard Forest. *Journal of Geophysical Research* 112, G02020,  
1995 doi:10.1029/2006JG000293.
- 1996 Waller, K., C. Driscoll, J. Lynch, D. Newcomb, and K. Roy. 2012. Long-term recovery of lakes  
1997 in the Adirondack region of New York to decreases in acidic deposition. *Atmospheric*  
1998 *Environment* 46:56–64.
- 1999 Wang, W. J., H. S. He, F. R. Thompson, J. S. Fraser, and W. D. Dijak. 2017. Changes in forest  
2000 biomass and tree species distribution under climate change in the northeastern United States.  
2001 *Landscape Ecology* 32:1399–1413.
- 2002 Wehr, R., J. W. Munger, J. B. McManus, D. D. Nelson, M. S. Zahniser, E. A. Davidson, S. C.  
2003 Wofsy, and S. R. Saleska. 2016. Seasonality of temperate forest photosynthesis and daytime  
2004 respiration. *Nature* 534:680–683.
- 2005 Williams, C. A., G. James Collatz, J. Masek, and S. N. Goward. 2012. Carbon consequences of  
2006 forest disturbance and recovery across the conterminous United States. *Global*  
2007 *Biogeochemical Cycles* 26, GB1005, doi:10.1029/2010GB003947.
- 2008 Williams, C. A., M. K. Vanderhoof, M. Khomik, and B. Ghimire. 2013. Post-clearcut dynamics  
2009 of carbon, water and energy exchanges in a midlatitude temperate, deciduous broadleaf  
2010 forest environment. *Global Change Biology* 20:992–1007.
- 2011 Williams, C. A., H. Gu, R. MacLean, J. G. Masek, and G. James Collatz. 2016. Disturbance and  
2012 the carbon balance of US forests: A quantitative review of impacts from harvests, fires,  
2013 insects, and droughts. *Global and Planetary Change* 143:66–80.
- 2014 Wilson, H. F., J. E. Saiers, P. A. Raymond, and W. V. Sobczak. 2013. Hydrologic drivers and  
2015 seasonality of dissolved organic carbon concentration, nitrogen content, bioavailability, and  
2016 export in a forested New England stream. *Ecosystems* 16:604–616.
- 2017 Wofsy, S. C., M. L. Goulden, J. W. Munger, S.-M. Fan, P. S. Bakwin, B. C. Daube, S. L.  
2018 Bassow, and F. A. Bazzaz. 1993. Net exchange of CO<sub>2</sub> in a mid-latitude forest. *Science*  
2019 260:1314–1317.
- 2020 Yang, X., J. F. Mustard, J. Tang, and H. Xu. 2012. Regional-scale phenology modeling based on  
2021 meteorological records and remote sensing observations. *Journal of Geophysical Research:*  
2022 *Biogeosciences* 117, G03029, doi:10.1029/2012JG001977.
- 2023 Zhou, G., S., Z. Li, D. Zhang, X. Tang, C. Zhou, J. Yan, and J. Mo. 2006. Old-growth forests can  
2024 accumulate carbon in soils. *Science* 314:1417.

2025 Zhou, Z., S. V. Ollinger, and L. C. Lepine. 2018. Landscape variation in canopy nitrogen and  
2026 carbon assimilation in a temperate mixed forest. *Oecologia* 188:595–606.

2027

2028 **Data Availability**

2029 Data are publicly available from the Environmental Data Initiative:

2030 <https://doi.org/10.6073/pasta/e7113c9ea3ec7f99e400f2f0bc662c02>

2031

2032 **Table 1.** List of abbreviations used.

2033

Abbreviation	Definition	Units
$A_{\max}$	Ecosystem photosynthetic capacity	$\mu\text{mol C m}^{-2} \text{ s}^{-1}$
ANPP	Aboveground net primary production	$\text{g C m}^{-2} \text{ yr}^{-1}$
BNPP	Belowground net primary production	$\text{g C m}^{-2} \text{ yr}^{-1}$
C	Carbon	-
CC	Clear-cut (flux tower site)	-
CWD	Coarse woody debris	-
DBH	Diameter at breast height	cm
DOC	Dissolved organic carbon	$\text{g C m}^{-2}$
DOY	Day of year	-
EC	Eddy covariance	-
ECM	Ectomycorrhizal	-
EMS	Environmental Measurement Site (flux tower site)	-
FCRN	Fluxnet-Canada Research Network	-
FIA	Forest Inventory and Analysis	-
$\text{FR}_{\text{mass}}$	Fine root biomass	$\text{g C m}^{-2}$
$\text{FR}_{\text{production}}$	Fine root production	$\text{g C m}^{-2} \text{ yr}^{-1}$
$\text{FR}_{\text{turnover time}}$	Fine root turnover time	yr
FWD	Fine woody debris	-
GPP	Gross primary production	$\text{g C m}^{-2} \text{ yr}^{-1}$
GSL	Growing season length	d

HEM	Hemlock (flux tower site)	-
LAI	Leaf area index	m <sup>2</sup> leaves m <sup>-2</sup> ground
LTER	Long-Term Ecological Research	-
LUE	Light use efficiency	μmol C μmol <sup>-1</sup> PPFD
MAP	Mean annual precipitation	mm
MAT	Mean annual temperature	°C
N	Nitrogen	-
NEE	Net ecosystem exchange	g C m <sup>-2</sup> yr <sup>-1</sup>
NEP	Net ecosystem production	g C m <sup>-2</sup> yr <sup>-1</sup>
NPP	Net primary production	g C m <sup>-2</sup> yr <sup>-1</sup>
PAI	Plant area index	m <sup>2</sup> plant tissue m <sup>-2</sup> ground
PI	Principal investigator	-
PPFD	Photosynthetic photon flux density	μmol photon m <sup>-2</sup> s <sup>-1</sup>
R <sub>a</sub>	Autotrophic respiration	g C m <sup>-2</sup> yr <sup>-1</sup>
R <sub>above</sub>	Aboveground respiration	g C m <sup>-2</sup> yr <sup>-1</sup>
R <sub>e</sub>	Ecosystem respiration	g C m <sup>-2</sup> yr <sup>-1</sup>
R <sub>h</sub>	Heterotrophic respiration	g C m <sup>-2</sup> yr <sup>-1</sup>
R <sub>r</sub>	Root respiration	g C m <sup>-2</sup> yr <sup>-1</sup>
R <sub>s</sub>	Soil respiration	g C m <sup>-2</sup> yr <sup>-1</sup>
SD	Standard deviation	-
SE	Standard error	-
SOC	Soil organic carbon	-
WUE	Water use efficiency	-

2034

2035

2036 **Table 2.** Contemporary C stocks for mature hemlock- and hardwood-dominated stands at the  
 2037 Harvard Forest. Units are g C m<sup>-2</sup> ± SD (*n*). Carbon stocks for aboveground live biomass and  
 2038 coarse roots are based on the most recent plot measurements (2008–2015, depending on the  
 2039 study), since these C pools have increased over the study period. All other C pools are based on  
 2040 means across all plots and years of measurement. The hemlock and hardwood means are  
 2041 significantly different at  $p < 0.05$  (\*),  $p < 0.01$  (\*\*),  $p < 0.001$  (\*\*\*), or not tested (†).

Component	Hemlock	Hardwood
Aboveground live biomass		
Wood + Foliage <sup>1</sup> *	14,007 ± 3,838 (34)	11,952 ± 3,730 (81)
Woody debris total†	2,047 ± 986	2,076 ± 1,248
Coarse woody debris (>7.5 cm diameter)*	643 ± 562 (38)	987 ± 955 (160)
Fine woody debris (0.6–7.5 cm diameter)***	344 ± 182 (35)	203 ± 135 (170)
Standing dead wood	1,060 ± 790 (38)	886 ± 792 (154)
Fine roots total†	547 ± 149	416 ± 118
Fine roots organic horizon***	148 ± 85 (73)	100 ± 45 (134)
Fine roots mineral horizon 0–15 cm	177 ± 80 (102)	191 ± 109 (200)
Fine roots mineral horizon 15–30 cm	117 ± 84 (23)	70 ± 8 (4)
Fine roots mineral horizon 30–45 cm*	105 ± 40 (8)	55 ± 6 (4)
Coarse roots total <sup>1</sup> ***	2,913 ± 811 (34)	2,285 ± 707 (81)
Soil total†	15,059 ± 3,548	12,851 ± 2,560
Soil organic horizon***	4,305 ± 2,624 (54)	2,700 ± 1,322 (145)
Soil mineral horizon 0–15 cm	5,170 ± 1,931 (98)	5,324 ± 1,649 (291)
Soil mineral horizon 15–30 cm	3,052 ± 1,326 (22)	2,907 ± 1,032 (30)
Soil mineral horizon 30–45 cm*	2,532 ± 464 (8)	1,920 ± 1,010 (21)
Total C content†	34,573 ± 5,382	29,580 ± 4,747
Distribution (% of total)		
Live aboveground	40%	40%
Woody debris	6%	7%
Roots	10%	9%
Soils	44%	44%

2042 <sup>1</sup>Based on allometric equations.

2043 **Table 3.** Average rates of net primary production for mature hemlock- and hardwood-dominated  
2044 stands throughout the Harvard Forest. Units are g C m<sup>-2</sup> yr<sup>-1</sup> ± 1 SD (*n*, plot × year). The hemlock  
2045 and hardwood means are significantly different at *p* < 0.05 (\*), *p* < 0.01 (\*\*), *p* < 0.001 (\*\*\*), or  
2046 not tested (†).

Flux	Hemlock	Hardwood
Aboveground biomass increment [wood + foliar increment] (1998 – 2014) <sup>†</sup>	166 ± 99 (191)	200 ± 118 (508)
Foliar litterfall	157 ± 49 (204)	160 ± 36 (681)
Non-foliar litterfall <sup>***</sup>	74 ± 68 (204)	41 ± 29 (681)
Litterfall total (1989 – 2015) <sup>1 ***</sup>	231 ± 94 (204)	201 ± 51 (681)
<b>Aboveground net primary production (ANPP)<sup>†</sup></b>	<b>397 ± 137</b>	<b>401 ± 129</b>
Fine root net primary production (<2mm) <sup>2†</sup>	218 ± 174	225 ± 136
Coarse root biomass increment (1998 – 2014)	34 ± 20 (191)	38 ± 23 (508)
Root exudates (2010 – 2013)	97 ± 88 (8)	69 ± 56 (14)
<b>Belowground net primary production (BNPP)<sup>†</sup></b>	<b>349 ± 196</b>	<b>332 ± 149</b>
<b>Total net primary production (NPP)<sup>†</sup></b>	<b>746 ± 239</b>	<b>733 ± 197</b>

2048 <sup>1</sup> Before calculating the mean foliar, non-foliar, and total litterfall of all studies listed in  
 2049 Appendix S1: Table S5, we estimated the fractions of foliar and non-foliar litterfall for the  
 2050 studies where both components were reported and applied them to the studies where only foliar  
 2051 or total litterfall was reported.

2052 <sup>2</sup> Fine root net primary production in hardwood forests is the average of estimates from  
 2053 McClaugherty et al. (1982), Gaudinski et al. (2010), and Abramoff and Finzi (2016). Fine root  
 2054 net primary production in hemlock forests is based on data from Abramoff and Finzi (2016); no  
 2055 other data were available for this type of forest.

2056 **Table 4.** C fluxes within the EMS and HEM tower footprints only. NEP, GPP,  $R_e$ , and  $R_s$  are the average of 1992–2015 (EMS) and  
 2057 2005–2012 (HEM). Units are  $g\ C\ m^{-2}\ yr^{-1} \pm 1\ SD\ (n; plot \times year)$ . The hemlock and hardwood means are significantly different at  $p <$   
 2058  $0.05$  (\*),  $p < 0.01$  (\*\*),  $p < 0.001$  (\*\*\*), or not tested (†). The uncertainty for the eddy-flux data includes interannual variability, but  
 2059 not gap-filling uncertainty. As discussed in the text, there is more gap-filling in the HEM tower data than the EMS tower data.  
 2060

		HEM	EMS
Input flux	Gross primary production (GPP; tower-calculated)	1,441 ± 97 (8)	1,526 ± 227 (24)
Net primary production	Total net primary production (NPP)†	688 ± 197	678 ± 182
	<b>Aboveground</b>		
	Wood + foliage (plot-measured, allometries)	158 ± 84 (124)	199 ± 119 (575)
	Foliar litterfall*** (plot-measured)	182 ± 58 (84)	149 ± 34 (416)
	Non-foliar litterfall*** (plot-measured)	89 ± 72 (84)	41 ± 28 (416)
	Litterfall total <sup>1</sup> ***	271 ± 109 (84)	191 ± 44 (416)
	Aboveground net primary production (ANPP)†	429 ± 138	390 ± 127
	<b>Belowground</b>		
	Fine root net primary production <sup>2</sup> †	129 ± 107	199 ± 110
	Coarse root biomass increment (estimated from allometries)	33 ± 18 (124)	38 ± 23 (575)
	Root exudates	97 ± 88 (8)	51 ± 65 (6)
	Belowground net primary production (BNPP)†	259 ± 140	288 ± 130
Soil sequestration	OH to 50 cm depth (isotope-estimated) <sup>3</sup>	20 ± 10	20 ± 10

Output flux	Tower-based ecosystem respiration ( $R_{e, \text{tower}}$ )*	$976 \pm 82$ (8)	$1,228 \pm 255$ (24)
Component fluxes	Soil respiration ( $R_s$ )* (chamber measurement)	$682 \pm 27$ (8)	$727 \pm 54$ (24)
	Aboveground respiration ( $R_{\text{above}}$ ): $R_e - R_s$	$294 \pm 86$ (8)	$501 \pm 261$ (24)
	Autotrophic respiration ( $R_a$ ): $GPP - NPP - \text{soil}$ sequestration	$733 \pm 220$	$828 \pm 291$
	Root respiration ( $R_r$ ): $R_a - R_{\text{above}}$	$439 \pm 236$	$327 \pm 391$
	Heterotrophic respiration ( $R_h$ ): $R_s - R_r$	$243 \pm 238$	$400 \pm 395$
Net ecosystem production (NEP)	Tower-based [ $NEP_{\text{tower}}$ ]	$465 \pm 83$ (8)	$298 \pm 153$ (24)
	Inventory-based [ $NEP_{\text{inv}}$ ]: Net change in live biomass + net change in soil C	$183 \pm 109$	$190 \pm 82$
	Comparison of NEP calculations: $NEP_{\text{tower}} -$ $NEP_{\text{inv}}$	$282 \pm 137$	$108 \pm 174$
	Percentage NEP difference (relative to tower)	61	36

2061 <sup>1</sup> Before calculating the mean foliar, non-foliar, and total litterfall of all studies listed in Appendix S1: Table S5, we estimated the  
 2062 fractions of foliar and non-foliar litterfall for the studies where both components were reported and applied them to the studies where  
 2063 only foliar or total litterfall was reported.

2064 <sup>2</sup> Between the top of the organic horizon and 15 cm depth in the mineral soil. Fine root net primary production in the EMS tower  
 2065 footprint is the average of estimates from McLaugherty et al. (1982), Gaudinski et al. (2010), and Abramoff and Finzi (2016). Fine  
 2066 root net primary production in the HEM tower footprint is based on data from Abramoff and Finzi (2016); no other data were  
 2067 available for this location.

2068 <sup>3</sup> We assume a standard deviation equal to 50% of the mean value of the range reported by Gaudinski et al. (2000).



2069 **Figure legends**

2070 **Figure 1.** a) A timeline of ecosystem C measurements at the Harvard Forest. The timeline is  
2071 divided into biomass components, soil components, fluxes, and global change experiments.  
2072 Lines indicate measurements across all studies. Asterisks on the mineral SOC line indicate the  
2073 years in which mineral soil C sampling was repeated in the same set of plots. b) Map of the  
2074 Harvard Forest tracts, eddy-flux towers, and plots. The types of measurements collected varied  
2075 across plots and studies; for plots with aboveground biomass measurements, forest type was  
2076 determined using *k*-means cluster analysis.

2077  
2078 **Figure 2.** Regional comparison of production and C stocks in biomass. Distribution of C in  
2079 biomass in FIA plots (black dots) within EPA ecoregions 58g and 59b (green polygon) is lower  
2080 than that at the Harvard Forest (red outline). GPP estimated from AVIRIS (blue box) does not  
2081 differ between the Harvard Forest and full AVIRIS footprint.

2082  
2083 **Figure 3.** Long-term (1964–2015) annual mean air temperature (a) and total precipitation (b) at  
2084 the Harvard Forest. Also presented are trends in annual mean CO<sub>2</sub> concentration (c) at the Mauna  
2085 Loa Observatory (1959–2015), ground-level O<sub>3</sub> concentration (d) in Ware Center, MA, 25 km  
2086 south of the Harvard Forest (1981–2015), and total N deposition (e) and SO<sub>4</sub><sup>2-</sup> deposition (f) at  
2087 the Quabbin Reservoir, 17 km southwest of the Harvard Forest (1982–2015). Statistically  
2088 significant ( $p < 0.05$ ) linear relationships in (a), (b), (d), (e), and (f) are shown for the full record  
2089 (solid lines) and for the period of interest for this study (1992–2015; dashed lines).

2090  
2091 **Figure 4.** (a) Changes in aboveground carbon stocks (mean  $\pm$  SD) of the four major tree species  
2092 at the Harvard Forest, based on 60 plots distributed across the Prospect Hill Tract (the  
2093 PHOREST study). The plots were originally sampled in 1937, the year prior to a major hurricane  
2094 that resulted in 70% loss of timber volume at the Harvard Forest. Through time stand biomass  
2095 has steadily increased with red oak emerging as the dominant species. (b) Tree-ring analysis  
2096 shows annual aboveground carbon increment of trees in the oak–maple-dominated Lyford Plot  
2097 and EMS plots. Red oak dominated biomass increment at this site for the past >50 years, with  
2098 minor contributions from red maple and other species. There was a drought in the mid-1960s,  
2099 and a severe gypsy moth defoliation in 1981.

2100

2101 **Figure 5.** Components of NPP at the Harvard Forest over time for hardwood-dominated plots: a)  
2102 biomass increment (aboveground and coarse roots), SE of slope = 1.22,  $p < 0.001$ ,  $\text{Adj-}r^2 = 0.07$ ;  
2103 b) foliar litter production, SE of slope = 0.37,  $p < 0.001$ ,  $\text{Adj-}r^2 = 0.05$ ; c) NPP combining woody  
2104 increment aboveground, coarse root increment, and total litter production, SE of slope = 3.3,  $p =$   
2105 0.016,  $\text{Adj-}r^2 = 0.32$ . Data for total litterfall began in 1999 for the hardwood plots, which is why  
2106 panel (c) shows data only from 2000–2014.

2107

2108 **Figure 6.** Components of NPP at the Harvard Forest over time for hemlock-dominated plots: a)  
2109 biomass increment (aboveground and coarse roots); b) foliar litter production; c) NPP combining  
2110 woody increment aboveground, coarse root increment, and total litter production. None of these  
2111 showed a significant trend over time. Data for total litterfall began in 2005 for the hemlock plots,  
2112 which is why panel (c) shows data only from 2006–2014.

2113

2114 **Figure 7.** Cumulative (a) and annual (b) net ecosystem production and its component fluxes  $R_e$   
2115 (c) and GPP (d). Star symbols represent years during which hemlocks were in decline. The black  
2116 lines in (b–d) represent the significant (solid) or non-significant (dashed) trends in increasing  
2117 NEP,  $R_e$ , and GPP with time at the EMS site (NEP:  $\text{Adj-}r^2 = 0.06$ ,  $p = 0.127$ ;  $R_e$ :  $\text{Adj-}r^2 = 0.17$ ,  $p$   
2118 = 0.026; GPP:  $\text{Adj-}r^2 = 0.51$ ,  $p < 0.001$ ).

2119

2120 **Figure 8.** Notable features of the eddy-covariance and plant-area index data sets. July GPP as a  
2121 function of photosynthetic photon flux density for the (a) HEM, (b) EMS, and (c) CC tower sites.  
2122 The fitted lines model light-use-efficiency using Eq. 3. Data were averaged within 50  $\mu\text{mol}$   
2123  $\text{photon m}^{-2} \text{s}^{-1}$  bins of PPFD. (d) The seasonal time course of LAI at the EMS site, and (e)  
2124 median July mid-day GPP as a function of plant area index. Data from the HEM site are  
2125 restricted to the time before clear sign of HWA-associated decline (2005–2012). The black line  
2126 in (e) is the regression between CC-tower PAI and GPP.

2127

2128 **Figure 9.** Relationship between (a) NEP and LUE ( $\text{Adj-}r^2 = 0.13$ ,  $p = 0.045$ ), (b) GPP and  $A_{\text{max}}$   
2129 ( $\text{Adj-}r^2 = 0.20$ ,  $p = 0.018$ ), (c) NEP and PAI ( $\text{Adj-}r^2 = 0.23$ ,  $p = 0.035$ ), and (d) NEP and red oak  
2130 tree-ring-based biomass increment ( $\text{Adj-}r^2 = 0.35$ ,  $p = 0.003$ ) at the EMS site.

2131  
2132 **Figure 10.** Median daily fluxes of C at the (a) EMS and (b) HEM sites. The data in this figure  
2133 were first published in Giasson et al. (2013) but were updated through the end of 2015.  
2134 Ecosystem respiration is based on new data from the two eddy-covariance tower sites. No  
2135 additional soil respiration data have been collected since Giasson et al. (2013) and the time series  
2136 is extended based on an empirical model fit between flux and soil temperature data collected  
2137 between 1992 and 2010 (see Figure A4 in Giasson et al. 2013). For the HEM site, data from the  
2138 period during which hemlocks were declining (2013–2015) were not used. The shaded regions  
2139 above and below the points reflect 1 SD of the average daily flux across the 24- and 8-year  
2140 records, respectively. Soil temperature was measured 20 cm below the soil surface at the EMS  
2141 site and 10 cm below the surface at the HEM site. (c) The ratio of soil and total ecosystem  
2142 respiration at the two sites. The median daily (d) ecosystem respiration, (e) soil respiration, and  
2143 (f) aboveground respiration at the EMS and HEM sites. Open symbols represent the HEM site  
2144 and closed symbols the EMS site. In (c), star symbols indicate years during which hemlocks  
2145 were in decline.

2146  
2147 **Figure 11.** Mean daily DBH increment ( $\text{mm d}^{-1}$ ), mean daily aboveground respiration ( $R_{\text{above}}$ ,  $\text{g}$   
2148  $\text{C m}^{-2} \text{d}^{-1}$ ), and plant area index (PAI,  $\text{m}^2 \text{m}^{-2}$ ) at the EMS site for 1998–2003 and 2006. A total  
2149 of 1320 trees ( $>5 \text{ cm DBH}$ ) of 16 species were measured 6–19 times per year.

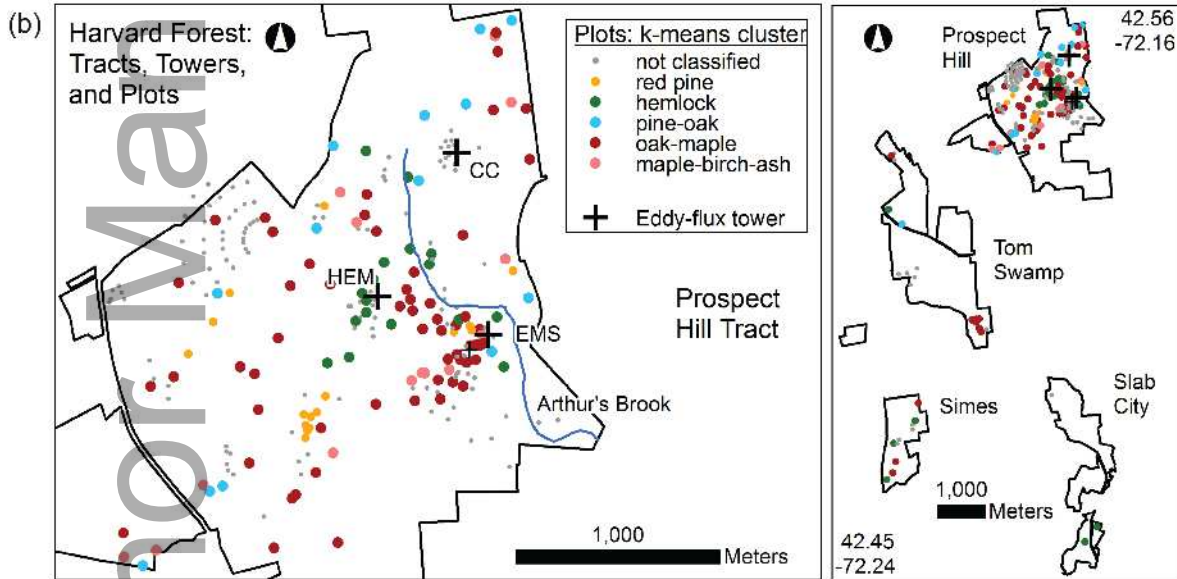
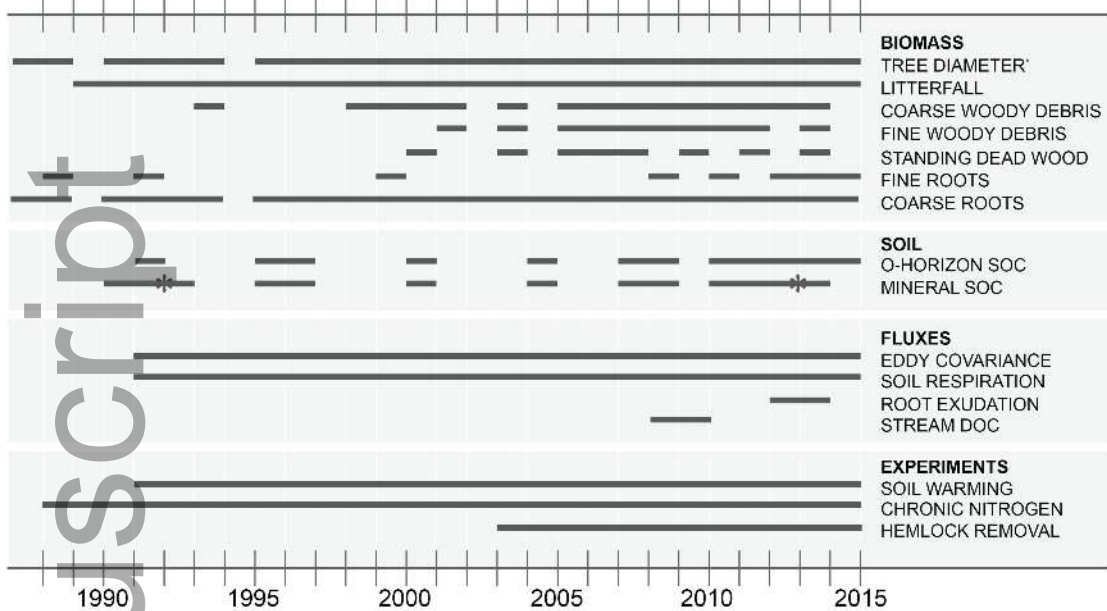
2150  
2151 **Figure 12.** Climate metrics at the Harvard Forest. Start and end dates of the growing season and  
2152 the length of the growing season at the (a) EMS and (b) HEM eddy-covariance sites. All  
2153 regressions for the EMS site are statistically significant ( $\text{Adj-}r^2 = 0.15$ ,  $p = 0.0351$ ;  $\text{Adj-}r^2 = 0.13$ ,  
2154  $p = 0.0459$ ;  $\text{Adj-}r^2 = 0.27$ ,  $p = 0.0052$  for the start, end, and length of the growing season,  
2155 respectively). No regression was statistically significant at the HEM site ( $\text{Adj-}r^2 = 0.03$ ,  $p =$   
2156  $0.310$ ;  $\text{Adj-}r^2 = -0.09$ ,  $p = 0.531$ ;  $\text{Adj-}r^2 = -0.01$ ,  $p = 0.368$  for the start, end, and length of the  
2157 growing season, respectively). The 95% confidence interval of the slopes are indicated. Solid  
2158 lines show statistically significant relationships and dashed lines insignificant ones.

2159  
2160 **Figure 13.** Relationship between the date of the onset of the growing season and springtime NEP  
2161 for the EMS (a) and HEM (b) sites. Also, relationship between the date of the end of the growing

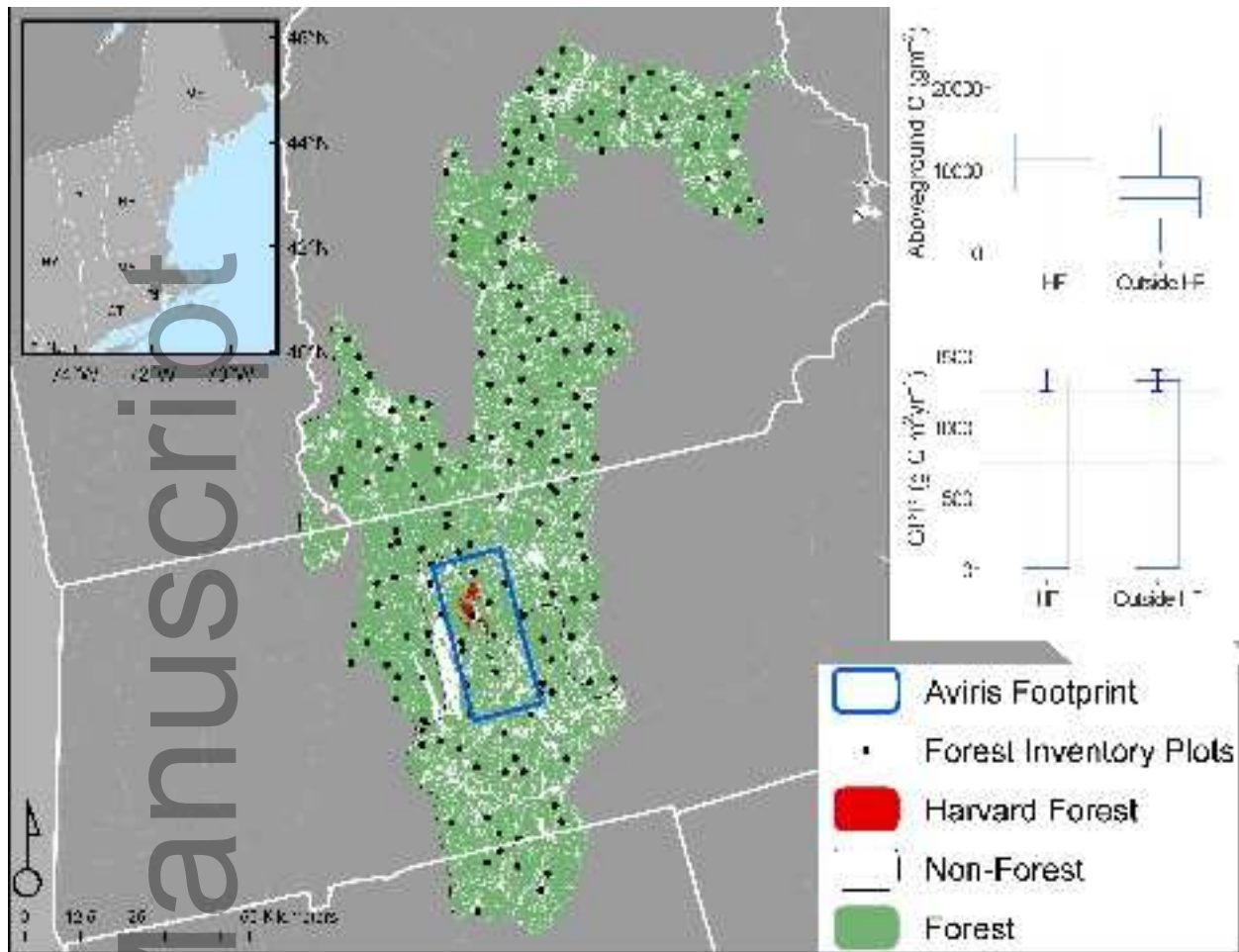
2162 season and autumn NEP for the EMS (c) and HEM (d) sites. The onset of the growing season is  
2163 defined as the first day of the year when daily NEP was above a threshold of 30% of the mean  
2164 maximum daily NEP. Similarly, the last day when NEP was above the threshold was considered  
2165 the end of the growing season. Spring is defined as March–May and autumn is September–  
2166 November. Regressions are statistically significant (EMS-spring:  $\text{Adj-}r^2 = 0.27$ ,  $p = 0.006$ ; EMS-  
2167 autumn:  $\text{Adj-}r^2 = 0.61$ ,  $p < 0.001$ ; HEM-spring:  $\text{Adj-}r^2 = 0.42$ ,  $p = 0.049$ ) except in the autumn at  
2168 the HEM site ( $\text{Adj-}r^2 = 0.02$ ,  $p = 0.333$ ). The 95% confidence interval of the slopes are indicated.  
2169 Solid and dashed lines represent significant and insignificant relationships, respectively.

(a) HARVARD FOREST  
CARBON DATA SETS

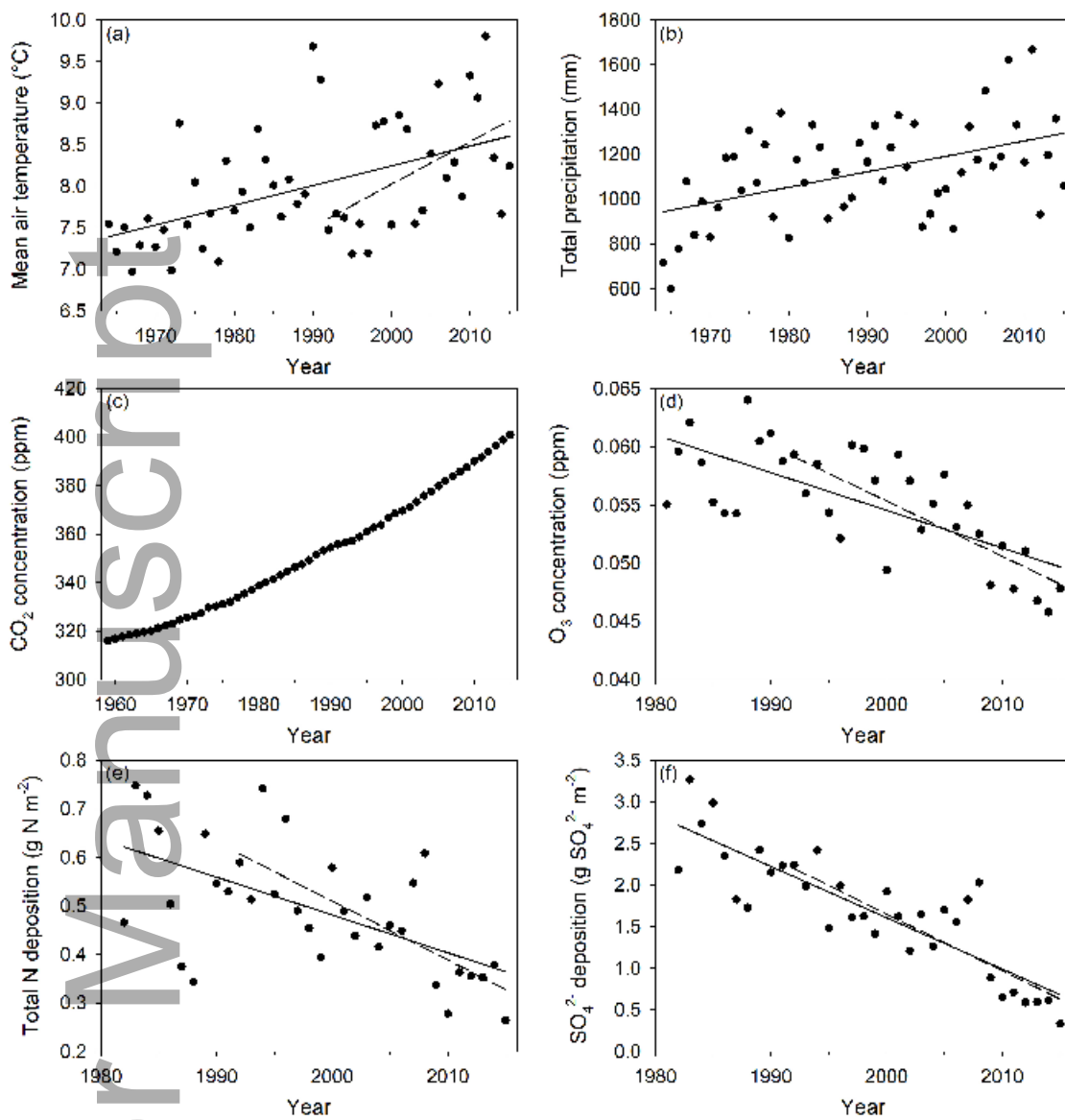
Ongoing measurements for all variables extend through the present. Tree diameter also available for 1937, 1969, and 1975.



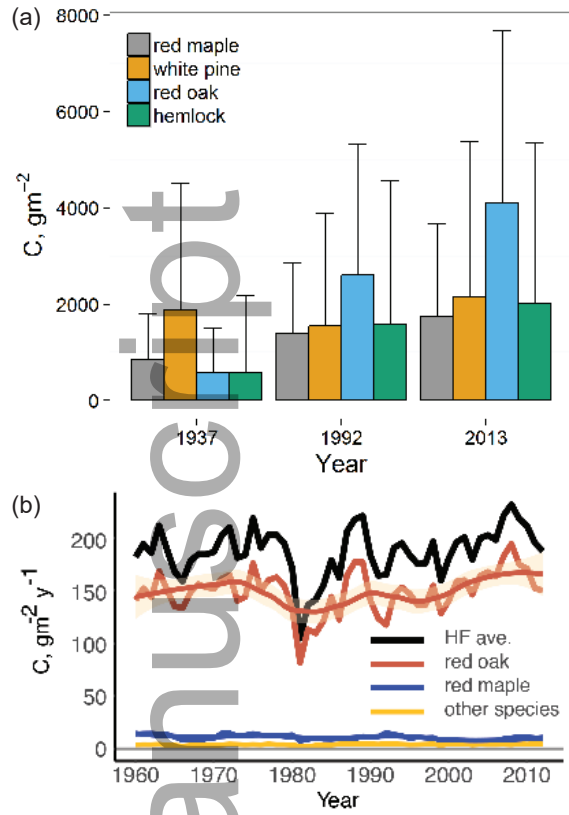
ecm\_1423\_f1.tif



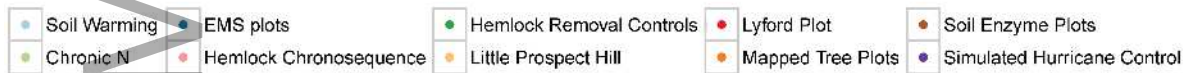
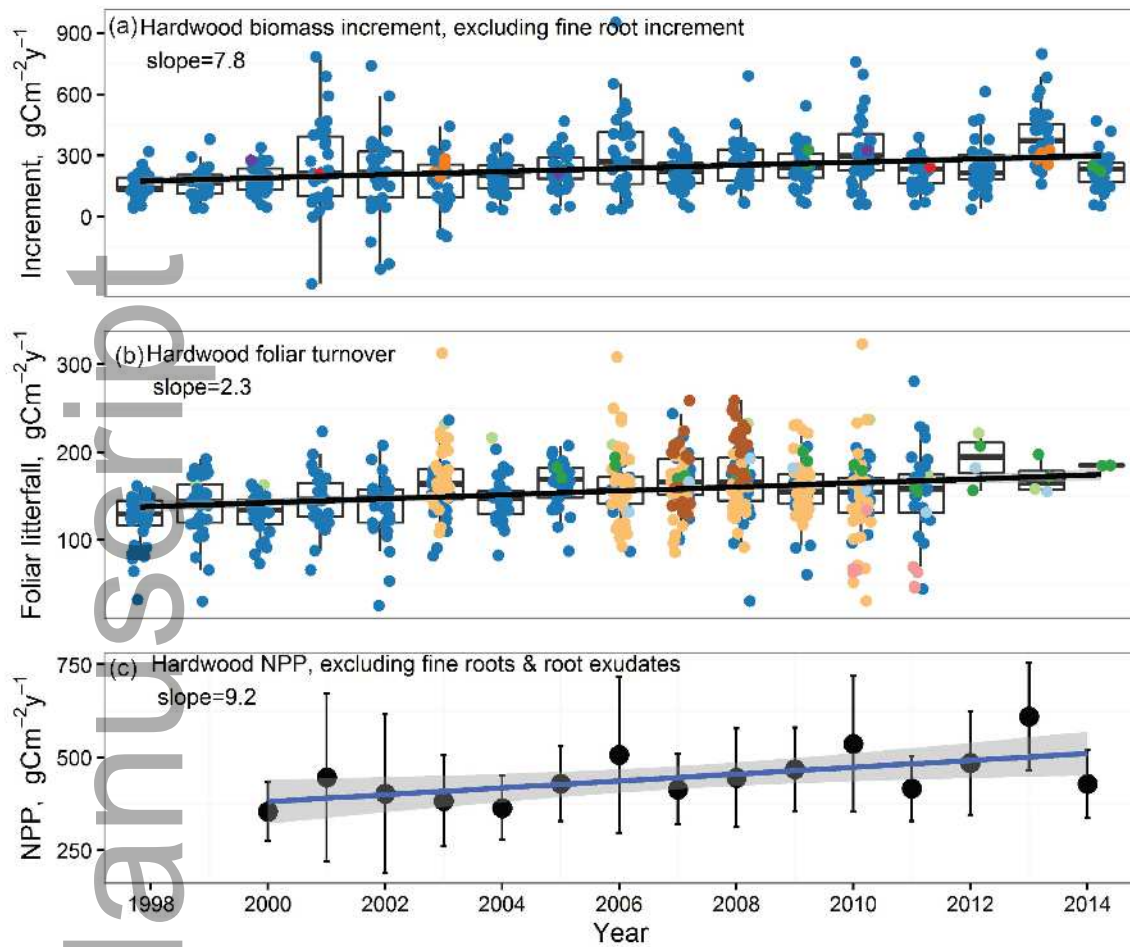
ecm\_1423\_f2.jpg



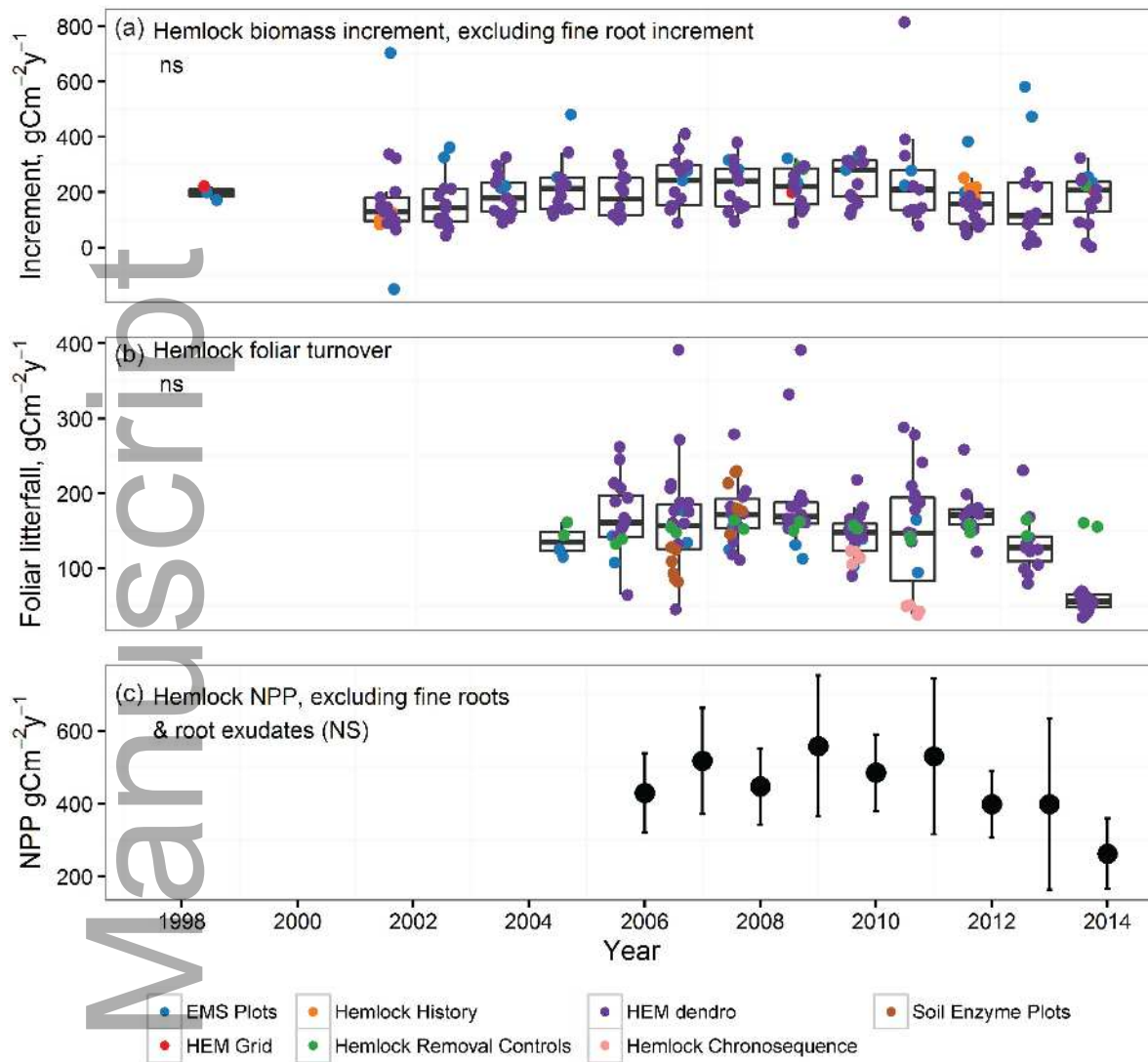
ecm\_1423\_f3.jpg



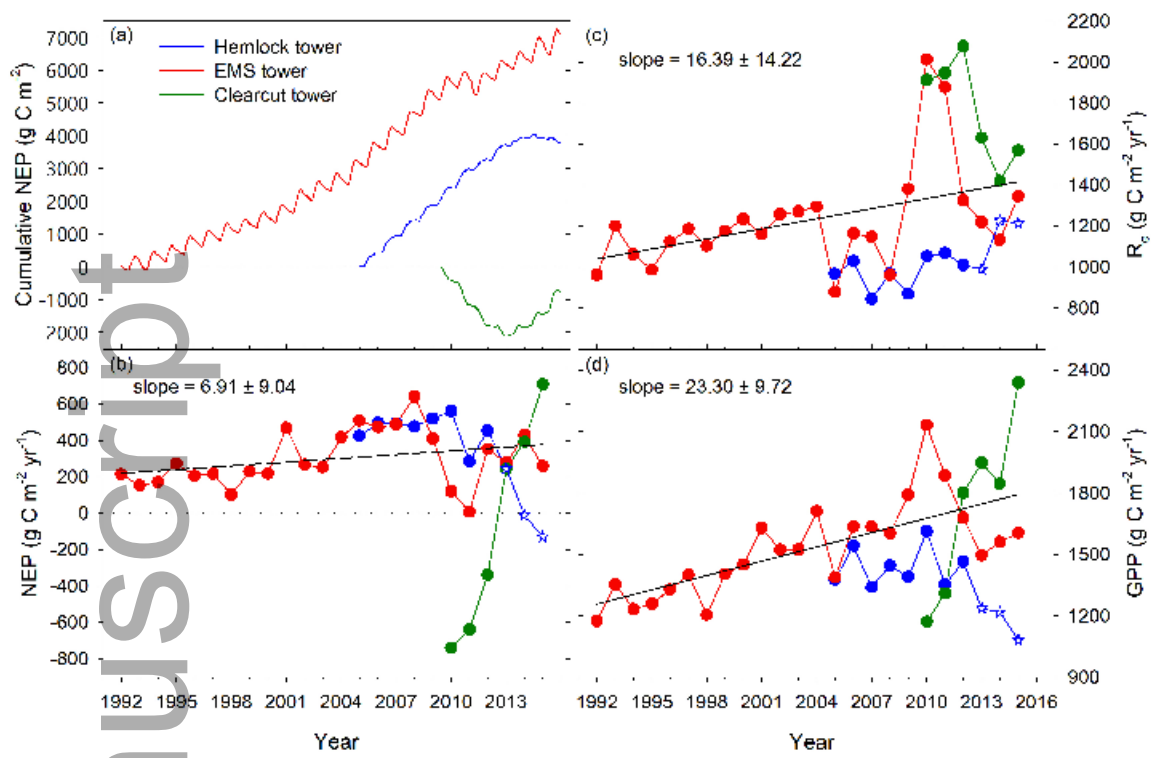




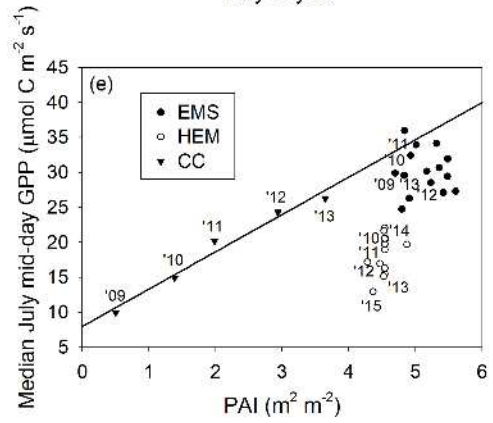
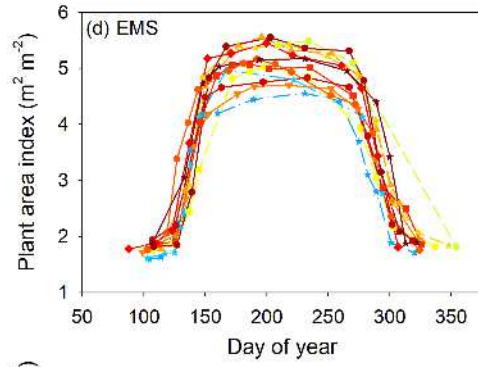
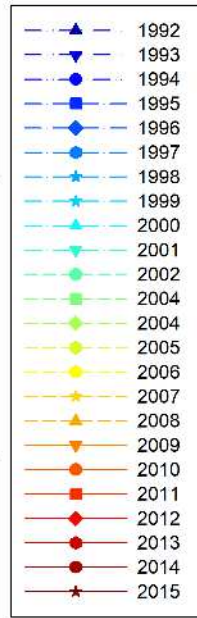
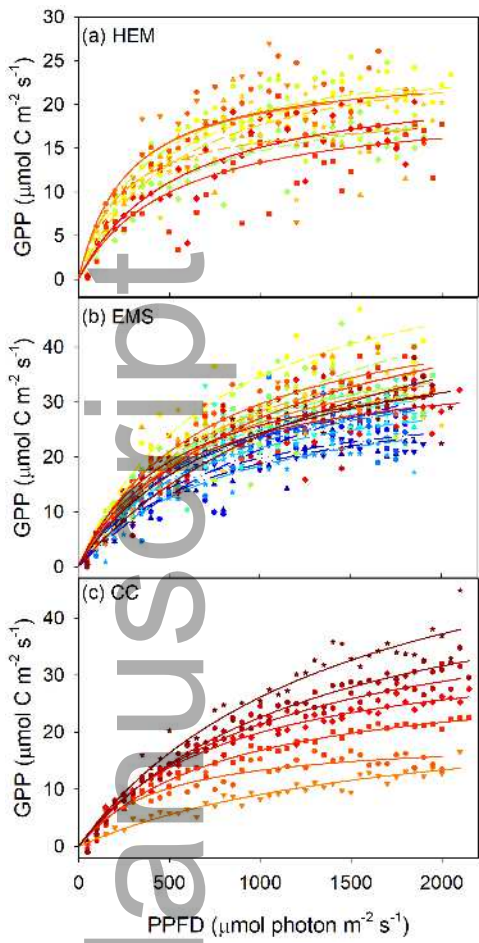
ecm\_1423\_f5.tif



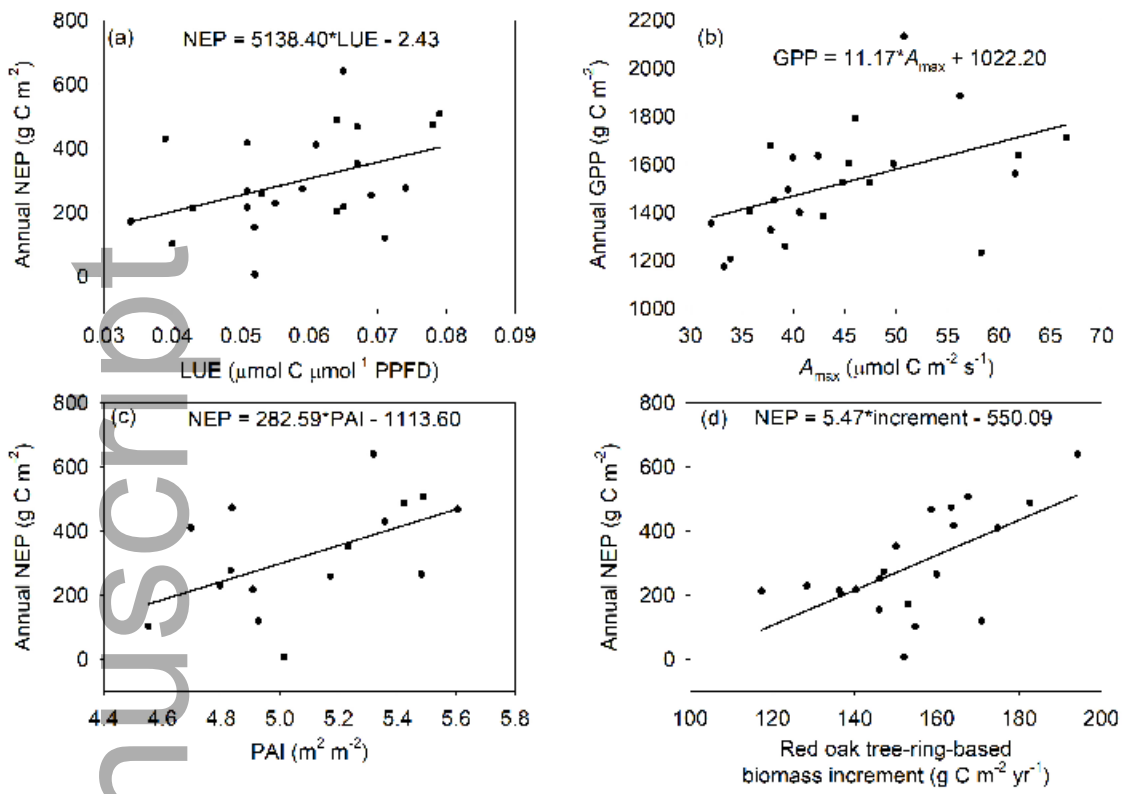
e cm\_1423\_f6.tif



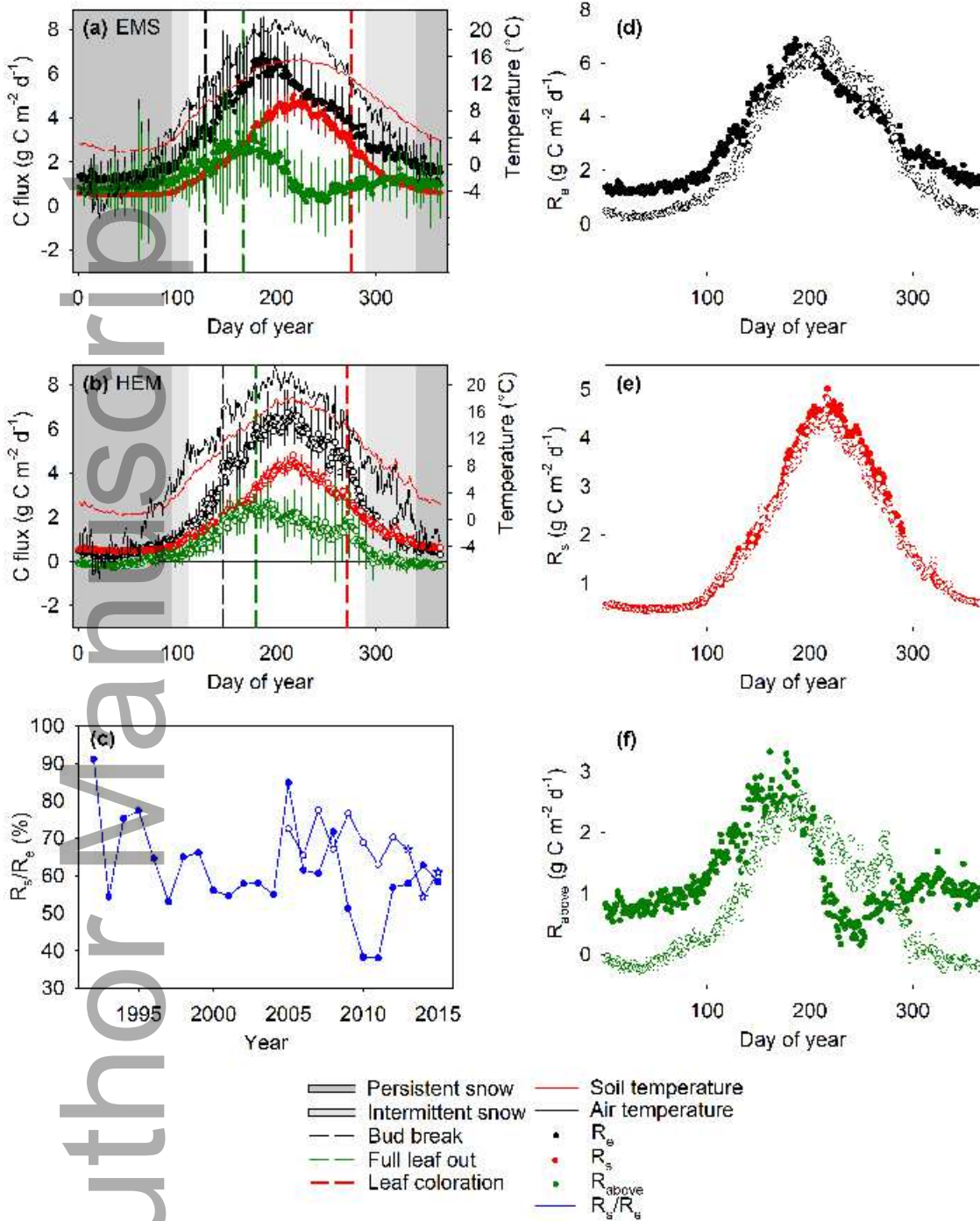
ecm\_1423\_f7.jpg



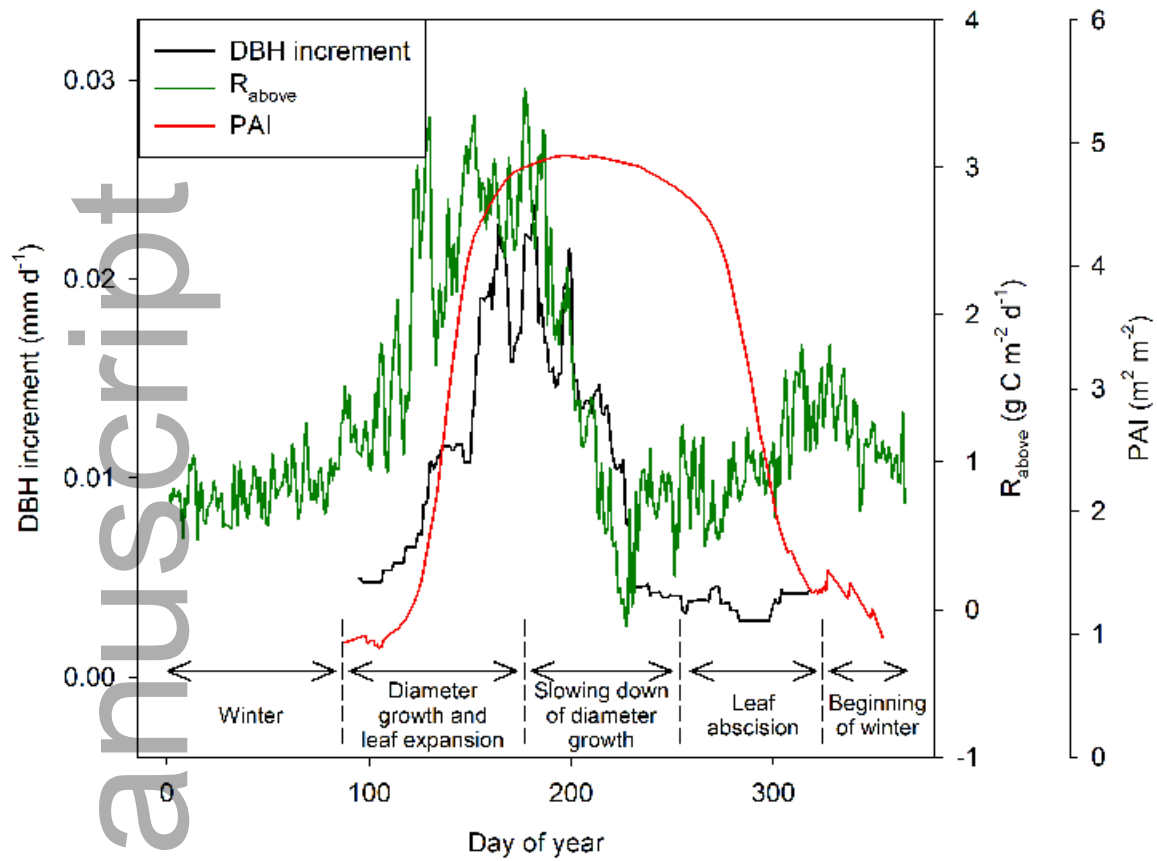
ecm\_1423\_f8.jpg



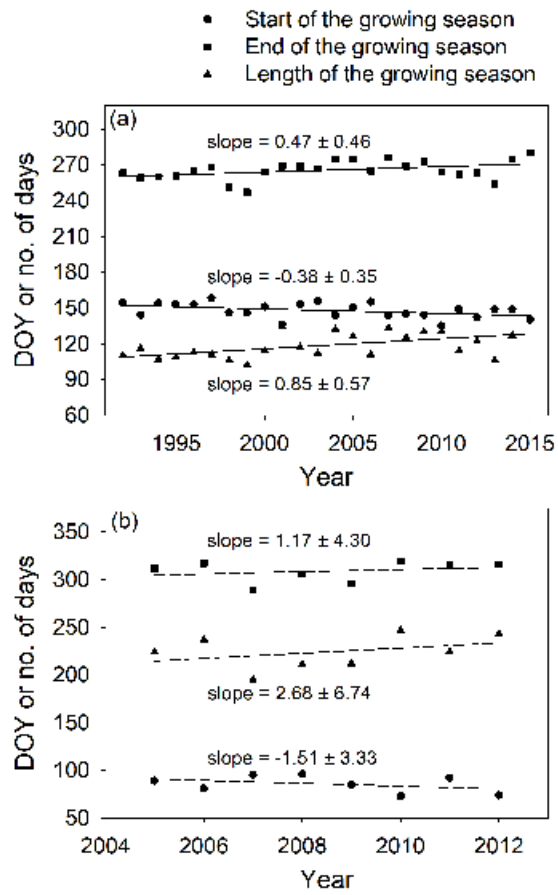
ecm\_1423\_f9.jpg



ecm\_1423\_f10.jpg

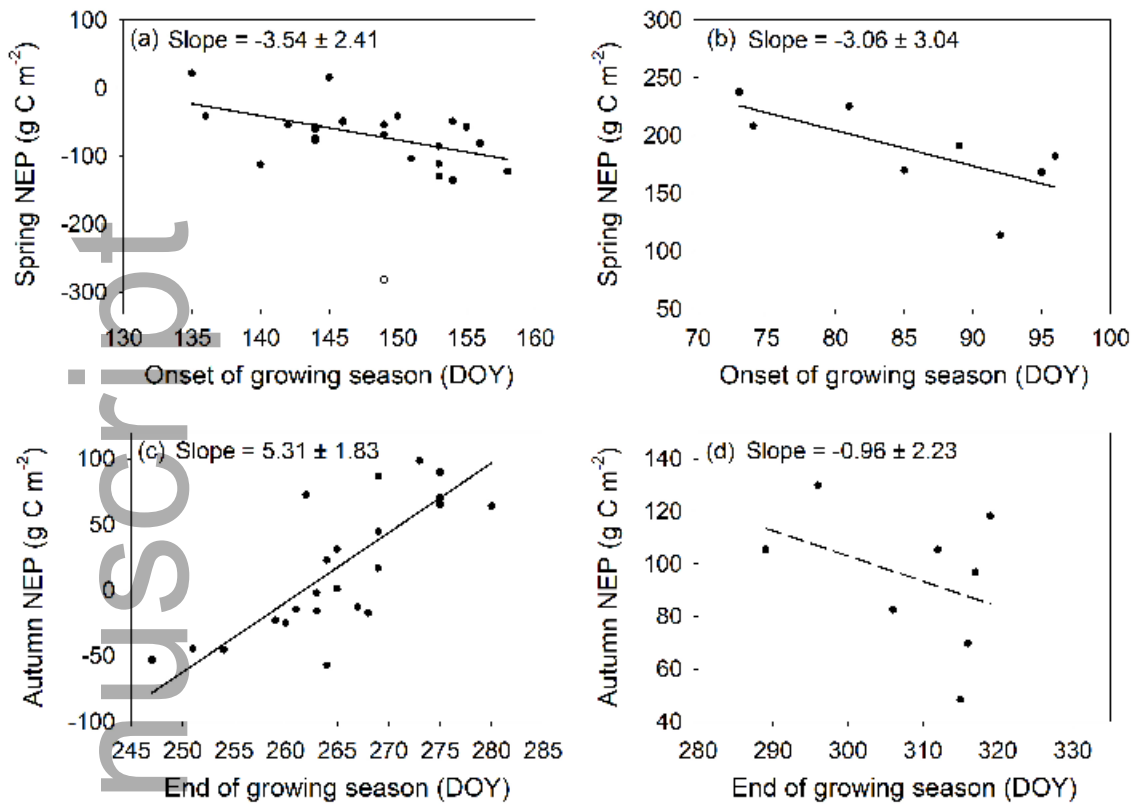


ecm\_1423\_f11.jpg



ecm\_1423\_f12.jpg





ecm\_1423\_f13.jpg